This is to certify that the
dissertation entitled

IN VIVO AND IN VITRO MECHANISMS FOR DISRUPTION OF THE
TOLL-LIKE RECEPTOR ACTIVATED IMMUNOGLOBULIN M
RESPONSE BY 2,3,7,8-TETRACHLORODIBENZO-P-DIOXIN

presented by

Colin M. North

has been accepted towards fulfillment
of the requirements for the

___Ph.D.___ degree in ___Pharmacology & Toxicology___

_____
Major Professor's Signature

8·21·09
_____
Date

PLACE IN RETURN BOX to remove this checkout from your record.
TO AVOID FINES return on or before date due.
MAY BE RECALLED with earlier due date if requested.

DATE DUE	DATE DUE	DATE DUE

5/08 K:/Proj/Acc&Pres/CIRC/DateDue.indd

IN VIVO AND *IN VITRO* MECHANISMS FOR DISRUPTION OF THE TOLL-LIKE RECEPTOR ACTIVATED IMMUNOGLOBULIN M RESPONSE BY 2,3,7,8-TETRACHLORODIBENZO-*P*-DIOXIN

By

Colin M. North

A DISSERTATION

Submitted to
Michigan State University
in partial fulfillment of the requirements
for the degree of

DOCTOR OF PHILOSOPHY

Pharmacology & Toxicology

2009

2,3,7,8-te

causes profound

models of T-ind

are directly sens

the primary IgN

cells (ASC), ca

1). B-cell CLL

1). Paired Box

that TCDD dis

activated prim

regulate of pla

increase in the

or 30 µg kg).

elicited increa

dose-depende

Relati

in purified B

0.3, 3 or 30 r

TCDD cause

ABSTRACT

IN VIVO AND *IN VITRO* MECHANISMS FOR DISRUPTION OF THE TOLL-LIKE RECEPTOR ACTIVATED IMMUNOGLOBULIN M RESPONSE BY 2,3,7,8-TETRACHLORODIBENZO-*P*-DIOXIN

By

Colin M. North

2,3,7,8-tetrachlorodibenzo-p-dioxin (TCDD) is a persistant organic pollutant that causes profound suppression of the primary immunoglobulin M (IgM) response in animal models of T-independent humoral immunity. B cells, the antibody producing cell type, are directly sensitive to TCDD, but a mechanistic understanding for TCDD disruption of the primary IgM response is incomplete. B cell differentiation into antibody-secreting cells (ASC), called plasmacytic differentiation, is regulated by Activator Protein-1 (AP-1), B-cell CLL/lymphoma (BCL-6), B lymphocyte induced maturation protein-1 (Blimp-1), Paired Box gene 5 (Pax5), and X-box Binding Protein-1 (XBP-1). It was hypothesized that TCDD disrupts the Toll-like receptor (TLR) ligand lipopolysacchride (LPS)-activated primary IgM response by altering expression of transcription factors known to regulate of plasmacytic differentiation. *In vivo* LPS administration induced a significant increase in the number of ASCs, which was dose-dependently impaired by TCDD (3, 10, or 30 μg/kg). Gene and protein expression analysis showed TCDD suppressed LPS-elicited increases in CD138 and IgM components. Blimp-1 and XBP-1 expression were dose-dependently impaired by TCDD.

Relationships between transcription factors regulating plasmacytic differentiation in purified B cells were assessed *in vitro* using LPS and combinations of TCDD (0.03, 0.3, 3 or 30 nM), then analyzed by flow cytometry 24, 48, and 72 h post-treatment. TCDD caused a concentration-related suppression of Blimp-1 and phosphorylated c-Jun

expression. and e

TCDD treatment

CD69. CD80. an

    Kinases

TCDD alters B(

JNK phosphory

activated by LP

assess the time-

TCDD suppress

min post-treatm

ERK. and JNK

IgM response b

potentially as a

expression, and elevated BCL-6 expression, relative to LPS + DMSO treated B cells. TCDD treatment caused a concomitant suppression of LPS-activated MHC Class II, CD69, CD80, and CD86 upregulation as early as 24 h post-treatment.

Kinases directly and indirectly regulate AP-1 and BCL-6. It was hypothesized that TCDD alters BCL-6 expression and AP-1 phosphorylation by changing AKT, ERK, and JNK phosphorylation. Multiparametric analysis of AKT, ERK, and JNK phosphorylation activated by LPS, R848, or CpG DNA in the B cell lymphoma CH12.LX was used to assess the time- and concentration-dependent effects of TCDD (0.003, 0.03, or 0.3 nM). TCDD suppressed TLR-activated AKT, ERK, and JNK phosphorylation at 15, 30, and 60 min post-treatment. TCDD at 30 nM impaired R848-activated phosphorylation of AKT, ERK, and JNK in primary B cells. These results suggest TCDD suppresses the primary IgM response by altering transcription factor and activation marker expression, potentially as a result of TCDD interference in TLR-activated kinase phosphorylation.

To Elizabeth N

in spite of my b

To Simone. Ce

do and remind

To Charles an

stumbled thro

completed gr

To John and

curiosity thr

To God. w

your glory

Dedication

To Elizabeth North, who believed in me even as times were difficult, and who stuck it out in spite of my belief that I could graduate by next year if everything went right.

To Simone, Cecily, and Felicity, who teach me about myself with every little thing they do and remind me that science is not the highest pursuit in life.

To Charles and Chris Jalovec, who have been the light of Christ in my life as I have stumbled through graduate school. Without their help and support I could not have completed graduate school.

To John and Terry North, who set the stage for my education and encouraged my curiosity throughout life.

To God, without whom all our efforts are for naught. My gifts and talents are solely for your glory.

Acknowledgments

TABLE OF CONTENTS

Table 1. Dir

Table 2. Dir

LIST OF TABLES

LIST OF FIGURES

293T

293T-HAG

293T-HAHR

3-MC

Ax488

Ax647

AHR

AHR-GFP

APC

ASC

BCR

BSA

Ca^{2+}

CMV

CYP

CYP1A1

CpG

DNA

DLC

DNP-Ficoll

DRE

EMSA

ABBREVIATIONS

293T	human embryonic kidney 293T cell line
293T-HAG	human embryonic kidney 293T cell line expressing human AHR-GFP
293T-HAHR	human embryonic kidney 293T cell line expressing human AHR
3-MC	3-methylcholanthrene
Ax488	AlexaFluor 488
Ax647	AlexaFluor 647
AHR	aryl hydrocarbon receptor
AHR-GFP	aryl hydrocarbon receptor with C-terminal fused GFP
APC	antigen presenting cell or allophycocyanin
ASC	antibody secreting cell
BCR	B cell receptor
BSA	bovine serum albumin
Ca^{2+}	calcium
CMV	cytomegalovirus
CYP	cytochrome P450
CYP1A1	cytochrome P450 1A1
CpG	CpG oligonucleotide 1826
DNA	deoxyribonucleic acid
DLC	dioxin like chemical
DNP-Ficoll	dinitrophenol-Ficoll
DRE	dioxin response element
EMSA	electromobility shift assay

ERK

FACS

GFP

h

HsAHR

IgH

IgJ

Igκ

Igλ

IgM

JNK

LPS

MACS

MAPK

min

mRNA

ORF

pAKT

pERK

PE

PBS

PCR

PFC

ERK	extracellular signal-regulated kinase
FACS	fluorescence activated cell sorter
GFP	green fluorescent protein
h	hours
HsAHR	*Homo sapiens* aryl hydrocarbon receptor
IgH	immunoglobulin μ heavy chain
IgJ	immunoglobulin J chain
Igκ	immunoglobulin κ light chain
Igλ	immunoglobulin λ light chain
IgM	immunoglobulin M
JNK	Jun N-terminal kinase
LPS	lipopolysacchride
MACS	Buffer for B cell isolation
MAPK	mitogen-activated protein kinase
min	minutes
mRNA	messenger ribonucleic acid
ORF	open reading frame
pAKT	phosphorylated AKT (Serine 473)
pERK	phosphorylated Extracellular signal Regulated Kinase 1 and 2 (Threonine 202/Tyrosine 204)
PE	phycoerythrin
PBS	Phosphate Buffered Saline
PCR	polymerase chain reaction
PFC	plaque forming cell

pNK

PKC

PuroR

QRT-PCR

RS48

RPMI

s

SKWA

SKWAG

SV40

TCDD

TCR

pJNK	phosphorylated Jun N-terminal Kinase 1 and 2 (Threonine 183/Tyrosine 185)
PKC	Protein Kinase C
PuroR	puromycin resistance
QRT-PCR	quantitative real-time reverse transcribed polymerase chain reaction
R848	Resiquimod
RPMI	Roswell Park Memorial Institute
s	seconds
SKWA	SKW 6.4 AHR$^+$
SKWAG	SKW 6.4 AHR-GFP$^+$
SV40	simian virus 40
TCDD	2,3,7,8-tetrachlorodibenzo-*p*-dioxin
TCR	T cell receptor

CHAPT

Overarch

Prot

for scientifi

risk assessm

the fundame

practices in

risk assessme

factors.

In the

key mechanis

enzyme induc

toxicities asso

tissues affecte

mechanistic un

potential health

undertaken and

immunotoxicity

mechanisms und

CHAPTER 1. INTRODUCTION

Overarching Purpose

Protection of human and animal health is considered one of the highest purposes for scientific endeavor. Making regulatory policies designed to protect health depends on risk assessment to make qualitative and quantitative evaluation of hazards. Understanding the fundamental biology underlying chemical toxicity allows the possibility of best practices in risk assessment. The optimal result of mechanism-based decision making in risk assessment is health protection, without unintentional harm due to unanticipated factors.

In the case of dioxin and dioxin like chemicals (DLCs), a basic understanding of key mechanisms exists for adaptive biological responses such as drug metabolizing enzyme induction. Unfortunately, a similar level of knowledge does not exist for toxicities associated with dioxin exposure in experimental animal models. Among many tissues affected by dioxins, the immune system is highly sensitive to dioxin and DLCs. A mechanistic understanding of dioxin immunotoxicity would be useful in estimating potential health risks posed by exposure to environmental dioxins and DLCs. The studies undertaken and described in this dissertation aim to advance knowledge of TCDD immunotoxicity, in an effort to fill data gaps in the understanding of molecular mechanisms underlying dioxin-associated health effects.

Overview

The i

organism thr

mediated (re

The innate ir

for undesiral

the dynamic

complement

recognize ur

efficiency or

branches. ce

humoral imr

undesirable

The

name derive

(Lindenman

antigen pres

macrophage

antigens the

either an eff

memory. Fir

native antige

form of antit

Overview of Immune System

The immune response is a highly complex and regulated process, protecting the organism through innate (soluble factors such as complement and defensins), cell-mediated (recognizing and killing foreign cell types), and humoral (antibody) immunity. The innate immune system is inherently anti-pathogenic, creating a hostile environment for undesirable agents. While important for host defense, innate immunity cannot adapt to the dynamic environment in which an organism lives. The innate immune system is complemented in vertebrate mammals by an adaptive immune system, which learns to recognize undesirable agents in the host and attack them with increasing speed and efficiency on subsequent encounters. The adaptive immune system exists as two branches, cell-mediated immunity protecting the host from conditions such as cancer, and humoral immunity that generates antibodies to identify, neutralize, and destroy undesirable agents.

The humoral, or antibody, response is specific for an agent termed the antigen, a name derived from the hypothesis that an agent causes generation of an antibody (Lindenmann 1984). Several cell types interact to produce a robust humoral response: antigen presenting cells (APCs), helper T cells (T_H cells), and B cells. APCs, such as macrophages and dendritic cells, sample the surrounding microenvironment and present antigens they find to T cells. Antigens recognized as foreign activate the T cell to become either an effector T cell producing cytokines, or a memory T cell maintaining antigenic memory. Finally, the B cell is the antibody producing cell type. The B cell recognizes native antigen in the environment if its B cell receptor (BCR), a non-secreted cell surface form of antibody, binds antigen with moderate affinity. B cells internalize BCR-antigen

2

complex foll

cells as an A

survival and

balance betw

host, and spe

in either spec

Indivi

stem cell pop

to new locatic

immune syste

first line sentr

marrow into t

without a suff

the host. T cel

to lymphoid o

recognized by

moves out into

the lymphoid t

The cel

and secrete larg

antibody molec

chains (as κ or λ

The light and he

complex following antigen binding, process the antigen, and present the antigen to T_H cells as an APC. In turn, stimulated T_H cells secrete cytokines that increase B cell survival and proliferation. The coordinated interaction of several cell types maintains a balance between specificity of response, in which the immune system does not attack the host, and speed of response, in which an immune response is rapidly initiated. Imbalances in either specificity or speed of response lead to disease in the host.

Individual cell types responsible for the antibody response arise from a common stem cell population in the bone marrow. Immune cells leave the bone marrow and move to new locations around the body as they differentiate into the various cell types of the immune system. APCs are distributed throughout the periphery of the body, acting as first line sentries to monitor the cellular environment. T cells travel from the bone marrow into the thymus where they undergo a maturation process that removes T cells without a sufficiently capable T cell receptor (TCR) or a TCR that is strongly reactive to the host. T cells that complete the maturation process and egress from the thymus migrate to lymphoid organs where they remain resident, waiting for APCs presenting an antigen recognized by the TCR. The B cell builds a functional BCR within the bone marrow, then moves out into the periphery, and similarly to the T cell, most B cells become residents of the lymphoid tissues.

The cellular function for which B cells are recognized is the ability to synthesize and secrete large amounts of antibody, sometimes called immunoglobulin. Individual antibody molecules have a general structure consisting of a combination of two light chains (as κ or λ chains) and two heavy chains (as μ, γ_1, $\gamma_{2a/2b}$, γ_3, α_1, α_2, ε, or δ chains). The light and heavy chains are further subdivided into variable regions and constant

3

regions. The

produced. wi

and δ produc

biological ac

initial humor

predominant'

individual an

cells differen

biological fu:

thesis.

  With

microscopy c

providing a p

while still pro

their expressi

infection. B1

mostly in the

associated mo

and have a lo

marginal zone

threshold for a

al 2002). It is

system that ca

regions. The constant region of the heavy chain designates the isotype of antibody produced, with µ producing IgM, γ producing IgG, α producing IgA, ε producing IgE, and δ producing IgD. Antigen binding occurs in the variable region, while many of the biological activities of antibodies depend on the constant region of the antibody. The initial humoral immune response to antigen, termed the primary response, consists predominantly of IgM. Secreted IgM is distinct from other antibody isotypes in that five individual antibodies are joined as a pentamer by the immunoglobulin J-chain (IgJ). B cells differentiate into a specialized cell type, the plasma cell, in order to accomplish the biological function of copious antibody secretion, a process that is discussed later in this thesis.

With the advent of fluorescence activated cell sorting (FACS) and fluorescent microscopy distinctions among types of B cells have arisen in scientific literature, providing a partial explanation for how the antibody response can be activated rapidly, while still providing specificity of response. Some B cells, termed B1 cells on the basis of their expression of Ly-1 (CD5), appear to play an important role in control of bacterial infection. B1 cells have a restricted repertoire of BCR (Bendelac *et al.* 2001), are resident mostly in the peritoneum and pleural cavities (Hayakawa *et al.* 1985), bind pathogen-associated molecules such as lipopolysacchride (LPS) (Kantor and Herzenberg 1993), and have a lower stimulus requirement for activation (Fagarasan *et al.* 2000). The marginal zone (MZ) B cells are very similar to the B1 cells, particularly in their lower threshold for activation (Lopes-Carvalho *et al.* 2005), but reside in the spleen (Balazs *et al.* 2002). It is thought that B1 and MZ cells provide a layer to the humoral immune system that can react more rapidly to bacterial infection, limiting the initial rate of

4

pathogen exp

specificity an

primary hum

(Fairfax *et al.*

follicular B c

et al. 1983). E

presented by

BCR outcomp

an activated, a

producing hig

memory. The

in antibody-se

cell to reach th

examined prio

The ac

stimulus: T-de

thymus is requ

which induces

dependent stim

produce antibod

not be discussed

(CpG), and resiq

pathogen expansion and allowing time for other B cell subsets producing higher specificity antibodies to differentiate. In LPS-activated experimental models the observed primary humoral IgM response is likely to reflect a high proportion of B1 and MZ (Fairfax *et al.* 2007; Martin *et al.* 2001). The third widely recognized B cell subset is the follicular B cell, named for its histologic localization in the "follicle" of the spleen (Hsu *et al.* 1983). B cell selection occurs via B cell competition for binding of native antigen presented by dendritic cells at the center of the follicle. B cells expressing high affinity BCR outcompete B cells expressing lower affinity BCR for survival signals provided by an activated, antigen-bound BCR. Through this competitive process only those B cells producing high affinity, high specificity antibody survive to provide robust immunologic memory. The time required for selective competition within the germinal center to result in antibody-secreting cells is typically greater than the time required for a B1 or MZ B cell to reach the antibody-secreting stage; thus, for antibody-secreting cell responses examined prior to five days much of the response is attributed to B1 and MZ B cells.

The activation of B cells has been studied in the context of 2 different types of stimulus: T-dependent stimuli such as sheep erythrocytes (sRBC), in which an intact thymus is required for a humoral response, and T-independent stimuli such as LPS, which induces a humoral response in the absence of an intact thymus (Wortis 1971). T-dependent stimuli require the coordinated interaction of the APC, T_H cell, and B cell to produce antibody, and have not been utilized for studies in this dissertation and thus will not be discussed further. T-independent stimuli, such as LPS, CpG oligonucleotides (CpG), and resiquimod (R848), activate B lymphocytes via Toll-like Receptors (TLR),

evolutionarily conserved pattern recognition receptors facilitating a rapid, robust response

to bacterial and viral pathogens (Rehli 2002).

The B cell is commonly referred to as naïve following egress from the bone

marrow. Antigen encounter subsequently activates the B cell, and like many receptor-

mediated processes an activation threshold exists for the B cell (DeFranco *et al.* 1985).

TLR activation leads to activation of key cell signaling agents such as AKT and Nuclear

Factor κ B (NFκB), many of which are convergent on the mitogen-activated kinases

(MAPK) (Campbell 1999; Harnett *et al.* 2005). Intracellular signals are integrated on an

individual cell basis, resulting in differentiation into either a memory B cell or antibody-

secreting plasma cell (ASC).

Control of

The s

engagement

and intracellu

transcription

Jun N-termina

MAPK. JNK

transcription f

ERK also play

circuit by contr

ubiquitinated a.

releasing a brak

contradiction to

differentiation. o

plasmacytic diff

controlling plasn

expected to alter

Control of Plasmacytic Differentiation

The signaling cascade feeding into plasmacytic differentiation begins with engagement of receptors such as the BCR or TLRs, causing activation of protein kinases and intracellular calcium (Ca^{2+}) increases, both of which feed into MAPK cascades and transcription factor networks. B cell signaling converges on several kinases, including Jun N-terminal Kinase (JNK), extracellular signal-regulated kinase (ERK), and p38 MAPK. JNK phosphorylates c-Jun, one component of the Activation Protein 1 (AP-1) transcription factor, increasing the transcriptional activity of AP-1 (Smeal *et al.* 1991). ERK also plays an important role in regulation of the plasmacytic differentiation control circuit by controlling BCL-6 abundance. Following phosphorylation by ERK, BCL-6 is ubiquitinated and targeted for proteasomal degradation (Niu *et al.* 1998), in effect releasing a brake controlling expression of Blimp-1. Interestingly, and in seeming direct contradiction to the role of ERK-induced degradation of BCL-6 controlling plasmacytic differentiation, constitutively active MEK, thought to activate ERK, inhibits LPS-induced plasmacytic differentiation (Rui *et al.* 2006). Given the apparent dual nature of ERK in controlling plasmacytic differentiation, treatments affecting ERK activation can be expected to alter frequency of plasmacytic differentiation.

7

Figure 1. The Plasmacytic Differentiation Control Circuit. Regulatory relationships are depicted as → to indicate positive regulation and ⊣ to indicate negative regulation.

Unfolded
Protein

P
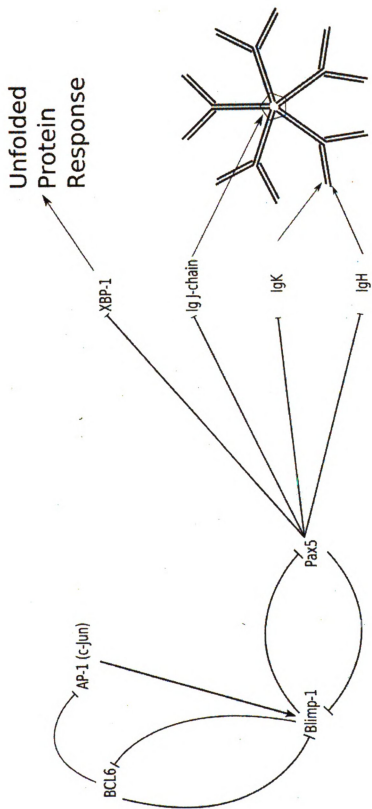
Plasmacy

alteration

activation.

gene expre

differentiati

induced mat

1 (XBP-1) a

regulatory in

depicted *in F*

6. *Blimp-1*. ar

2004). so call

In this case Bl

and Pax5 prev

quiescent. but

initiator of plas

AP-1 through a

family members

AP-1 *binds to re*

(Ohkubo et al. 2(

of BCL-6 and Pa

Blimp-1 expressi

expression profile

Profound remodeling of the B cell occurs for vigorous antibody secretion. Plasmacytic differentiation requires coordinated changes in gene expression preceding alteration in cellular phenotype. On the intracellular level this is accomplished through activation, repression, and induction of transcription factors responsible for control of the gene expression program in B cells. Research into the cellular mechanism of plasmacytic differentiation establishes AP-1, B-cell CLL/lymphoma 6 (BCL-6), B lymphocyte induced maturation protein 1 (Blimp-1), Paired Box 5 (Pax5), and X-box Binding Protein 1 (XBP-1) as key transcription factors regulating B cell fate (Igarashi *et al.* 2007). The regulatory interactions controlling the "plasmacytic differentiation control circuit" are depicted in Figure 1. The central axis of cell fate control is the interaction between BCL-6, Blimp-1, and Pax5. Such an interaction results in a "bistable switch" (Markevich *et al.* 2004), so called because the switch exist in one of two stable, mutually exclusive states. In this case Blimp-1 expression is stably on or stably off. In resting mature B cells BCL-6 and Pax5 prevent expression of Blimp-1, maintaining the gene expression program of a quiescent, but vigilant, B cell. Additionally, BCL-6 directly interacts with a keystone initiator of plasmacytic differentiation, AP-1, by reducing the transcriptional activity of AP-1 through a specific interaction with c-Jun (Vasanwala *et al.* 2002), one of the Jun family members that commonly participates in the AP-1 complex (Karin *et al.* 1997). AP-1 binds to response elements within in the Blimp-1 promoter to drive gene expression (Ohkubo *et al.* 2005), and once translated into protein, Blimp-1 silences gene expression of BCL-6 and Pax5 (Shaffer *et al.* 2002), creating a positive feedback loop in which Blimp-1 expression increases and allows for wholesale alteration of the cellular gene expression profile. *In vivo* profiling of the *prdm1* locus, from which *Blimp-1* is

transcribed. d

phenotype. as

2004).

Pax5 i

on the basis o

the B cell line

2007b). Loss c

types (Cobalec

Pax5 expressic

Pax5 expressic

2006). Cumula

Pax5 expressio

of interest are t

IgJ. Conversely

(Delogu et al. 2

Beyond

XBP-1 expressi

the unfolded pro

evidence sugges

transduction thro

Recent evidences

simply the result

course of BCR si

transcribed, demonstrates Blimp-1 expression is quantitatively related to plasma cell phenotype, as cells with the highest *prdm1* locus activation are plasma cells (Kallies *et al.* 2004).

Pax5 is required for generation of mature B cells (Maitra and Atchison 2000), and on the basis of functions promoting B cell maturation and repressing genes unsuitable for the B cell lineage named the "guardian of B cell identity and function" (Cobaleda *et al.* 2007b). Loss of Pax5 expression allows B cell dedifferentiation into either progenitor cell types (Cobaleda *et al.* 2007a) and T cells (Mikkola *et al.* 2002). Furthermore, loss of Pax5 expression promotes transition of B cells into an ASC phenotype, and restoration of Pax5 expression in Pax5$^{-/-}$ B cells reduces expression of Blimp-1 and XBP-1 (Nera *et al.* 2006). Cumulative evidence suggests B cells maintain their cellular character because of Pax5 expression, with loss of Pax5 allowing B cells to change phenotype. Several genes of interest are targeted by Pax5 for repression, including CD138, Blimp-1, IgH, Igκ, and IgJ. Conversely, Pax5 positively regulates genes involved in forming a functional BCR (Delogu *et al.* 2006).

Beyond regulation of Ig genes (Calame *et al.* 2003), Pax5 also directly regulates XBP-1 expression (Reimold *et al.* 1996). XBP-1 is best known for its role in resolution of the unfolded protein response observed in plasma cells (Yoshida *et al.* 2001). Emerging evidence suggests XBP-1 plays additional roles in B cell biology, aiding in signal transduction through the BCR and potentially indirectly regulating Blimp-1 expression. Recent evidences suggests XBP-1 induction is a differentiation-dependent event, not simply the result of an unfolded protein response, and plays a role in controlling the time course of BCR signaling (Hu *et al.* 2009). Both the role of XBP-1 in resolving the

unfolded protei

potential import

importance of X

XBP-1 expressi

downregulation

with a decrease

1(Shen and Hen

and is required.

indirect regulati

Different

in phenotypically

cells. Protein an

differentiation cc

programs to secr

decrease as Blim

unfolded protein response and the newly identified role in BCR signaling accentuate the potential importance of XBP-1 in B cell function. Further accentuating the potential importance of XBP-1 in regulating plasmacytic differentiation, RNA interference in XBP-1 expression reduced *IgH* gene expression in plasmacytoma cell lines. The downregulation of *IgH* expression resulting from XBP-1 interference was concomitant with a decrease in the expression of the transcription factor Octamer Binding Factor 1(Shen and Hendershot 2007). Because Octamer Binding Factor 1 upregulation precedes, and is required, for *prdm1* locus activation (Corcoran *et al.* 2005) the potential for indirect regulation of Blimp-1 expression by XBP-1 is apparent.

Differentiation from the activated B cell to antibody-secreting plasma cell occurs in phenotypically identified stages, and appears in Figure 2 beginning with resting B cells. Protein and mRNA abundance for transcription factors of the plasmacytic differentiation control circuit changes over time as B cells remodel their transcriptional programs to secrete antibody. As conceptualized in Figure 2, levels of Pax5 function decrease as Blimp-1 expression increases.

Figure 2. B cell to plasma cell transition. Reprinted by permission from Macmillan Publishers Ltd: Nature Reviews Immunology (Nutt et al. 2007).

Resting B cell | Activated B cells | Plasmablasts (short lived) | Plasma cells (long lived)

B-cell receptor

Memory B cell (BCL-6^{low})

GC (BCL-6^{hi})

Pre-plasmablast

Follicular B cell (BCL-6^{low})

MZ B cell (BCL-6^{low})

B-cell precursor

B-1 B cell (BCL-6^{low})

PAX5 (function)

BLIMP1
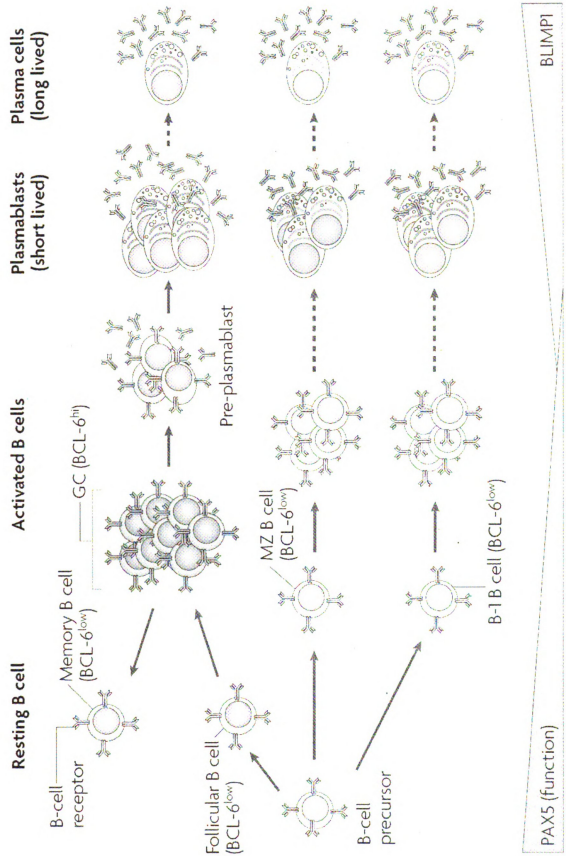
In sum

into classic M.

MAPK signali

an increase in

maintaining its

Increased synth

cell.

In summary, plasmacytic differentiation begins with receptor activation feeding into classic MAPK signaling cascades. In B cells destined for the ASC phenotype, MAPK signaling converges on the plasmacytic differentiation control circuit, resulting in an increase in Blimp-1 expression. Blimp-1 upregulation represses BCL-6 and Pax5, thus maintaining its own expression, and initiating changes that increase Ig synthesis. Increased synthesis of Ig allows for increasing secretion of Ig, the hallmark of the plasma cell.

History of

Deca

with exposur

such as poly

dibenzodioxi

appears in 19

of chemical i

reviewed rep

(Bowen and

from tetrachl

1973). Of all

dioxin (TCDD

with dioxin an

Attenti

widely publici

and for Operat

garnered large

public eye, DL

dietary exposur

food web (Kelly

consistent and li

industry workers

particular, have

History of Dioxin and Dioxin-like Chemicals

Decades of research have been dedicated to understanding toxicities associated with exposure to halogenated aromatic hydrocarbons, particularly for dioxin and DLCs such as polychlorinated biphenyls, polychlorinated dibenzodifurans, and polychlorinated dibenzodioxins. The first published reports of intentional synthesis for dibenzodioxins appears in 1957 (Gilman and Dietrich 1957), but unintentional production as a byproduct of chemical industry activity occurred as early as 1848 (Weber *et al.* 2008). Peer-reviewed reports of health effects attributable to DLCs began to surface in the 1950's (Bowen and Moursund 1957; Meigs *et al.* 1954), with evidence for adverse health effects from tetrachlorinated dibenzodioxins appearing in the 1970's (Jensen *et al.* 1972; May 1973). Of all the chemical structures classified as DLCs, 2,3,7,8-tetrachlorodibenzo-*p*-dioxin (TCDD) is the most studied and potent congener for inducing toxicities associated with dioxin and DLC exposure.

Attention focused on health risks posed by dioxin and DLCs increased following widely publicized exposure events, including Times Beach in Missouri, Seveso in Italy, and for Operation Ranchhand participants (Weber *et al.* 2008). While all the above events garnered large amounts of media attention at the time, and continue to remain in the public eye, DLCs in the environment are encountered by almost all humans through dietary exposure. The highly lipophillic nature of DLCs causes bioaccumulation in the food web (Kelly *et al.* 2007), such that top level consumers such as humans have consistent and life-long exposure to DLC. Additionally, some individuals, chemical industry workers (Patterson *et al.* 1989) and incinerator workers (Kumagai *et al.* 2000) in particular, have higher body burdens of DLCs owing to occupational exposure.

Widesp

literature. but I

models establi

hepatomegaly

carcinogenesis

syndrome (See

doses of TCDI

tissue and spec

TCDD. show in

1983).

Unlike r

story of the dio:

profiling progre

the fore in the 1

major determina

hydrocarbon. or

cytochrome P45

of mice. such as

Conversely. nonr

response to 3-M(

CYP activity than

nonresponsive str

to TCDD between

Widespread exposure to DLCs, including TCDD, is well established in the literature, but human health effects beyond chloracne are tenuous. Experimental animal models establish TCDD as an agent with pleitropic biologic effects, including hepatomegaly (Alsharif and Hassoun 2004), endocrine disruption (Safe 1995), carcinogenesis (Huff *et al.* 1991), teratogenesis (Abbott and Birnbaum 1989), wasting syndrome (Seefeld *et al.* 1984), and immunological defects (Luebke *et al.* 2006). The doses of TCDD required for eliciting biological effects listed above range from tissue to tissue and species to species, but the immune response is highly sensitive to disruption by TCDD, showing functional perturbations at concentrations as low as 4 ng/kg (Clark *et al.* 1983).

Unlike many contemporary nuclear receptors first cloned then characterized, the story of the dioxin receptor discovery is a fascinating example of classical biochemical profiling progressing to identification of the receptor. As the effects of TCDD came to the fore in the 1970's and 1980's, mouse breeding studies identified a genetic locus as a major determinant in sensitivity to biological effects associated with dioxin. The *Aryl hydrocarbon*, or *Ah*, locus conferred phenotypic differences for effects of DLCs on cytochrome P450 (CYP) induction by 3-methylcholanthrene (3-MC). Responsive strains of mice, such as the C57BL/6, induce CYP enzyme expression in response to 3-MC. Conversely, nonresponsive strains, such as the DBA/2, do not induce CYP enzymes in response to 3-MC (Nebert *et al.* 1972). TCDD is a 30,000-fold more potent inducer of CYP activity than 3-MC, and was shown to induce CYP activity in both responsive and nonresponsive strains of mice, albeit with approximately 10-fold differences in sensitivity to TCDD between the strains (Poland and Glover 1974). Further examination identified

17

that TCDD se

differential se

DLCs (Poland

With t

responses to D

cellular compo

high affinity to

protein for TCI

1976). Bestowe

methodology fo

Poland 1988), a

a partial N-term

With a p

oligonucleotide

characterization

encoding AHR re

the C57BL/6 mou

helix domain con

transcription facto

heat shock protein,

ligand activation .

Translocator (AR

that TCDD sensitivity was inherited as an autosomal dominant trait, and conferred

differential sensitivity to both the biochemical and toxicologic responses to TCDD and

DLCs (Poland *et al.* 1979).

With the *Ah* locus implicated as being responsible for the biochemical and toxic

responses to DLCs, many laboratories began using radiolabelled TCDD as a probe for the

cellular component encoded by the *Ah* locus. Poland et al showed that TCDD binds with

high affinity to a cytosolic protein, and quantified the B_{max}, K_d, and specificity of the

protein for TCDD, characteristics implicating the protein as a receptor (Poland *et al.*

1976). Bestowed the name *Ah* receptor (AHR), Perdew and Poland developed a

methodology for enriching liver homogenates for receptor purification (Perdew and

Poland 1988), a technique that allowed Bradfield et al to purify enough AHR to perform

a partial N-terminal sequencing (Bradfield *et al.* 1991).

With a partial protein sequence in hand, Burbach et al used degenerate

oligonucleotide probes to interrogate cDNA libraries. Culminating years of biochemical

characterization for AHR and its interaction with TCDD, the identification of cDNA

encoding AHR resulted in the cloning and sequencing of the mouse AHR^{b-1} allele from

the C57BL/6 mouse. DNA sequence analysis identified the AHR as a basic helix-loop-

helix domain containing protein and member of the *Per-ARNT-Sim* family of

transcription factors (Burbach *et al.* 1992). AHR resides in the cytosol complexed with

heat shock protein 90, p23, and aryl hydrocarbon receptor associated protein 9. Upon

ligand activation AHR translocates to the nucleus and dimerizes with the AHR Nuclear

Translocator (ARNT), forming a heterodimeric transcription factor capable of binding a

dioxin response element (DRE), 5'-TNGCGTG-3', and altering gene expression

(Denison and Nagy 2003).

History of

The p

the 1970's. F

gluococortico

by chemicals

and humoral

Vecchi and c

immunity up

The pi

by DLCs oper

longitudinally.

a requirement

to TCDD. char

and have since

the B cell.

During t

determinant in b

factor in TCDD-

humoral response

to immunotoxicity

relationship comp

correlated potency

Harper et al. 1995

History of TCDD and Dioxin Immunotoxicity

The potential for immune response suppression by DLCs was recognized early in the 1970's. Because TCDD causes thymic atrophy, a result associated with gluococorticoid suppression of immunity, awareness of potential for immunosuppression by chemicals came to exist. TCDD was shown to impair function of both cell-mediated and humoral responses in rodents (Vos *et al.* 1973; Vos *et al.* 1974). Later work by Vecchi and colleagues found that a single dose of TCDD caused suppression of humoral immunity up to 42 days following treatment (Vecchi *et al.* 1980a; Vecchi *et al.* 1980b).

The pioneering discoveries of Joseph Vos in the area immune response disruption by DLCs opened a path for many investigators to expand on his initial findings. Viewed longitudinally, research on TCDD-mediated disruption of humoral immunity established a requirement for AHR, identified the humoral immune response cell types most sensitive to TCDD, characterized the kinetics of TCDD-mediated humoral immunity disruption, and have since delved into the molecular mechanism of TCDD immunotoxicity within the B cell.

During the early 1980's the *Ah* locus received increasing attention as a major determinant in biological responses to TCDD, and with time proved to be an essential factor in TCDD-mediated disruption of humoral immunity. Initial comparisons of humoral response disruption by TCDD in Ah^{bb} and Ah^{dd} mouse stains showed sensitivity to immunotoxicity segregated with the *Ah* locus (Vecchi *et al.* 1983). Structure-activity relationship comparisons for AHR ligand-mediated effects on the primary IgM response correlated potency for AHR activation with immune suppression (Harper *et al.* 1995a; Harper *et al.* 1995b; Tucker *et al.* 1986). Conclusive proof for AHR involvement in

TCDD disruption of the primary IgM response comes from multiple lines of evidence. Sulentic et al found that an AHR expressing B cell line, CH12.LX, is highly sensitive to TCDD, showing antibody response impairment at concentrations of TCDD as low as 30 pM. The antibody response of a second cell line that does not express AHR, BCL-1, is unaffected by TCDD even at 3 nM concentrations (Sulentic *et al.* 1998). Using AHR knockout mice Vorderstrasse et al proved the *in vivo* primary IgM response to sRBC unperturbed by 10 µg/kg TCDD treatment, whereas the primary IgM response decreased 80% in TCDD-treated AHR sufficient mice (Vorderstrasse *et al.* 2001).

As the role of AHR in TCDD-mediated immunotoxicity was established, questions remained regarding which cell types of the humoral immune response were sensitive to TCDD. To determine the sensitive cell type in the primary IgM response comparisons of *in vitro* cultures stimulated using sRBC, DNP-Ficoll, or LPS are useful. While the primary IgM response to sRBC requires the participation of T cells, B cells, and antigen presenting cells, the responses to DNP-Ficoll is T-independent, requiring only APCs and B cells, and the response to LPS requires only the B cell. By comparing the ability of TCDD to suppress responses to each stimulus it is possible to exclude T cells or APCs from a role in IgM response suppression. The first evidence for sensitivity of B cells to TCDD came in the form of parallel, concentration-dependent TCDD suppression of primary IgM responses to sRBC, DNP-Ficoll, and LPS (Holsapple *et al.* 1986), thus excluding T cells and APCs. Additionally, cultures of purified mouse B cells are directly sensitive to disruption of LPS-stimulated IgM secretion (Morris *et al.* 1993). In effort to conclusively establish the relative roles for different immune cell types in primary IgM response disruption by TCDD, Dooley et al used separation/reconstitution

studies examining contributions of different cell types to the primary IgM response elicited by sRBC or DNP-Ficoll. Mice were treated *in vivo* with TCDD, then individual cell types (T cells, B cells, and APCs) were separated and used to reconstitute *in vitro* cultures. After excluding TCDD effects on APCs in preliminary results, focus turned to cultures containing all three cell types with either B cells and APCs or T cells and APCs supplied by TCDD treated mice. Only cultures containing B cells from TCDD treated mice showed the profound suppression of the primary IgM response normally associated with TCDD treatment (Dooley and Holsapple 1988). Later follow-up experiments further confirmed that T cells from TCDD exposed mice do not impair the *in vitro* IgM response (Dooley *et al.* 1990).

Due to the nature of the immune system and primary humoral immune response it is necessary to stimulate a response before any disruption of that response can be observed. Many events occur within the cell following stimulation, some within seconds while others will not occur for days. It is possible for a "window of sensitivity" to exist in such a scenario, during which an event may be disrupted, in this case by TCDD. Should the disrupting agent exposure occur outside the window of sensitivity, alterations in the immune response do not occur. While *in vivo* exposure to TCDD prior to immune response activation causes long lasting perturbations in the immune system (Holladay *et al.* 1991), *in vitro* studies show that TCDD significantly inhibits the primary IgM response only if added within 24 hours of sRBC addition (Tucker *et al.* 1986) or 3 hours for LPS addition (Holsapple *et al.* 1986). In addition, TCDD causes relatively minor alterations in circulating Ig compared to the profound impairment of the induced IgM . response (Fan *et al.* 1996), suggesting that *in vivo* TCDD does not directly inhibit the

activity of plasma cells, but rather the ability of an activated B cell to differentiate into a plasma cell. Considering the relatively short window of sensitivity, a single day or less following activation, it is likely that TCDD interferes in some early event in activation-induced B cell differentiation. Interestingly, a window of sensitivity for TCDD disruption of differentiation processes also exists for adipocytes, as demonstrated in the ability of TCDD to inhibit hormone induced preadipocyte differentiation into adipocytes (Hanlon *et al.* 2003).

The window of sensitivity for TCDD disruption of the IgM response brought research focus to early post-activation events in B cells. TCDD affects many aspects of B cell activation, including protein phosphorylation and intracellular Ca^{2+}. In purified unactivated B cells, TCDD treatment increased basal kinase activity, but did not affect Protein Kinase C (PKC) activity. The combined treatment of phorbol-12-myristate-13-acetate (PMA) and TCDD caused greater protein phosphorylation than single treatments alone, which was interpreted as resulting from activation of multiple kinases (Kramer *et al.* 1987). Examining both global protein phosphorylation and tyrosine phosphorylation in B cells following TCDD, *in vitro* cultures revealed concentration-related increases in protein phosphorylation within minutes of treatment (Clark *et al.* 1991; Snyder *et al.* 1993). B cells treated with the combination of PMA and the Ca^{2+} ionophore ionomycin (PMA/Io) are an experimental model of BCR activation. In examining the potential for TCDD disruption of BCR signaling, Karras et al showed PMA/Io-induced proliferation decreased as much as 50% in TCDD treated B cells. The authors attributed to the decreased proliferation caused by TCDD to alteration in intracellular Ca^{2+} levels

downstream of phospholipase C activation due to the dependence on ionomycin, not

PMA, concentration (Karras and Holsapple 1994). Followup studies indicated TCDD

treatment interfered with stability of intracellular Ca^{2+} concentrations in resting B cells

(Karras *et al.* 1996). Taken together, evidence suggests TCDD affects some early event in

B cell signaling, but direct evidence of TCDD effects on any single factor to which all the

above effects can be attributed remains elusive.

In addition to evidence for TCDD disruption of an early event in signaling, there

is also support for intracellular signaling preventing TCDD disruption of the IgM

response. Unlike *in vivo* responses or *in vitro* stimulated responses from *in vivo* treated

mice, inconsistent suppression of *in vitro* stimulated primary IgM response hampered

initial efforts to model *in vivo* effects until it was recognized that different serum lots

supported *in vitro* TCDD suppression of the IgM response (Morris and Holsapple 1991).

Serum was also demonstrated to modulate TCDD-induced CYP enzyme induction in

both splenocytes and hepatocytes (Morris *et al.* 1994), suggestive of the possibility that

serum factors can alter TCDD-induced AHR signaling. Human Interferon-γ (IFNγ)

causes a concentration-related reversal for TCDD suppression of both LPS and sRBC

AFC response, as well as TCDD-induced protein phosphorylation, for cultured mouse

splenocytes. In a return to the window of sensitivity paradigm, only addition IFNγ to

culture within 18 h of activation could reverse TCDD suppression of the IgM

response(Snyder *et al.* 1993). IFNγ also prevented TCDD-induced CYP expression in

cultured primary hepatocytes, an effect attributed to a soluble, heat-labile, protease-

sensitive factor that was not IFNγ (Jeong *et al.* 1993). Taking into account the window of

sensitivity and cell signaling alteration resulting from TCDD treatment, as well as results

demonstrating

response. evid

from alteration

cell to plasma

In summ

response is an

signaling occur

precede. or occ

differentiation

demonstrating that a protein-mediated signal can prevent TCDD suppression of the IgM response, evidence indicates the disruption of the primary IgM response by TCDD results from alterations at, or preceding, the level of cell signals that converge on control of B cell to plasma cell differentiation.

In summary, previous literature indicates TCDD disruption of the primary IgM response is an AHR-dependent phenomenon, likely the result of TCDD alteration in cell signaling occurring within 24 h of B cell activation. The kinetics of this alteration likely precede, or occur concurrently with, cell signaling inputs feeding into the plasmacytic differentiation control circuit.

Intracellular Signaling involved in TCDD Disruption of the Primary IgM Response

As the techniques underpinning scientific investigation advanced so did efforts to understand how TCDD disrupts B cell differentiation at the intracellular level. Clues as to how TCDD impairs the antibody response can be found in the quantity of AHR in immune cells, direct regulation of *Ig* genes by AHR, alteration in posttranslational modification of regulatory proteins, and activity of transcription factors important in control of plasmacytic differentiation.

The ED_{50} for TCDD inhibition of the sRBC-induced IgM response is 0.7 µg/kg (Smialowicz *et al.* 1994) and 7 nM for the TNP-LPS induced *in vitro* IgM response (Harper *et al.* 1995b) in the B6C3F1 mouse. One likely reason for the sensitivity of immune cells to TCDD is cell activation causes AHR and ARNT levels increase 2 to 6 fold (Crawford *et al.* 1997; Williams *et al.* 1996). In ligand-receptor interactions one primary determinant dictating tissue response to a ligand in the amount of receptor available for binding (Clark 1933), therefore, the increase in AHR associated with leukocyte activation should increase tissue responsiveness to TCDD treatment. Indeed, even in the absence of exogenous ligand addition, activation of leukocytes causes AHR translocation into the nucleus, DNA binding, and transcription of CYP1A1, all classically associated with TCDD-induced AHR activation (Crawford *et al.* 1997).

Development of a cell line-based model for TCDD disruption of the IgM response allowed assessment of TCDD effects in ways that were difficult or impossible to perform using primary cells. The CH12.LX B cell line is a subclone of the CH12 lymphoma that responds to sRBC or LPS treatment by differentiating into an ASC (Bishop and

Haughton 1986). CH12.LX cell line, due to its TCDD- and LPS-responsive phenotype, is

a highly suitable *in vitro* model for elucidating mechanisms of TCDD-mediated

disruption of the IgM response. Because both TCDD suppression of IgM secretion and

AHR dependence was well established *in vivo* and *in vitro* for both primary cells and the

CH12.LX cell line, one approach to elucidating mechanism is to work upstream from a

known event, such as TCDD suppression of immunoglobulin μ heavy chain (IgH)

expression. Activity of the 3' α enhancer of the *IgH* gene plays an important role in

antibody production (Arulampalam *et al.* 1994; Dariavach *et al.* 1991; Grant *et al.* 1995;

Pettersson *et al.* 1997; Pettersson *et al.* 1990). Two DRE sites within the 3' α enhancer

were identified and shown to bind AHR (Sulentic *et al.* 2000), both of which were later

confirmed to alter transcriptional activity of the 3' α enhancer (Sulentic *et al.* 2004a) and

directly bind AHR in intact cells (Sulentic *et al.* 2004b). Together, the observations of

Sulentic et al were the first published evidence for a direct regulation of Ig secretion by

AHR.

During the intervening time between identification of DREs within the 3' α

enhancer and evidence for direct modulation of transcriptional activity for the 3' α

enhancer by AHR, additional observations within CH12.LX cells further established

potential effects of TCDD on signaling important for plasmacytic differentiation. Two

key transcriptional regulators known to enhance the activity of the 3' α enhancer are AP-

1 (Matthias and Baltimore 1993) and NFκB (Kanda *et al.* 2000). There are marked

increases in both DNA binding and transcriptional activity for AP-1 and NFκB following

LPS activation of CH12.LX cells, with TCDD treatment causing significant impairment

of AP-1 activity, but not NFκB. TCDD inhibits LPS-activated AP-1 DNA binding in

CH12.LX cells. bu

binding. EMSA su

present in the AP-

correlated with im

Since a direct. inhi

2002). and the AP

contain Fos. a part

transcriptional act

treatment.

Earlier stu

identifying protei

with increasing c

development of

to be an importa

facilitates B cell

Additionally. li

inhibition incre

CH12.LX cells

modification.

further confirr

TCDD treatm

CH12.LX cells, but not BCL-1 cells, implying that AHR is required to decrease AP-1

binding. EMSA supershifts were able to establish Jun, but not Fos, as one of the proteins

present in the AP-1 complex induced by LPS in CH12.LX cells, an outcome that directly

correlated with immunoblot results assessing nuclear c-Jun quantity (Suh *et al.* 2002b).

Since a direct, inhibitory interaction between BCL-6 and c-Jun exists (Vasanwala *et al.*

2002), and the AP-1 complex induced by LPS treatment of CH12.LX cells does not

contain Fos, a partial explanation for TCDD disruption of AP-1 DNA binding and

transcriptional activity could be maintenance of BCL-6 activity resulting from TCDD

treatment.

Earlier studies illustrating TCDD-induced protein phosphorylation, without

identifying proteins specifically, demonstrated a limitation that became surmountable

with increasing commercial availability of antibodies, quantitative PCR techniques, and

development of the CH12.LX cell line model. In example, regulation of $p27^{kip1}$, known

to be an important regulator of differentiation in the several cell types (Lloyd *et al.* 1999),

facilitates B cell cycle arrest to allow for differentiation (Schrantz *et al.* 2000).

Additionally, linking the plasmacytic differentiation control circuit with $p27^{kip1}$, BCL-6

inhibition increases expression of $p27^{kip1}$ (Shaffer *et al.* 2000). LPS activation of

CH12.LX cells induced increases in $p27^{kip1}$ expression and posttranslational

modification, while TCDD treatment prevented an LPS-induced alteration of $p27^{kip1}$. In

further confirmation for a window of sensitivity, greatest modulation of $p27^{kip1}$ by

TCDD treatment occurred within 24 h of activation. Given the known importance of

BCL-6 in regulation of plasmacytic differentiation, documented TCDD effects on the common downstream target p27^{kip1}, and the coinciding window of sensitivity for regulation by TCDD, the disruption of a signal event upstream of the plasmacytic differentiation control circuit depicted in Figure 1 seems likely.

With an effect on the *IgH* locus established in CH12.LX, efforts were applied to determining if regulatory steps preceding *IgH* expression were similarly disrupted. Pax5 directly controls expression of several components of IgM, including *IgH* (Singh and Birshtein 1993). Concentration-response profiling of TCDD effects on Pax5 expression in LPS-stimulated CH12.LX showed that TCDD prevents downregulation of Pax5 mRNA, protein, and DNA binding (Yoo *et al.* 2004). Further extending the observation of TCDD effects on Pax5, Schneider et al showed TCDD caused concentration-related increases in *Pax5* gene expression and prevented LPS-induced downregulation of Pax5 protein in both splenocytes and CH12.LX cells (Schneider *et al.* 2008). In a more detailed follow up examination of both Pax5 regulation and Blimp-1 expression in splenocytes and CH12.LX, the DNA binding activity of Blimp-1 to response elements within the *Pax5* promoter was markedly reduced by TCDD treatment, and correlated with TCDD suppression of LPS-induced Blimp-1 mRNA expression. Confirming previous *in vitro* observations of reduced AP-1 transcriptional activity, TCDD caused a concentration-dependent reduction in LPS-stimulated DNA binding of specific AP-1 response elements identified in the promoter of Blimp-1 (Schneider *et al.* 2009).

Cumulatively, the knowledge of intracellular events leading to suppression of the *in vitro* IgM response provide clear evidence for TCDD, directly and indirectly, affecting multiple regulatory points within B cells, including AP-1 DNA binding, Blimp-1

upregulation, Pax5 downregulation, and *IgH* 3' α enhancer activity. Above the level of intracellular signaling, the immunotoxicity of TCDD can be summarized as a dose- and AHR-dependent phenomenon, for which a window of sensitivity within the first 24 hours following *in vitro* activation exists. Verification and extension of *in vitro* mechanisms using *in vivo* systems would represent a valuable step forward in understanding immunotoxicity caused by TCDD.

CHAPTER 2. MATERIALS AND METHODS

Animals

Female 6-8 week old C57BL6 mice were purchased from the National Cancer

Institute and housed in accordance with Michigan State University Institutional Animal

Care & Use Committee policy. For *in vivo* studies mice were dosed by single oral

gavage according to individual weights 4 days prior to LPS administration, with final

doses equal to 0, 3, 10, or 30 µg/kg TCDD in sesame oil. On day 0 mice received

intraperitoneal injections of phosphate buffered saline vehicle or 25 µg *Salmonella*

typhosa LPS to activate as primary humoral IgM response. Each time point and treatment

group consisted of 6 mice. Tissue samples were collected from mice receiving sesame oil

vehicle or TCDD treatment alone on the day 0 to establish baseline effects of TCDD for

all outcomes measured, then tissues were collected from all treatment groups on

subsequent days. Mice were euthanized by carbon dioxide asphyxiation and spleens

removed for processing into single cell suspensions by mechanical disruption.

Splenocytes from individual mice were divided into separate aliquots for flow cytometry,

RNA and DNA isolation, protein isolation, and IgM ASC response enumeration.

Chemicals

TCDD was purchased from Accustandard (New Haven, CT) and prepared in

sesame oil (Sigma-Aldrich). *Salmonella typhosa* LPS was purchased from Sigma-Aldrich

and prepared immediately prior to administration.

For *in vitro* studies stocks of LPS, R848, and CpG ODN 1826 were prepared in

individual aliquots and stored at -20° C until use. LPS was reconstituted in RPMI-CH12

at a concentration of 10 μg/μL without serum and other culture supplements. R848 was purchased from Alexis Biochemicals (Plymouth Meeting, PA) and prepared in cell culture grade DMSO (Sigma-Aldrich) at a concentration of 1 μg/μL. HPLC-purified thioester modified CpG with a sequence of 5'-TCCATGACGTTCCTGACGTT-3' was purchased from Eurofins MWG Operon (Huntsville, AL) and prepared in Tris-buffered water at a concentration of 1.2 μg/μL.

B cell Isolation

Purified mouse B cells were isolated using Miltyeni Biotec B cell Isolation kits (Auburn, CA) according to manufacturer's instructions. In brief, spleens were collected from three mice and mechanically disrupted into a single cell suspension. Following passage through a 40 μm nylon mesh, splenocytes were pelleted and resuspended in MACS buffer (sterile pH 7.2 phosphate buffered saline containing 0.5% bovine serum albumin (BSA) and 2 mM ethylenediaminetetraacetic acid). A cocktail of biotinylated antibodies specific for T cells, natural killer cells, neutrophils, dendritic cells, and macrophages were incubated with the splenocytes, then cells were washed to remove excess antibody. Following resuspension, splenocytes were incubated with anti-biotin antibodies conjugated to magnetic beads, then washed to remove excess antibody. Splenocytes were resuspended in MACS buffer and passed through a single magnetic column followed by three washes to isolate B cells. During column purification non-B cells are retained in the magnetic column while B cells pass into a collection tube. Purity of isolated B cells was verified by FACS analysis of CD19 expression, and were routinely found to be 95-98% CD19$^+$.

Cell Culture

SKW 6.4 cells purchased from ATCC were maintained according to ATCC recommendations in Roswell Park Memorial Institute-1640 media containing 10% bovine calf serum, 4.5 g/L glucose, 2 g/L sodium bicarbonate, 1.5 mM HEPES, 1 mM sodium pyruvate, non-essential amino acids, and 50 µM 2-mercaptoethanol (Complete RPMI-SKW). Cells were passed every two to three days and maintained at a density between $1x10^5$ and $2x10^6$ cells/mL.

CH12.LX cells, obtained from Dr. Gregory Haughton (University of North Carolina, Chapel Hill, NC), were maintained in Roswell Park Memorial Institute-1640 media containing 10% bovine calf serum, 2.5 g/L glucose, 3 g/L sodium bicarbonate, 1 mM HEPES, 1 mM sodium pyruvate, non-essential amino acids, and 50 µM 2-mercaptoethanol (Complete RPMI-CH12). Cells were passed every 2-3 days and maintained at a density between $1x10^4$ and $1x10^6$ cells/mL.

HEK 293T (293T) cells were purchased from Open Biosystems and maintained in Dulbecco's Modified Eagle Medium supplemented with 10% bovine calf serum, 4.5 g/L glucose, 3 g/L sodium bicarbonate, 1 mM sodium pyruvate, and non-essential amino acids (Complete DMEM). Cells were passed every 2-3 days upon reaching 90% confluence.

Primary B cells were cultured in RPMI-CH12 at an initial density of $3x10^6$ cells/mL.

Flow Cytometry Analysis

For *in vivo* studies splenocyte samples were depleted of erythrocytes by ammonium chloride lysis. Suppliers and fluorescent labels on antibodies used can be found in Appendix A. FcγIII/II (CD16/CD32) receptors were blocked to prevent non-specific labeling with Fc Block followed by incubation with phycoerythrin-labeled anti-CD19 antibodies to identify B cells. For cell surface marker staining antibodies specific for MHC Class II and CD138 were added following CD19 antibody addition. Cells were washed two times to remove excess antibody, then fixed with Cytofix (BD Biosciences). For detection of intracellular proteins splenocytes were fixed following CD19 staining, then permeabilized with Perm/Wash (BD Biosciences). Excess antibody was removed with two washes before cells were resuspended in FACS staining buffer (1x Hank's Balanced Salt Solution with 1% BSA and 0.09% sodium azide). For indirect staining of Blimp-1 and IgJ cells were incubated with the appropriate species-specific secondary antibody, then washed two time to remove excess antibody prior to analysis. 20,000 CD19$^+$ events were collected on a BD FACSCalibur (BD Biosciences) using CellQuest Pro for acquisition. Data were analyzed using FlowJo 7.2 (Treestar Software, Ashland, OR).

For *in vitro* studies of activation marker and transcription factor expression purified B cells were seeded at a density of $3x10^6$ cells/mL in 1 mL per well on 24 well plates. Cells were treated with 0, 0.03, 0.3, 3, or 30 nM TCDD in DMSO vehicle, then activated with 30 μg/mL *Salmonella typhosa* LPS. At 1, 8, or 24 h post-treatment $5x10^5$

cells were transferred to individual wells of a 96 well U-bottom plate for staining. Antibodies used are listed in Appendix A. To identify viable populations LIVE/DEAD Near-IR dye (Invitrogen, Carlsbad, CA) was prepared according to manufacturer's instructions and cells incubated in 250 μL labeling buffer (Hank's Balanced Salt Solution containing diluted LIVE/DEAD Near-IR dye) for 30 minutes, then excess dye removed with a single wash of FACS buffer. FcγIII/II receptors were blocked with Fc Block. For activation marker determinations a cocktail of antibodies for detection of MHC Class II, CD69, CD80, and CD86 were added to individual wells following blocking. Cells were incubated at 4° C for 30 minutes to stain, washed twice to remove excess antibody, and fixed with Cytofix. 20,000 events were collected per sample on a BD FACS Canto II using FACS Diva software (BD Biosciences), then analyzed using FlowJo 7.2. Cells were gated to exclude doublets from analysis by plotting forward scatter pulse height compared to forward scatter pulse area.

For transcription factor expression measurements B cells fixation was performed following Fc Block incubation and washing. Samples were resuspended in 90% serum/10% DMSO and stored at -80° C until the day of analysis. For staining and analysis B cells were thawed at room temperature and washed twice with FACS buffer containing 0.5% saponin (Calbiochem, San Diego, CA), then incubated for 30 minutes at 4° C to allow for through permeabilization. Until the final resuspension in FACS buffer prior to analysis all buffers and washes contained 0.5% saponin to maintain permeabilization. Following permeabilization B cells were pelleted by centrifugation, resuspended in staining buffer containing antibodies specific for phosphorylated c-Jun, Blimp-1, and BCL-6 and incubated at room temperature for 30 minutes in the dark.

Excess antibody was removed by washing twice, then cells were resuspended in staining

buffer containing anti-rabbit IgG F(ab')$_2$ secondary antibody for detection of BCL-6 and

incubated for 30 minutes at room temperature in the dark. Following the second staining

excess antibody was removed with two washes, then cells were resuspended in staining

buffer containing antibody specific for c-jun. Cells were incubated for 30 minutes at

room temperature in the dark, then excess antibody was removed by washing twice.

20,000 events were collected per sample on a BD FACS Canto II using FACS Diva

software, then analyzed using FlowJo 7.2. Cells were gated to exclude doublets from

analysis by plotting forward scatter pulse height compared to forward scatter pulse area.

Studies measuring kinase phosphorylation utilized either CH12.LX or purified B

cells. CH12.LX cells were grown in log phase until reaching a density of 6x10^5 cells/mL,

then 1 mL of cells were transferred to 12x75 mm FACS tubes and placed in a 37° C water

bath to equilibrate for 2 to 3 hours. Primary B cells were diluted to a density of 1x10^6

cells/mL, then 1 mL of cells were transferred to 12x75 mm FACS tubes and placed in a

37° C water bath to equilibrate for 2 to 3 hours. 100x concentrated treatments were

prepared immediately prior to treatment addition. TCDD concentrations used were 0,

0.003, 0.03, or 0.3 nM TCDD in DMSO vehicle coupled with 30 μg/mL LPS, 12 μg/mL

CpG, or 200 ng/mL R848 for activation. Following treatment addition to individual

tubes, cells were vortexed briefly and returned to the water bath for the remainder of the

time course. At 15, 30, and 60 minutes (min) post-treatment cells were fixed by direct

addition of 32% electron microscopy grade paraformaldehyde (Electron Microscopy

Sciences, Hatfield, PA) for a final concentration of 10% paraformaldehyde, briefly

36

vortexed, then returned to the water bath for 30 minutes. At the completion of fixation

cells were pelleted by centrifugation, resuspended in 500 µL of cold ≥99.9% methanol,

and stored at 4° C until all time points were completed, then transferred to -80° C for

storage. On the day of analysis cells were pelleted, washed twice with staining buffer,

and $3.5x10^5$ cells were transferred to U bottom 96 well plates for staining. Following

centrifugation to pellet cells samples were resuspended in staining buffers containing

antibodies specific for phosphorylated ERK1/2 (Threonine 202/Tyrosine 204), JNK1/2

(Threonine 183/Tyrosine 185), or AKT (Serine 473). Samples were incubated for 30

minutes at room temperature in the dark, then pelleted and washed once to remove excess

antibody. 20,000 events were collected per sample on a BD FACS Canto II using FACS

Diva software for acquisition, then analyzed using FlowJo 7.2. For analysis cells were

gated to exclude doublets from analysis by plotting forward scatter pulse height

compared to forward scatter pulse area. To calculate % change the following formula was

used: ((Geometric Mean Fluorescence of stimulated samples - Geometric Mean

Fluorescence of untreated samples)/(Geometric Mean Fluorescence of untreated samples)

* 100 = % change

For detection of *Homo sapiens* AHR (HsAHR) by FACS CD16/CD32 receptors

were first blocked with Fc Block, washed twice to remove excess antibody, and fixed

with Cytofix for 15 min at 4° C. Cells were permeabilized using Perm/Wash, then

incubated with APC-conjugated rabbit anti-Human AHR or APC-conjugated rabbit IgG

isotype control for 30 min at 4° C prior to washing twice with Perm/Wash to remove

excess antibody. Cells were analyzed for AHR immunofluoresence using a BD

FACSCalibur with CellQuest Pro for acquisition and FlowJo 7.2 for analysis.

Gene Expression Analysis

RNA was isolated from splenocytes using Trizol (Sigma-Aldrich, Saint Louis, MO) according to manufacturer's protocol. RNA pellets obtained following isopropanol precipitation and ethanol wash were resuspended in Promega SV RNA Lysis Solution and then processed according to the manufacturer's protocol to further purify RNA (Promega, Madison, WI). cDNA was generated using Applied Biosystems High Capacity Archive kit according to manufacturer's instructions. TaqMan primer/probe sets were used for all gene expression analysis can be found in Appendix B, and quantified by $\Delta\Delta$Ct method using 18S for normalization (Livak and Schmittgen 2001). Real-time PCR was performed using ABI 7900HT or Prism 7000 real-time PCR machines.

IgM ASC Response

Detailed methods used for enumeration of ASC can be found in (Holsapple *et al.* 1984). TNP-haptenated sRBC were prepared as described in (Rittenberg and Pratt 1969). In brief, single cell suspensions of splenocytes were combined with a solution of warm 0.5% agar and TNP-haptenated sheep erythrocytes. Guinea pig complement (Cedar Lane Labs, Burlington, NC) was added, samples vortexed briefly, and aliqouted to a Petri dish. Samples were overlaid with a glass coverslip and incubated at 37°C in 95% air/5% carbon dioxide overnight. Hemolytic plaques were counted under magnification and normalized to cell number, as determined using Z1 series Coulter Counter (Beckman Coulter, Fullerton, CA), to calculate IgM ASC per 10^6 cells.

Mouse and Human IgM Sandwich ELISA

2×10^4 CH12.LX cells/mL were plated and incubated overnight prior to treatment

for mouse IgM ELISA. Following 48 h incubation cells were pelleted by centrifugation

and supernatants collected for assessment of secreted IgM. For quantification of mouse

IgM secretion Immulon 4 HBX strips (Thermo Electron Corporation, Milford, MA) were

coated overnight at 4° C with anti-mouse IgM capture antibody (Sigma-Aldrich). Plates

were then washed three times with PBS containing 0.5% Tween-20 (Sigma-Aldrich)

followed by four washes with distilled water. Wells were blocked with 250 µL PBS

containing 3% BSA for 1.5 h at room temperature. Following blocking, plates were either

washed as described above and used immediately or frozen at -20° C for future use. 100

µL of sample or purified mouse IgM standard (Sigma-Aldrich) was added to individual

wells and incubated at 37° C for 1.5 h, then washed as described above. 100 µL

horseradish peroxidase conjugated anti-mouse IgM was added to each well and incubated

for 1.5 h at 37° C for antigen detection. Plates were washed as described above and

developed using a kinetic reaction with 2,2'-azinobis(3-ethylbenz thiazoline-sulfonic

acid) (Roche, Indianapolis, IN) for detection on a Synergy HT plate reader (Bio-Tek,

Winooski, VT).

1×10^5 SKW 6.4 cells/mL were plated and incubated overnight prior to treatment

additions for human IgM ELISA. Following 96 h incubation cells were pelleted by

centrifugation and supernatants collected for assessment of secreted IgM. For

quantification of human IgM secretion Immulon 4 HBX high strips were coated

overnight at 4° C with 100 μL anti-human IgM x capture antibody (Sigma-Aldrich).

Plates were then washed three times with PBS containing 0.5% Tween-20 followed by 4

washes with distilled water. Wells were blocked with 250 μL PBS containing 3% BSA

for 1.5 h at room temperature. Following blocking, plates were washed and 100 μL of

sample or purified human IgM standard (Sigma-Aldrich) was added to individual wells

and incubated at 37° C for 1.5 h, then plates washed as described above. 100 μL

horseradish peroxidase conjugated anti-human IgM was added to each well and incubated

for 1.5 h at 37° C for antigen detection. Plates were washed as described above and

developed using a kinetic reaction with 2,2'-azinobis(3-ethylbenz thiazoline-sulfonic

acid) reagent for detection on a Synergy HT plate reader.

Immunoblot Analysis of HsAHR

For detection of HsAHR protein cells were lysed in radioimmunoprecipitation

buffer (phosphate buffer saline containing 1% NP-40, 0.5% sodium deoxycholate, and

0.1% sodium dodecyl sulfate) supplemented with Complete MINI protease inhibitor

(Roche, Indianapolis, IN). Following lysis, samples were centrifuged at 12,000 g for 15

minutes at 4° C to pellet insoluble material and supernatants assessed for total protein

concentration by bicinchoninic acid assay (Sigma-Aldrich).

Samples were heat-denatured and separated by sodium dodecyl sulfate-

polyacrylamide gel electrophoresis. Proteins were transferred overnight to nitrocellulose

membranes, followed blocking with a Tris-buffered saline solution containing 4% non-fat

dry milk and 1% BSA. Membranes were incubated for 2 h with antibody specific for

human AHR (H-211, Santa Cruz Biotech), washed, then incubated with an HRP-

conjugated goat anti-rabbit IgG antibody for 1 h. Supersignal Femto West (Pierce

Biotechnology) was used for chemiluminescent visualization of immunoreactive bands in conjunction with Kodak X-OMAT film.

Plasmid DNA isolation

Plasmid DNA was isolated according to manufacturer's instructions using Qiagen Miniprep or Maxiprep columns.

Plasmid Vector Construction

All DNA restriction enzymes utilized were purchased from New England Biolabs (Ipswich, MA).

The HsAHR insert for pcDNA3.1-TOPO (Invitrogen) was generated by PCR amplification of pSport-hAHR2, obtained from Dr. John J. LaPres, using Invitrogen *Platinum Taq* DNA polymerase with the forward primer NK634 (5'-CACCATGAACAGCAGCAGCGCC-3') and reverse primer NK636 (5'-TCAAAATTGGGCTTGGAATTAC-3'). PCR conditions were 2 min at 95° C to denature the template, 30 cycles of 30 seconds (s) at 94° C, 30 s at 58° C to anneal, and 3 min at 68° C to extend the product, with a final extension of 68° C for 30 min. PCR product was verified to be a single product of ~2.5 kb by visualization on an ethidium bromide containing agarose gel. PCR product was added directly to the TOPO cloning reaction and incubated according to manufacturer's instructions. TOPO cloning reactions were transformed into MAX Efficiency DH5α cells. Plasmids were verified by sequencing.

The HsAHR insert for pIRESneo3-HsAHR was generated by PCR from pSport-hAHR2 using the primers NK657 (5'-GCGCGCGGCCGCTTACAGGAATCCACTGGATGT-3') and NK658 (5'-

GCGCCGTACGCACCATGAACAGCAGCAGCGCCAAC-3') with Phusion High

Fidelity DNA polymerase (Finnzymes USA, Woburn, MA). Conditions used were an

initial denaturation phase of 98° C for 1 m, followed by 30 cycles of 98° C for 7 s and 72°

C for 50 s, with a final extension of 72° C for 2 min. PCR product was sequentially

digested with NotI followed by BsiWI, then gel purified. A PCR product of ~2.5 kb was

excised from the agarose gel, purified with Qiagen QIAQuick gel extraction columns,

ligated into pIRESneo3 using NEB T4 DNA ligase, and transformed into MAX

Efficiency DH5α cells. Plasmids were verified by restriction digestion and partial

sequencing.

To generate the C-terminal GFP fused form of HsAHR the plasmid phCMV-

CGFP was purchased from Genlantis (San Diego, CA). HsAHR suitable for insertion into

phCMV-CGFP was generated by PCR, introducing a 5' BglII site and 3'-HindIII site

using the primer NK675 (5'-GCCGCCGAGATCTGGGCACCATGAACAGCAGCA-3')

in combination with either NK676 (5'-TGGGCTTGGAAGCTTAGGAATCCACTG-3')

to maintain the native stop codon or NK677 (5'-

TCAAAATTAAGCTTGGAATTACAGGAATC-3') to mutate the final amino acid of

native HsAHR from valine to lysine and the stop codon to leucine, resulting in an in-

frame fusion of HsAHR to GFP. For all PCR reactions Phusion High Fidelity DNA

polymerase was used. PCR product was generated by first denaturing pSport-hAhR2 at

98° C for 30 s, followed by 30 cycles of 98° C for 10 s, 68° C for 10 s, and 72° C for 35 s,

with a final extension at 72° C for 2 min. The plasmid was digested with BglII and

HindIII, dephosphorylated using NEB Antarctic Phosphatase (New England Biolabs)

according to manufacturer's instructions, and gel purified to remove residual uncut
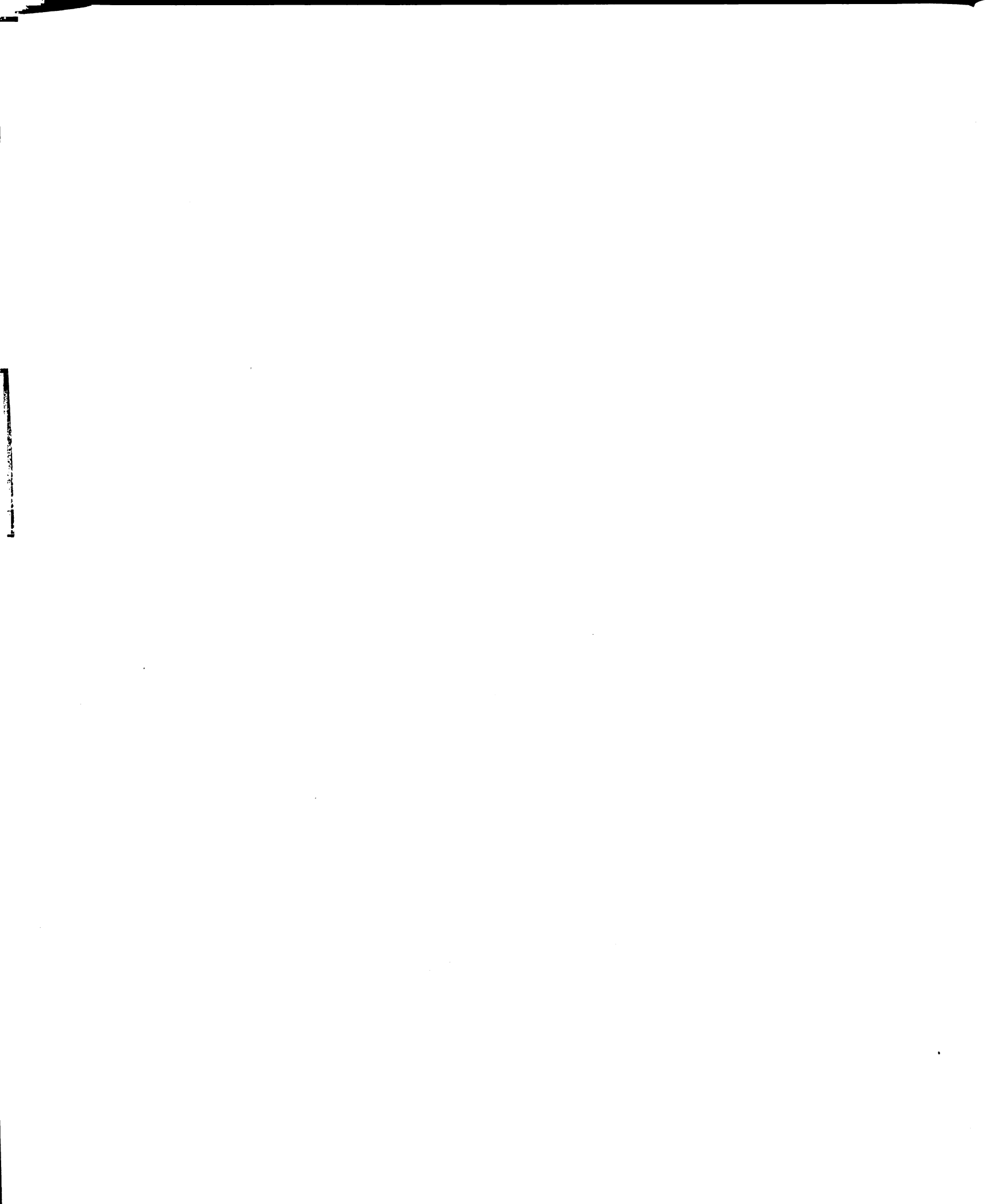
plasmid. HsAHR PCR product was also gel purified, then ligated into phCMV-CGFP

using a NEB Quick Ligation kit according to manufacturer's instructions. Ligation

reactions were transformed into ultracompetent XL-2 Blue cells (Stratagene, La Jolla,

CA). Colonies were screened by restriction digest, then verified by sequencing to contain

the desired HsAHR sequence.

For pZeoSV2-HsAHR-GFP the HsAHR-GFP ORF was liberated from phCMV-

HsAHR-GFP by digestion with BglII and NotI, followed by gel purification. pZeoSV2(+)

was prepared by digesting plasmid DNA with BglII and NotI, then dephosphorylating the

plasmid DNA with NEB Antarctic Phosphatase, and gel purified. HsAHR-GFP was

ligated into pZeoSV2(+) by using NEB T4 DNA ligase. The ligation reaction was

transformed into XL-2 Blue ultracompetent cells and verified by restriction digestion

followed by partial sequencing.

pLEX-HsAHR and pLEX-HsAHR-GFP were generated by digesting phCMV-

HsAHR and phCMV-HsAHR-GFP with BglII and NotI overnight, then gel purifying the

liberated DNA fragment containing AHR and AHR-GFP ORFs. To prepare pLEX-MCS

for insertion of HsAHR and HsAHR-GFP plasmid DNA was digested with BamHI and

NotI overnight, dephosphorylated, and gel purified to remove residual uncut plasmid.

DNA fragments were recovered from a 0.8% low melting temperature agarose gel using

Promega Wizard SV Gel Clean-up columns (Madison, WI) according to manufacturer's

instructions. HsAHR and HsAHR-GFP were ligated into pLEX-MCS using NEB Quick

Ligation kit, then transformed into Invitrogen Stbl2 competent *E. coli* (Carlsbad, CA)

according to manufacturer's instructions. Following overnight incubation at 30° C

individual colonies were screened by PCR using primers NK672 (5'-
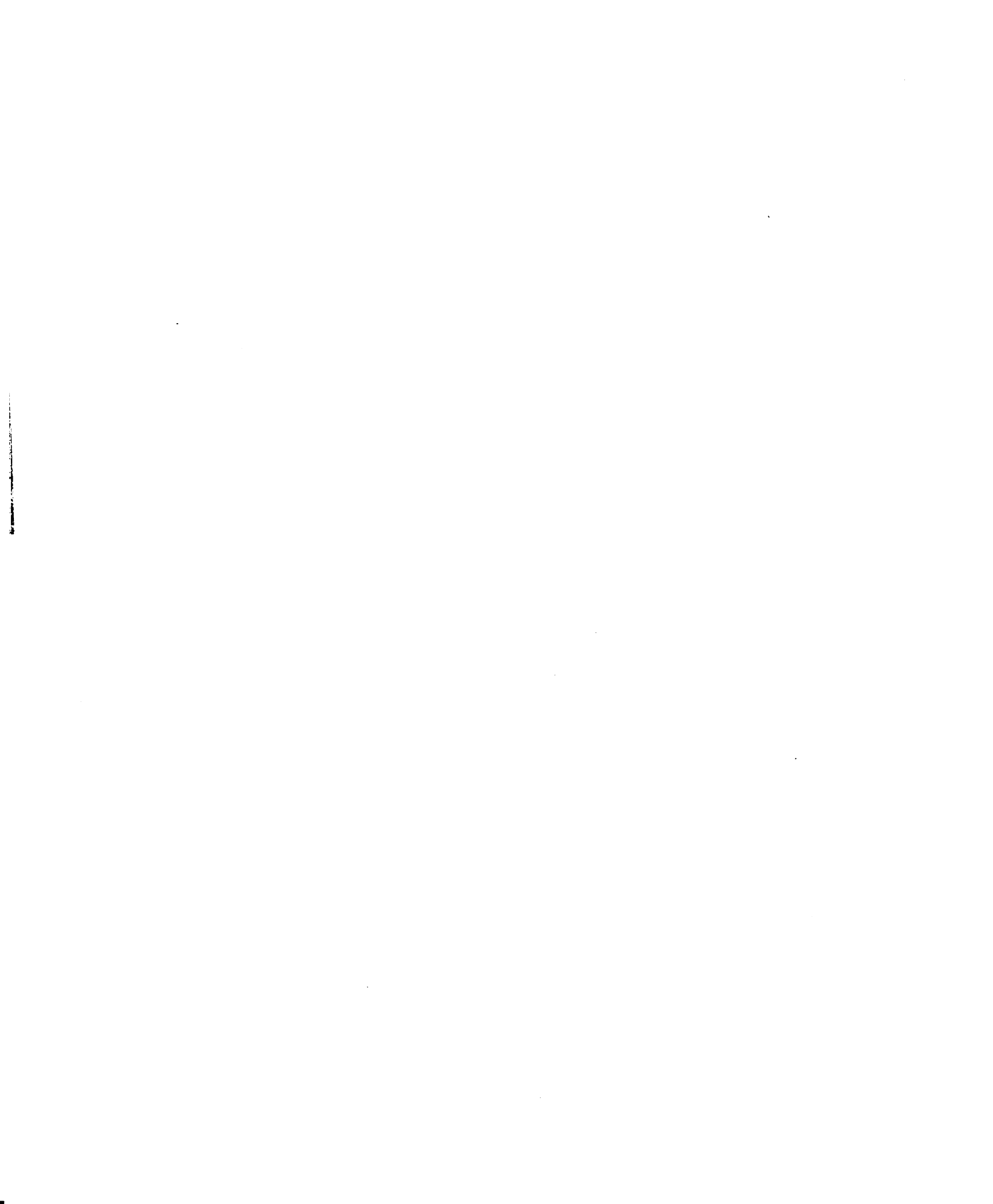
TTTCAGCGTCAGCTACACTG-3') and NK673 (5'-

TGACTGATCCCATGTAAGTCTGTAA-3') with an initial denaturation phase of 95° C

for 2 minutes followed by 25 cycles of 95° C for 30 s, 62° C for 30 s, and 72° C for 92

seconds, and a final extension phase of 72° C for 5 min. Positive colonies with PCR

product size of approximately 1.5 kb, indicative of AHR presence, were grown, plasmid

DNA purified, and verified by restriction digestion.

Transfection and Selection of Stably Transfected Cells

For pcDNA3.1-TOPO-HsAHR, pZeoSV2-HsAHR, pZeoSV2-HsAHR-GFP,

phCMV-HsAHR, and phCMV-HsAHR-GFP plasmids SKW 6.4 cells were grown in log

phase for 3 days prior to electroporation, starting at a density of 5×10^4 cells/mL. On the

day of electroporation cells were pelleted by centrifugation at $90g$ for 10 minutes and

resuspended in fresh Complete RPMI-SKW. Cells were counted by trypan blue

exclusion, then 2×10^6 cells were transferred to individual microcentrifuge tubes for

electroporation. Cells were pelleted again by spinning at $90g$ for 10 minutes, then

resuspended in premixed room temperature electroporation buffer consisting of 90 μL

Solution V with 20 μL Supplement 1 (Lonza Walkersville Inc., Walkersville, MD). 100

μL of cells were transferred to an electroporation cuvette and electroporated using an

amaxa Nucleofector set to program X-001. Following electroporation room temperature

Complete RPMI-SKW was added to each cuvette and cells transferred to individual 25

cm^2 culture flasks, which were placed in a vertical orientation in the incubator. After 24

h, recovery flasks were placed in a horizontal position and incubated an additional 24 h.

48 h post-electroporation 1.2 mg/mL G418 (pcDNA3.1-TOPO and phCMV-CGFP

derived vectors) or 50 μg/mL Zeocin (pZeoSV2 plasmids) was added to culture. Cells

monitored for outgrowth of antibiotic resistant populations by microscopy. For G418

resistance approximately 4-5 weeks were required to achieve a large antibiotic resistant

population.

Luciferase Assays

Luciferase activity was measured according to manufacturer's instructions using a

Promega Luciferase Assay System (Madison, WI) on a Synergy HT plate reader.

Lentivirus Preparation

293T cells were plated at a density of 6.5×10^6 cells per 10 cm^2 culture plate and

incubated 8 hours to allow for full attachment. 100 μg plasmid DNA was prepared for

transfection using calcium phosphate by diluting all plasmids into 0.25 M calcium

chloride solution. Diluted DNA was added as single drops to an equal volume of 2x

HEPES Buffered Saline while vortexing at high speed. Once all DNA had been added

precipitates were allowed for form for 5 minutes prior to dropwise addition of complexed

DNA to 293T cells. Following overnight incubation transfection media exchanged for

fresh Complete DMEM, then cells returned to the incubator for an additional 36 h.

Lentivirus containing culture media was collected and centrifuged at 3000 rpm for 30

minutes at 4° C to pellet cell debris, then supernatants were aliqouted and stored at -80° C

until use.

Direct Assessment of Lentiviral RNA

To isolate lentiviral RNA 400 μL of lentivirus containing culture supernatants

were combined with 1400 μL Trizol, mixed by vortexing, then incubated for 5 minutes.

200 µL 1-bromo-3-chloropropane were added to the sample, then thoroughly vortexed

and incubated at room temperature for 5 minutes. Samples were centrifuged at 12,000 g

for 10 minutes at 4° C, then the top phase aqueous solution was transferred to a new

sample tube. RNA was precipitated by adding 600 µL 100% isopropanol to each sample

tube, vortexing, then incubating for 1 h at -20° C. Following centrifugation to pellet RNA

a single wash with 70% ethanol was performed, samples were centrifuged again to pellet

RNA, dried, and RNA pellets resuspended in 20 µL of nuclease-free water. RNA was

quantified by NanoDrop, then reverse transcribed using a Superscript VILO cDNA

Synthesis kit (Invitrogen) according to manufacturer's instructions.

cDNA generated was analyzed by QRT-PCR using custom synthesized TaqMan

primers specific for HsAHR, GFP, and PuroR. For all PCR reactions a non-reverse

transcribed control reaction was also performed.

Lentiviral Transduction and Selection of Transduced Cells

Frozen lentiviral stocks were thawed at room temperature and supplemented with

8 µg/mL polybrene (SEQUABRENE, Sigma-Aldrich). Following 5 minutes incubation to

allow polybrene to coat viral particles, SKW 6.4 cells were resuspended in virus

containing media. $2x10^6$ SKW 6.4 cells in 250 µL were then added to each well of a 24

well tissue culture plate to achieve a monolayer of cells during spin infection. Cells were

centrifuged at 800g for 2 h, then washed twice with cell media prior to diluting cells to a

density of $1x10^5$ cells/mL. Following 96 h incubation puromycin was added to culture at

a final concentration of 1 µg/mL. Media was changed every 2-3 days until a puromycin

resistant populations arose and could be frozen for storage, cloned by limiting dilution, and analyzed for AHR gene and protein expression.

Transduction of 293T cells was accomplished by overlaying a 50% confluent culture with lentivirus containing media supplemented with 4 µg/mL polybrene for 4 h, then aspirating media and reculturing in Complete DMEM for an additional 48 h. Media was exchanged for fresh Complete DMEM containing 3 µg/mL puromycin and cells monitored for generation of antibiotic resistant colonies. Within 4 days puromycin resistant colonies could be observed. Polyclonal populations of 293T-HAG, expressing HsAHR fused to GFP, and 293T-HAHR, expressing the non-fused form of HsAHR, were used to validate the production of a full length HsAHR-GFP protein using immunoblot and a FACS-based method for detection of AHR.

Preparation of Conditioned Complete RPMI-SKW

SKW 6.4 cells were cultured at a density of 1×10^5 cells/mL, then following 48 h incubation cells were pelleted by centrifugation at 3000 rpm for 30 minutes. Supernatant was collected and centrifuged again prior to storage at 4° C for up to two weeks prior to use.

Cloning by Limiting Dilution

Stably transduced SKW 6.4 cells were diluted to a density of 3.333 cells/mL in conditioned RPMI-SKW and 100 µL of media, approximately 1/3 of a cell, was added to each well of a round bottom 96 well plate. An average of approximately 10 individual clones were obtained from each plate using this method.

Statistical Analysis

Results were analyzed by One-way ANOVA using Dunnet's post-hoc analysis compared to LPS + vehicle treatment for *in vivo* studies. Neuman-Keuls post-hoc analysis was used for determination of statistically significant differences for multiple comparisons between treatment groups of the *in vivo* studies. All analysis was performed using Graphpad Prism 4.05 (Graphpad Software, San Diego, CA). P-values less than or equal to 0.05 were considered significant.

For multivariate analysis of FACS data the Probability Binning approach was used. Probability Binning divides a control sample into discrete bins, 600 for all analyses performed in these studies, containing equal numbers of events. Bins derived from control samples, TLR ligand + vehicle treatment in these studies, are applied to experimental samples to compute a normalized chi-squared value. Based on the distribution of events in control and experimental samples the $T(\chi)$ value, analogous to a t-score, is derived. The $T(\chi)$ value allows ranking of experimental samples based on the relative distance of an experimental sample from the control sample (Roederer *et al.* 2001a; Roederer *et al.* 2001b). A $T(\chi)$ value of 0 indicates two populations are indistinguishable from each other. $T(\chi)$ values greater than 6 were considered significantly different. Flowjo 8.8.6 was used for all Probability Binning.

CHAPTER 3: EXPERIMENTAL RESULTS AND DISCUSSION FOR MURINE MODELS

Simultaneous *In vivo* Time Course and Dose Response Evaluation for TCDD-Induced Impairment of the LPS-stimulated Primary IgM Response

Suppression of the *in vivo* LPS-activated primary IgM response by TCDD

Different methods of B cell activation result in distinctly different cell signaling programs and cumulative responses (Donahue and Fruman 2007). To maximize the value of *in vivo* and *in vitro* comparisons it was deemed important to utilize similar modes of B cell activation as in previous studies. Many laboratories have reported TCDD suppression of the T cell-dependent anti-sRBC IgM antibody response (Dooley and Holsapple 1988; Holsapple *et al.* 1986; Luster *et al.* 1988; Smialowicz *et al.* 1994; Tucker *et al.* 1986; Vecchi *et al.* 1980a; Vorderstrasse *et al.* 2001), but no published studies have evaluated TCDD-mediated suppression of the *in vivo* primary IgM response in the context of the commonly used polyclonal B cell activating stimulus LPS. Moreover, no published study to date has correlated alteration in the expression of regulatory transcription factors with *in vivo* TCDD suppression of the IgM response to any stimulus. The rationale for using LPS in this study is that a strong polyclonal B cell activator may differentiate a proportionally larger fraction of B cells *in vivo* than antigens such as sRBC, resulting in a potentially greater sensitivity at early time points for detection of TCDD effects. To examine the *in vivo* effects of TCDD on the LPS-activated primary IgM response a dose of 30 µg/kg TCDD was selected, which is established to

cause near-maximal suppression of the sRBC-activated primary IgM response *in vivo* (Vecchi *et al.* 1980a), then selected half-log decreasing doses to profile the TCDD-mediated effects. LPS *in vivo* treatment induced a significant increase in the IgM ASC response, which was significantly suppressed by all concentrations of TCDD in a dose-dependent manner (Figure 3). This may be the first study to demonstrate that *in vivo* exposure to the polyclonal B cell activator, LPS, results in an increase in IgM ASC response, which is suppressed by TCDD.
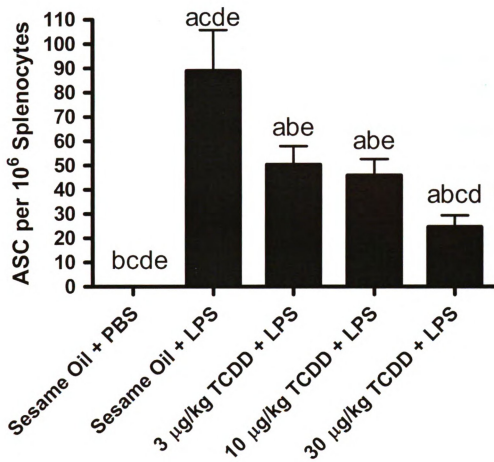
Figure 3. Suppression by TCDD of the LPS-activated IgM ASC response. Four days prior to LPS treatment mice were administered a single dose of TCDD (3, 10, or 30 µg/kg) and/or vehicle (sesame oil) by oral gavage. On day 0 mice received single intraperitoneal injections of either PBS or 25 µg LPS. IgM ASCs were enumerated on Day 3 following LPS. Results are depicted as mean ASC per 10^6 splenocytes ± SE of the mean. [a] P<0.05 compared to sesame oil + PBS, [b] P<0.05 compared to sesame oil + LPS, [c] P<0.05 compared to 3 µg/kg TCDD + LPS, [d] P<0.05 compared to 10 µg/kg TCDD + LPS, and [e] P<0.05 compared to 30 µg/kg TCDD + LPS.

LPS treatment induced a significant increase in spleen size, as reflected in the spleen weight/body weight ratio, which was significantly attenuated by TCDD treatment (Figure 4). Treatment with TCDD alone did not significantly alter spleen weight/body weight ratio, and no treatments caused significant changes in body weight. TCDD attenuation of LPS-induced increases in spleen weight/body weight ratio was associated with a commensurate decrease in total cellularity, suggesting a modest suppression in spleen cell proliferation.

Figure 4. Suppression by TCDD of LPS-induced spleen cell proliferation. Spleen weight, body weight, and total cell recovery per spleen were determined after mice were euthanized. (A) Ratio of spleen weight to total body weight. (B) Total splenocytes recovered per spleen following initial tissue processing into single cell suspensions. Results from 6 mice per group are depicted as mean ± SE of the mean. [a] P<0.05 compared to sesame oil + PBS and [b] P<0.05 compared to sesame oil + LPS.

A

Spleen Weight:Body Weight Ratio

- Sesame Oil + PBS
- Sesame Oil + LPS

Days Post-LPS

B

Cell Number (x10⁶)

-▲- 3 μg/kg TCDD + LPS
-★- 10 μg/kg TCDD + LPS
-◆- 30 μg/kg TCDD + LPS

Days Post-LPS
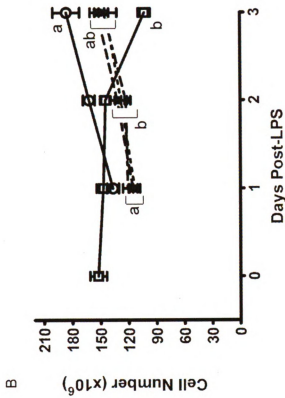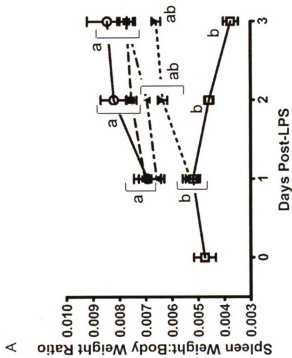
perfo

assoc

stud

intra

cell

II w

inc

Da

AS

aff

3(

C

a

An extensive phenotyping of splenic B cells from all treatment groups was performed, in which individual mice were evaluated for gene and protein expression associated with plasmacytic differentiation to maximize the statistical strength of this study. Fluorescence-activated cell sorting (FACS) was used to profile cell surface and intracellular protein abundance. LPS-activated B cells up-regulate expression of several cell surface proteins in the normal course of an immune response, including MHC Class II to aid in antigen presentation. Surface MHC Class II expression on $CD19^+$ B cells increased significantly in response to LPS, peaking on Day 1 and modestly declined by Day 3. Cell surface expression of MHC Class II declined as B cells proceed toward the ASC phenotype, consistent with our observation of peak MHC Class II expression 1 day after LPS treatment, which then declined on Days 2 and 3 (Figure 5). Administration of 30 µg/kg TCDD significantly attenuated the LPS-induced MHC Class II on the surface of $CD19^+$ B cells at all time points evaluated, while lower doses of TCDD marginally attenuated LPS-induced cell surface MHC Class II up-regulation.

Figure 5. Suppression by TCDD of LPS-induced cell surface MHC Class II expression. Isolated splenocytes were incubated with FcBlock, labeled with antibodies specific for CD19 and MHC Class II, then fixed with Cytofix. Cells were subsequently analyzed by FACS. Populations were gated by first identifying (A) CD19$^+$ events, then (B) the individual median fluorescence (MFI) for MHC Class II. Results from 6 mice per group are depicted as mean MFI ± SE of the mean. ^{a} P<0.05 compared to sesame oil + PBS and ^{b} P<0.05 compared to sesame oil + LPS.

A

B
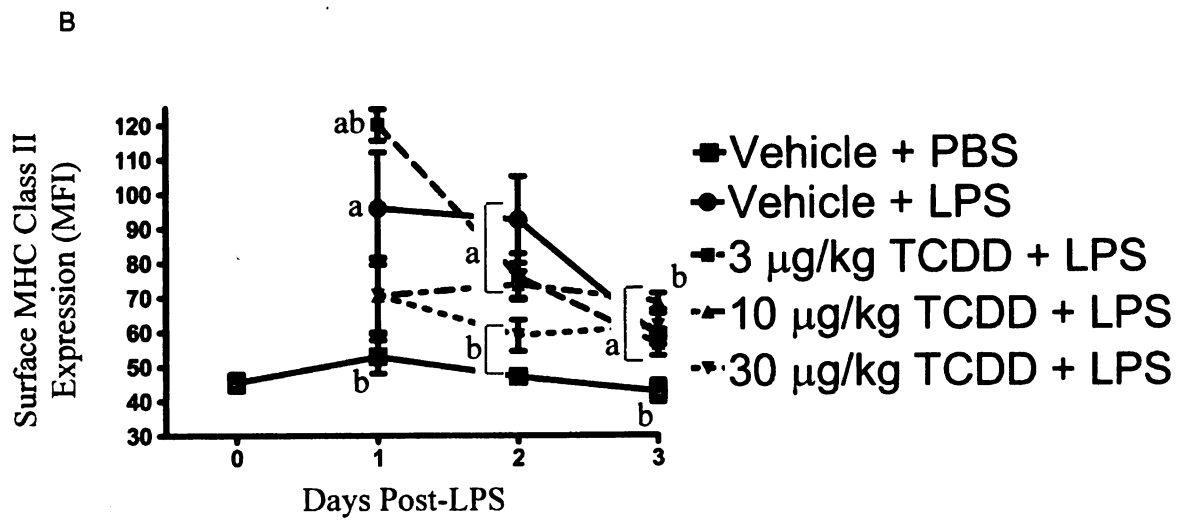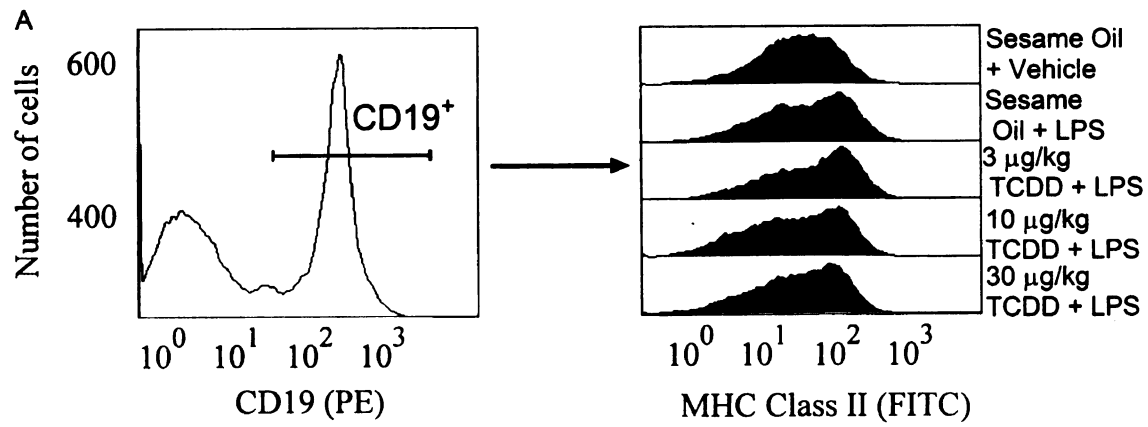
The IgM ASC response has been widely used to enumerate antibody secreting plasma cells. Our results show that intraperitoneal administration of LPS induced a significant increase in splenic ASCs, which was suppressed in a dose-dependent manner by TCDD treatment. Using the IgM ASC response as a phenotypic anchor, splenocytes were further characterized for CD138 expression, also termed syndecan-1, by flow cytometry as a complementary marker of plasma cells. Figure 6A shows LPS induced an increase in frequency of $CD19^+$ $CD138^+$ cells, which was attenuated by TCDD-treatment, an indication that suppression of the IgM ASC response was not simply due to suppression of antibody secretion, but also involved a blockade in LPS-activated B cell differentiation into ASCs. Extending the observation that appearance of $CD19^+$ $CD138^+$ cells was impaired by TCDD, LPS-induced generation of $CD19^+$ $Ig\kappa^{high}$ cells (Figure 6D) and $CD19^+$ IgJ^{high} cells (Figure 6E) in TCDD-treated mice was also impaired, suggesting that TCDD blocks B cell differentiation prior to the large increase in intracellular IgJ and Igκ associated with the plasma cell phenotype. Collectively, these results demonstrate TCDD-mediated suppression of the LPS-induced primary IgM response involves failure of individual cells to not only secrete IgM, but to express cell surface markers and intracellular proteins indicative of the ASC phenotype.

Figure 6. TCDD treatment impaired expression of phenotypic indicators for plasmacytic differentiation. To assess B cells for CD138 expression, isolated splenocytes were incubated with FcBlock, labeled with antibodies specific for CD19 and CD138, then fixed with Cytofix. For detection of total Igκ or IgJ, cells were blocked, labeled with CD19 antibodies, and fixed with Cytofix. At the completion of the time course, cells were permeabilized with BD Perm/Wash, incubated with antibodies specific for either IgJ or Igκ and analyzed by FACS. Populations were gated by first identifying CD19$^+$ events as depicted for (A) CD138 and (B)Igκ, and then gated on populations that expressed elevated levels of (C) CD138, (D) Igκ, or (E) IgJ. Results from 6 mice per group are depicted as mean frequency of CD19$^+$ cells ± SE of the mean for respective measurements. ^{a} *P<0.05 compared to sesame oil + PBS and* ^{b} *P<0.05 compared to sesame oil + LPS.*
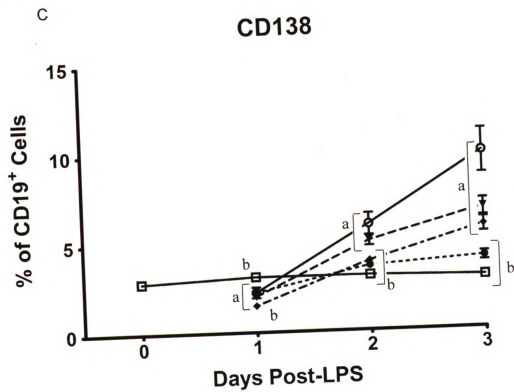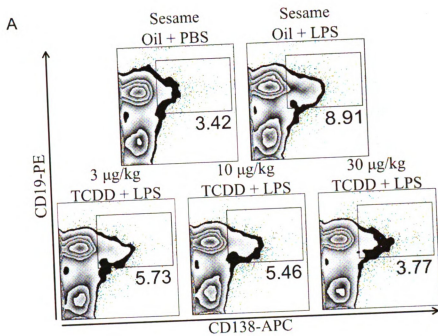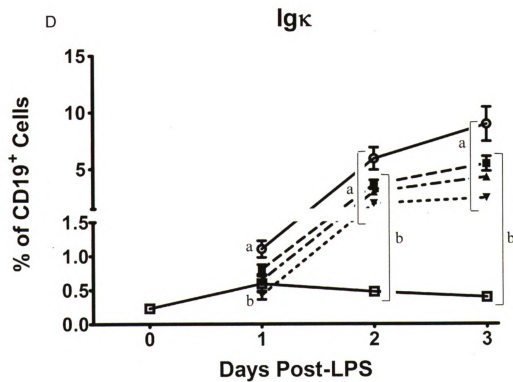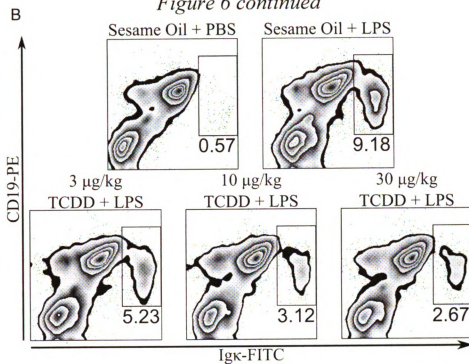
A

Sesame Oil + PBS — 3.42
Sesame Oil + LPS — 8.91
3 µg/kg TCDD + LPS — 5.73
10 µg/kg TCDD + LPS — 5.46
30 µg/kg TCDD + LPS — 3.77

CD19-PE

CD138-APC

C

CD138

% of CD19⁺ Cells

Days Post-LPS

Figure 6 continued

B

Sesame Oil + PBS

Sesame Oil + LPS

0.57

9.18

3 μg/kg
TCDD + LPS

10 μg/kg
TCDD + LPS

30 μg/kg
TCDD + LPS

5.23

3.12

2.67

CD19-PE

Igκ-FITC

D

Igκ

% of CD19⁺ Cells

Days Post-LPS

Figure 6 continued
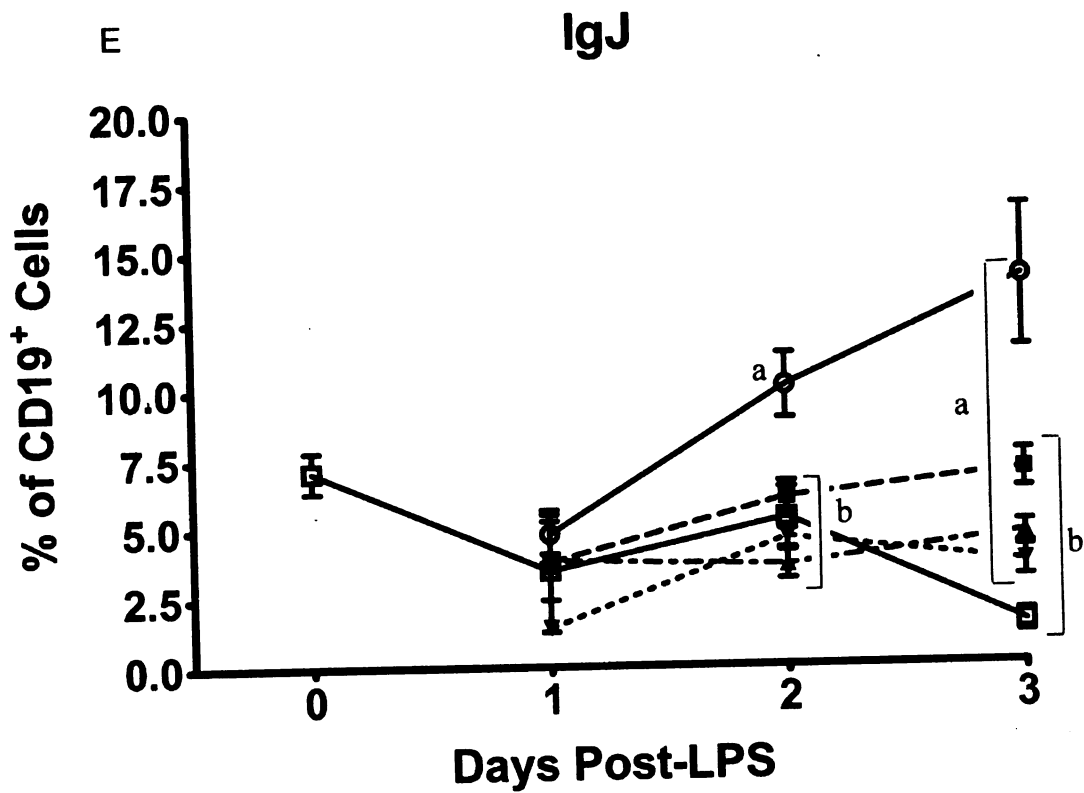
TCDD-mediated suppression of LPS-induced changes in gene and protein expression involved in B cell to ASC transition

Differentiation of a resting B cell into an ASC is regulated by a network of reciprocally acting transcription factors, conceptualized in Figure 1. Previous *in vitro* studies established that TCDD impaired expression of several latter components of the plasma cell phenotype, including expression of IgJ, Igκ, Igμ, Pax5, and Blimp-1 (Schneider *et al.* 2008; Schneider *et al.* 2009). High levels of IgJ, Igκ, Igμ, and XBP-1 are characteristic of antibody-secreting plasma cells, and splenocytes isolated from LPS-treated mice showed increasing levels of *IgJ*, *Igκ*, and *Igμ* mRNA peaking 2 to 3 days post-LPS treatment (Figure 7A, Figure 7C, and Figure 7D respectively), with the largest fold increase in the expression of *IgJ*. TCDD impaired LPS-induced increases of *IgJ*, *Igκ*, and *Igμ* mRNA levels with *IgJ* significantly impaired relative to LPS treatment at all time points evaluated. *Igκ* and *Igμ* have a relatively high level of constitutive expression in B cells because they form the B cell antigen receptor, whereas *IgJ* is required only for the production of secreted pentameric IgM and dimeric IgA. In this study *IgJ* is likely to be the best marker of Ig destined for secretion, and thus an indicator of antibody-secreting plasma cells. The expression profile for total and spliced *XBP-1* followed a similar pattern to *IgJ*, *Igκ*, and *Igμ*, peaking in response to LPS on Days 2 and 3. While not statistically significant, TCDD treatment did appear to impair induction of *XBP-1*, similar again to the patterns observed with *Igκ* and *Igμ* mRNA levels.

Figure 7. Gene expression profiles for LPS-induced plasmacytic differentiation in the absence and presence of TCDD treatment. Total RNA from splenocytes was isolated and cDNA synthesized for gene expression analysis. Target gene mRNA levels were normalized to 18S and the fold change was calculated by the $\Delta\Delta C_t$ method. (A) IgJ, (B) CD138, (C) Igκ, (D) Igμ, (E) total XBP-1, or (F) spliced XBP-1. Results from 6 mice per group are depicted as mean fold change ± SE of the mean. [a] P<0.05 compared to sesame oil + PBS and [b] P<0.05 compared to sesame oil + LPS.

A

IgJ

B

CD138

Figure 7 continued

Ig κ

C

Ig μ

D

Figure 7 continued

E

XBP-1(total)

F
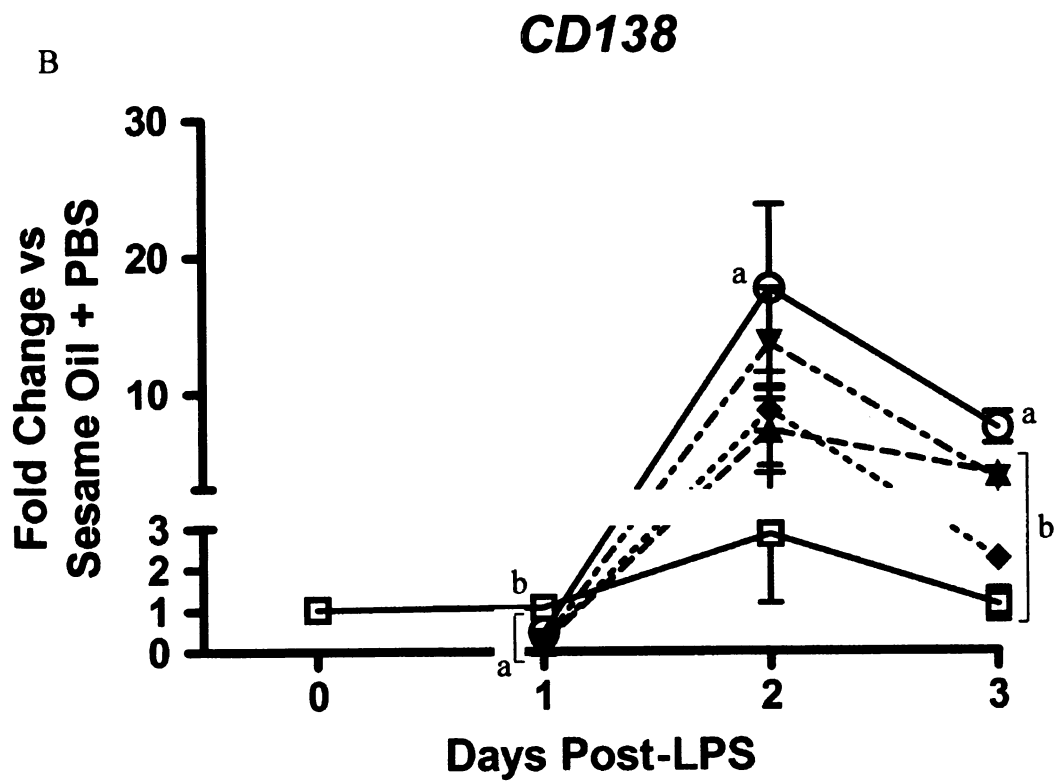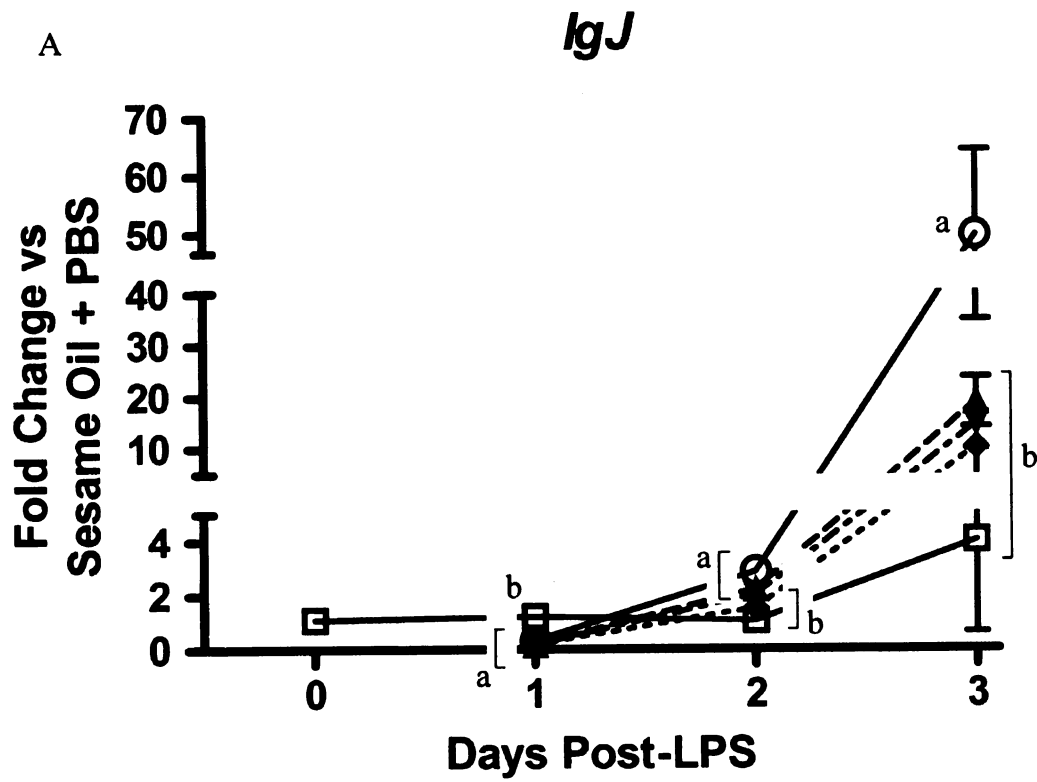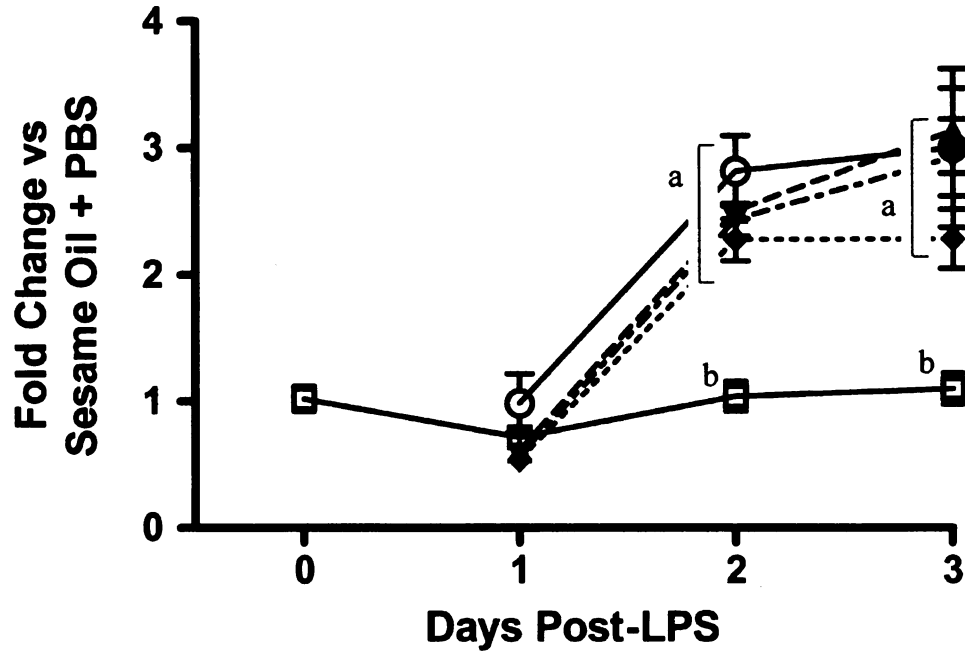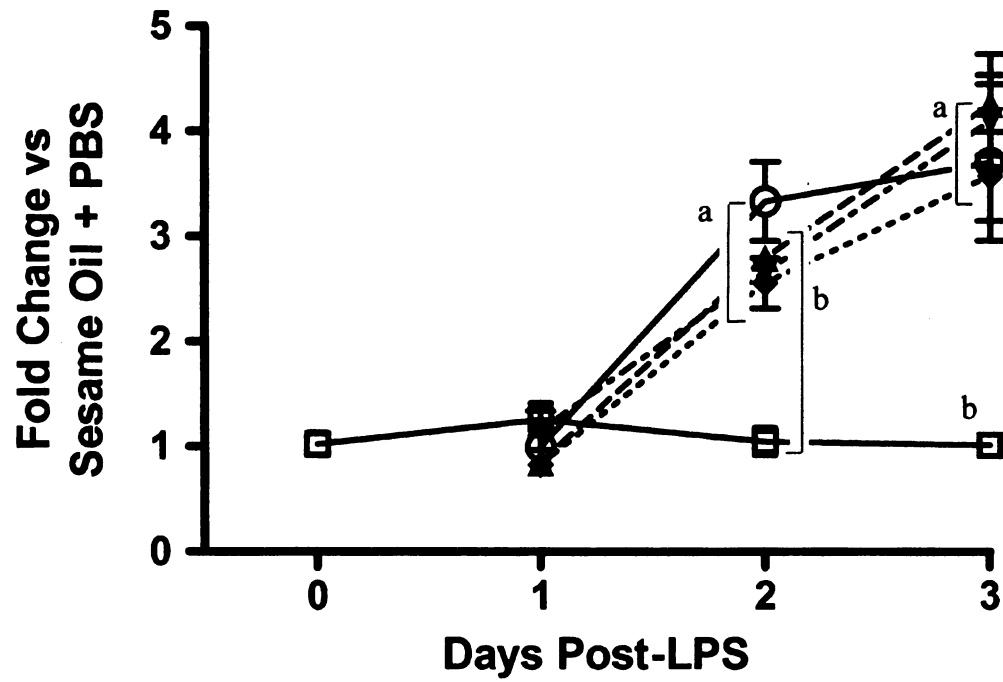
XBP-1(spliced)
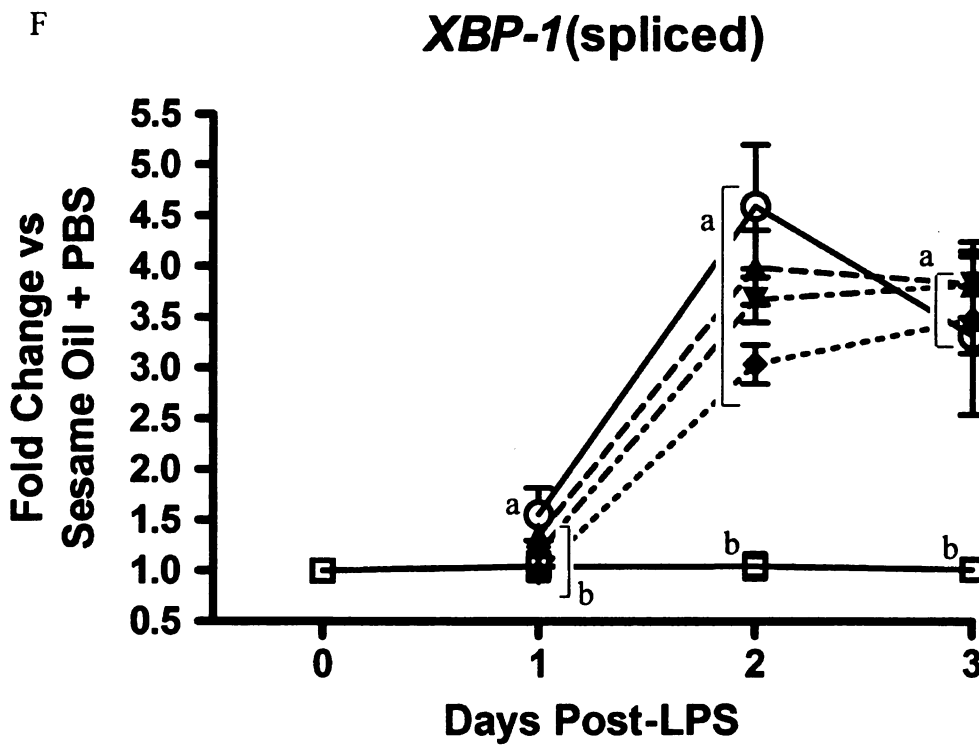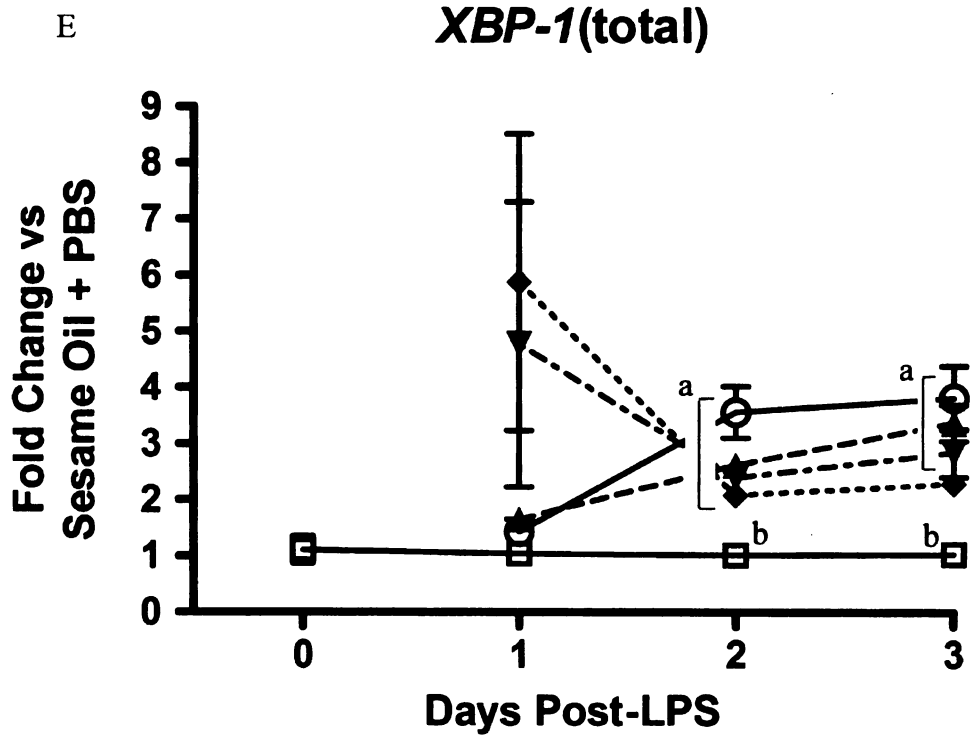
Previous *in vitro* studies with LPS-activated CH12.LX, a murine B cell line, and

mouse splenocytes suggested that TCDD treatment impaired down-regulation of Pax5

(Schneider *et al.* 2008; Yoo *et al.* 2004), a necessary regulatory event for plasmacytic

differentiation (Lin *et al.* 2002; Nera *et al.* 2006). In agreement with prior *in vitro*

observations, splenocytes from mice treated with LPS showed the greatest decrease in

mRNA abundance of *Pax5* on Day 2 of the time course. Mice treated with TCDD prior to

LPS had elevated *Pax5* mRNA levels on Day 1 of the time course, with 10 and 30 μg/kg

TCDD doses preventing the *Pax5* down-regulation associated with LPS treatment

observed most clearly on Day 2 of the time course (Figure 9A).

FACS analysis of Blimp-1 protein in $CD19^+$ B cells showed LPS treatment

induced an increase in the number of B cells expressing Blimp-1, consistent with

activation that precedes the ASC stage. Expression of Blimp-1 protein is quantitatively

associated with ASC phenotype, increasing as B cells differentiate into plasma cells

(Kallies *et al.* 2004), a finding supported by observations in Figure 8. The peak *in vivo*

ASC response occurs 3 to 4 days post-LPS (unpublished observation), correlating with

peak frequency for $CD19^+$ Blimp-1^{elevated} cells. TCDD treatment impaired generation

of $CD19^+$ Blimp-1^{elevated} B cells in LPS-treated mice (Figure 8A and B). In agreement

with protein expression, measurements of *Blimp-1* mRNA levels in isolated splenocytes

showed that LPS-treated mice possessed significantly increased *Blimp-1* mRNA levels on

Days 2 and 3. For example, 10 and 30 μg/kg TCDD treatment caused significant

suppression of LPS-induced *Blimp-1* mRNA levels on Day 3 (Figure 9B).

Figure 8. TCDD treatment suppressed LPS-stimulated generation of $CD19^{+}$ Blimp-$1^{elevated}$

cells. Isolated splenocytes were incubated with FcBlock, labeled with antibodies specific for

CD19, then fixed with Cytofix. At the completion of the time course cells were permeabilized with

BD Perm/Wash and incubated with antibodies specific for Blimp-1. Cells were subsequently

analyzed by FACS. (A) Representative plots from individual mice 3 days post-LPS showing the

$CD19^{+}$ Blimp-$1^{elevated}$ cell population. (B) Time course and dose response for generation of

$CD19^{+}$ Blimp-$1^{elevated}$ cell population. Results from 6 mice per group are depicted as mean

frequency of $CD19^{+}$ Blimp-$1^{elevated}$ cells ± SE of the mean. [a] P<0.05 compared to sesame oil +

PBS and [b] P<0.05 compared to sesame oil + LPS.

69

A

B
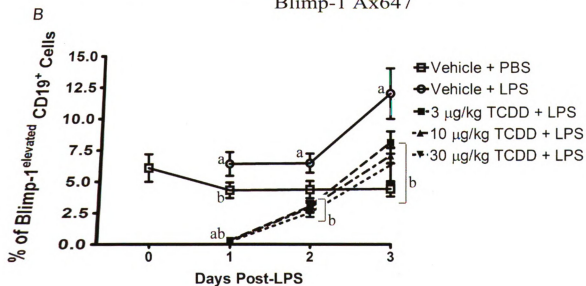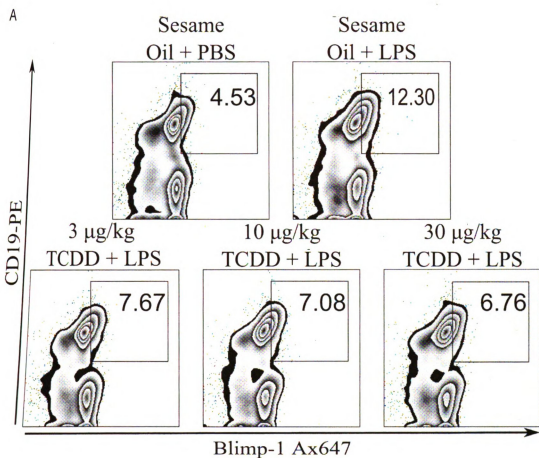
BCL-6, acting in concert with Pax5, is a negative regulator of Blimp-1 gene expression (Shaffer *et al.* 2000; Tunyaplin *et al.* 2004). B cells constitutively express BCL-6 under resting conditions, with initiation of the immune response causing a decrease in BCL-6 expression (Ohkubo *et al.* 2005), in turn allowing Blimp-1 expression to rise. *In vivo* LPS treatment decreased the level of *BCL-6* mRNA levels on Days 1 and 2, but concomitant treatment with TCDD did not appear to significantly alter BCL-6 gene expression (Figure 9C).

Figure 9. Gene expression profiles for transcription factors controlling plasma cell fate are influenced by LPS and TCDD treatments. Total RNA from splenocytes was isolated and cDNA synthesized for gene expression analysis. Target gene mRNA levels were normalized to 18S and the fold change was calculated by the $\Delta\Delta C_t$ method. (A) Pax5, (B) Blimp-1, or (C) BCL-6. Results from 6 mice per group are depicted as mean fold change ± SE of the mean. [a] $P<0.05$ compared to sesame oil + PBS and [b] $P<0.05$ compared to sesame oil + LPS.

A

Pax5

Fold Change vs Sesame Oil + PBS

B

Blimp-1

Fold Change vs Sesame Oil + PBS

C

BCL-6

Fold Change vs Sesame Oil + PBS

Days Post-LPS

- Sesame Oil + PBS
- Sesame Oil + LPS
- 3 μg/kg TCDD + LPS
- 10 μg/kg TCDD + LPS
- 30 μg/kg TCDD + LPS
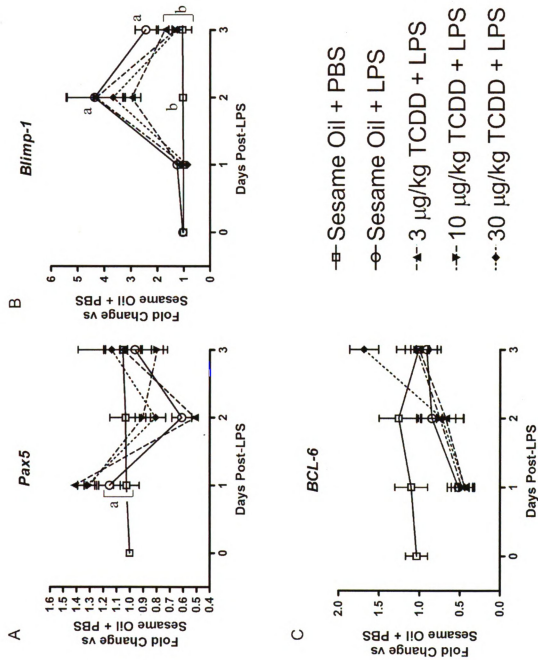
Simultaneous *In vitro* Time Course and Dose Response Evaluation for TCDD-Induced Impairment of the LPS-stimulated Primary IgM Response

Time and Concentration Response Profiling for TCDD Disruption of Transcription Factor Expression

In vivo profiling of LPS-elicited changes in transcription factor expression by FACS demonstrated a significant, dose-dependent impairment of Blimp-1 expression associated with TCDD treatment (Figure 8). While impairment of Blimp-1 mRNA expression has been demonstrated using both primary splenocytes and CH12.LX cells in vitro (Schneider et al. 2009), Blimp-1 protein expression in B cells was not directly assessed. Using Blimp-1 protein expression as a phenotypic anchor, multiparametric FACS was used to assess the time course and concentration response effects of TCDD on LPS-activated expression of Blimp-1, BCL-6, c-Jun, and phosphorylated c-Jun in purified splenic B cells.

Given that 0.03 and 0.3 nM TCDD shifted the distribution of TLR ligand treated cells to lower kinase phosphorylation, it stood to reason that alteration at the level of signal amplifier would impact downstream targets of phosphorylated JNK and ERK. JNK phosphorylates c-Jun, which in turn forms a portion of the AP-1 transcription factor that plays an important role in TLR ligand activated Blimp-1 expression (Ohkubo *et al.* 2005). ERK phosphorylates BCL-6, resulting in the ubiquitination and degradation of BCL-6 (Niu *et al.* 1998), and therefore plays a critical part in regulating plasmacytic differentiation. LPS treated primary B cells were assessed for c-Jun, phosphorylated c-Jun, BCL-6, and Blimp-1 expression at 24, 48, and 72 h post-treatment.

Figure 10 shows that LPS caused a time-related increase in the expression of c-Jun, phosphorylated c-Jun, and Blimp-1. BCL-6 initially increased with LPS treatment over the first 48 h relative to untreated B cells, but declined to expression levels below untreated B cells by 72 h post-treatment. Peak expression of c-Jun and Blimp-1 occurred 72 h post-LPS, while expression of phosphorylated c-Jun and BCL-6 peaked 48 h post-LPS. TCDD caused a concentration-related disruption of the normal pattern of LPS-activated transcription factor expression. Examined at their individual peak times of expression, TCDD increased BCL-6 expression while suppressing c-Jun, phosphorylated c-Jun, and Blimp-1 expression. Probability binning analysis of the examined transcription factors showed statistically significant alteration in the LPS + TCDD population relative to LPS + DMSO treated samples as early as 24 h post-treatment ($T(\chi)$ greater than 36 for all LPS + TCDD treated groups), but is maximally different 72 h post-treatment ($T(\chi)$ greater than 336 for all LPS + TCDD treated groups). $T(\chi)$ values can be used as a metric to rank how different samples are from a control population, and based on $T(\chi)$ values of LPS + TCDD treated groups the 0.03 and 0.3 nM TCDD ($T(\chi)$ of 457.3 and 336.3 respectively) treatments cluster nearer to LPS + DMSO treatment than 3 and 30 nM TCDD treated B cells ($T(\chi)$ values of 980.1 and 811.2 respectively).

LPS treatment caused an increase in phosphorylated c-Jun over untreated cells at all time points evaluated, as much as 269% over untreated values at 48 h. 30 nM TCDD treatment caused a significant impairment of LPS-activated c-Jun phosphorylation compared to LPS + DMSO treated B cells at all times evaluated ($T(\chi)$ greater than 6.9 at all time points), but caused the most significant suppression at 24 h post-LPS ($T(\chi)$ of 86.7), a decrease of 14.3% from the LPS + DMSO treated B cells. 3 nM TCDD causes

statistically significant suppression at 24 and 48 h post-LPS (T(χ) greater than 28.3), but

not at 72 h. 0.03 and 0.3 nM TCDD both significantly impaired c-Jun phosphorylation at

24 h (T(χ) greater than 33.3), but not at 48 or 72 hours.

Total c-Jun expression increased over the 72 h time course for all LPS treated

samples. LPS + DMSO B cells peaked at 72 h with a 24.5% increase over untreated B

cells. All concentrations of TCDD caused a significant increase in the total amount of c-

Jun at 24 h post-LPS (T(χ) greater than 16.9), but did not persist for all TCDD

concentrations at 48 and 72 h.

An inverse relationship for protein expression was expected for BCL-6 and

Blimp-1, as depicted in Figure 1. BCL-6 expression is silenced and Blimp-1 increased

within plasma cells (Shaffer *et al.* 2002), so TCDD-elicited alterations in the ratio of

these two transcription factors can tip the balance of the plasmacytic differentiation

control circuit away from the antibody-secreting cell fate. Simultaneous analysis of both

transcription factors at 48 h post-LPS, the peak time for BCL-6 expression and

intermediate time for Blimp-1 expression, shows that LPS treatment induced increases in

both transcription factors (Figure 11). 30 nM TCDD treatment shifted the B cell

population to a higher expression of BCL-6, as demonstrated by 54.8% of LPS + DMSO

treated B cells expressing elevated levels of BCL-6 compared to 69.4% of LPS + 30 nM

TCDD treated B cells elevating BCL-6 expression. TCDD treatment did not affect

Blimp-1 expression at 48 h as much as BCL-6, as 44.3% of LPS + DMSO treated B cells

had elevated Blimp-1 expression compared to 42.14% of LPS + 30 nM TCDD treated B

cells, a difference of 2.16%.

At 72 h post-treatment the effect of 30 nM TCDD on the percentage of B cells expressing elevated levels of Blimp-1 is slightly greater, 43.8% in LPS + DMSO treated B cells compared to 40.3% in LPS + 30 nM TCDD, a difference of 3.5% (Figure 12). In contrast, the percentage of Blimp-1^{High} BCL-6^{Low} B cells was markedly different between LPS + DMSO and LPS + 30 nM TCDD treatments, 25.2% versus 12.6% respectively. Furthermore, the percentage of Blimp-1^{Low} BCL-6^{High} B cells was also affected by TCDD treatment, going from 9.2% of viable cells in the LPS + DMSO treated group to 25.0% of cells in the LPS + 30 nM TCDD treated group.

Figure 10. In vitro TCDD treatment disrupts LPS-activated transcription factors expression.

Purified B cells were treated with 0, 0.03, 3, or 30 nM TCDD in DMSO vehicle and activated

with LPS (30 µg/mL). 24, 48, and 72 h following treatment B cells were analyzed by multivariate

FACS for expression of c-Jun, phosphorylated c-Jun, BCL-6, and Blimp-1. Values depicted are

mean ± SEM. Results are representative of 2 separate experiments.

Phosphorylated c-Jun

Phosphorylated c-Jun Expression (Geometric Mean Fluorescence)

c-Jun

c-Jun Expression (Geometric Mean Fluorescence)

Blimp-1

Blimp-1 Expression (Geometric Mean Fluorescence)

BCL-6

BCL-6 Expression (Geometric Mean Fluorescence)

Hours
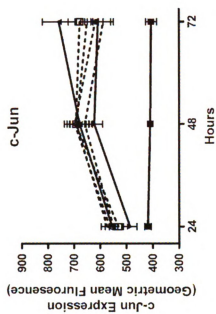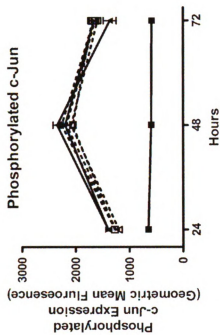
- - - - LPS + 0.03 nM TCDD
- - - - LPS + 0.3 nM TCDD
- -o- - LPS + 3 nM TCDD
- -◇- - LPS + 30 nM TCDD
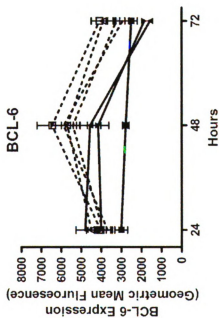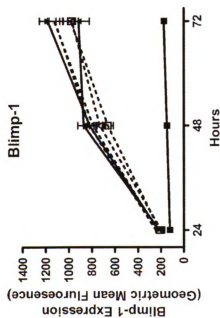
—■— Untreated
—■— LPS
—■— LPS + DMSO
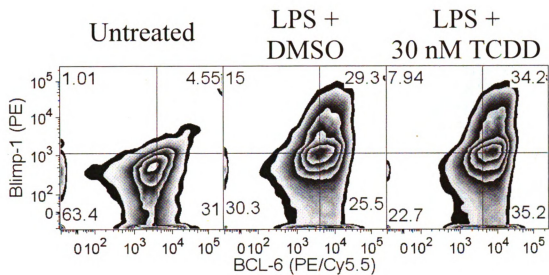
Figure 11. Relationship of Blimp-1 to BCL-6 expression at 48 h. Purified B cells were assessed simultaneously for Blimp-1 and BCL-6 expression 48 h post-treatment by FACS. Results depicted are concatenated analysis of at least 4 biological replicates. Plots depict immunofluoresence for viable cells, with each level of contour corresponding to 5% of the population. Numbers in the corner of each quadrant depict the percentage of viable cells within the quadrant. Results are representative of 2 separate experiments.
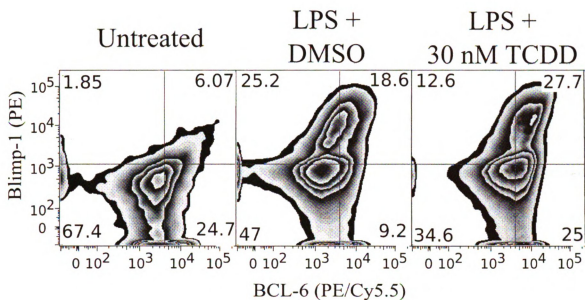
Figure 12. Relationship of Blimp-1 to BCL-6 expression at 72 h. Purified B cells were assessed simultaneously for Blimp-1 and BCL-6 expression 72 h post-treatment by FACS. Results depicted are concatenated analysis of at least 4 biological replicates. Plots depict immunofluoresence for viable cells, with each level of contour corresponding to 5% of the population. Numbers in the corner of each quadrant depict the percentage of viable cells within the quadrant. Results are representative of 2 separate experiments.

Time and Concentration Response Profiling for TCDD Disruption of Cell Surface Activation Marker Expression

TCDD dose-dependently impaired LPS-induced MHC Class II upregulation on the surface of B cells following *in vivo* treatment (Figure 5). In experimental models of cell-mediated immunity, 15 µg/kg TCDD reduced P815-elicited increases in CD86 on the cell surface of CD45R^{+} B cells (Prell and Kerkvliet 1997). Based on the *in vivo* observations that TCDD treatment impaired both MHC Class II and CD86, it was hypothesized that TCDD impairs upregulation of activation markers following *in vitro* immune response activation. An examination of both the time- and concentration-dependent changes in surface expression for activation markers CD69, CD80, and CD86 following *in vitro* LPS stimulation of B cells was performed

LPS caused a time-dependent increase in all activation markers examined during the first 24 h following treatment (Figure 13). MHC Class II expression declined in untreated B cells *in vitro* following isolation, while LPS treatment maintained and increased MHC Class II expression. CD69 expression peaked at 8 h post-treatment and remained sustained through the initial 24 h period. Both CD80 and CD86 increased throughout the 24 h time course. 89.3% of B cells treated with LPS + DMSO upregulated at least one cell surface activation marker expression by 24 h, compared with 14.7% of untreated B cells.

Multivariate probability binning analysis of cell surface marker expression showed TCDD caused a significant impairment of LPS-stimulated activation marker expression beginning 8 h post-treatment compared to LPS + DMSO treatment (from T(χ)=6.5 for LPS + 0.03 nM TCDD to T(χ)=50.0 for LPS + 30 nM TCDD), and extended

to 24 h (from $T(\chi)$=20.5 for LPS + 0.03 nM TCDD to $T(\chi)$=64.3 for LPS + 30 nM TCDD).

Most of the suppressive effect of TCDD on LPS-elicited cell surface activation marker upregulation during the first 24 h is attributable to effects on MHC Class II and CD69, as probability binning considering only CD80 and CD86 expression showed LPS + TCDD treated B cells are indistinguishable from LPS + DMSO treated B cells ($T(\chi)$ less than 1.5 for all concentrations of TCDD).

Figure 13. Simultaneous time course and concentration response for TCDD alteration of LPS-stimulated cell surface activation marker expression. Primary splenic B cells were isolated by negative selection and cultured at $3x10^6$ cells/mL. Cells were treated with 0, 0.03, 0.3, 3, or 30 nM TCDD in DMSO vehicle (0.025%) and activated with LPS (30 µg/mL). 1, 8, and 24 h post-treatment cells were collected for FACS analysis of MHC Class II, CD69, CD80, and CD86 expression. Results depicted are geometric mean fluorescence ± SEM for at least 4 biological replicates.

Results are representative of 2 experiments.

Cell Surface Activation Marker Expression
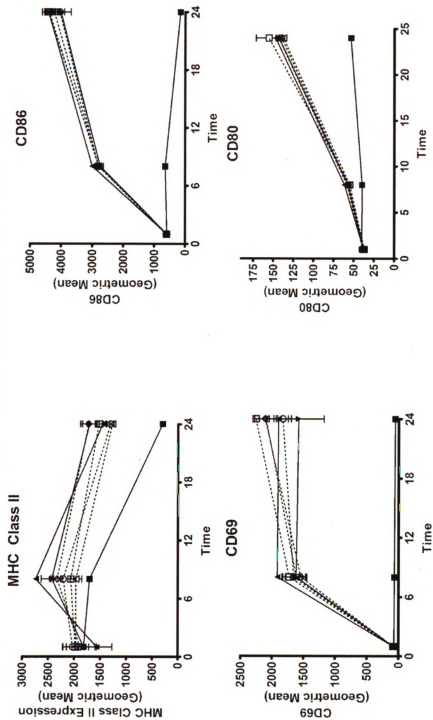
Significant upregulation of all activation markers occurred by 24 h following LPS and was decreased by TCDD treatment, but the primary IgM response develops over the course of 72 h. While previous *in vivo* results showed TCDD suppressed LPS-activated MHC Class II expression as early as 24 h post-treatment, purified B cells cultured *in vitro* may respond to LPS differently from their *in vivo* counterparts. The time course of activation marker examination was therefore increased to 24, 48, and 72 h post-treatment to extend and maximize the value of data obtained from experiments assessing expression of transcription factors.

LPS treatment caused a time-related increase in total surface expression of MHC Class II, CD69, CD80, and CD86 (Figure 14), with highest observed expression occurring 72 h post-LPS. Multivariate probability binning analysis of activation marker expression in LPS + DMSO treated B cells to all other treatment groups showed that 30 nM TCDD impaired expression of activation marker expression as early as 24 h post-LPS $(T(\chi)=69.4)$, but as activation marker expression increased in LPS + DMSO treated groups over time the impairment caused by TCDD became more apparent. By 72 h TCDD significantly impaired activation marker expression from 0.03 nM $(T(\chi)=73.5)$ to 30 nM TCDD $(T(\chi)=415.6)$.

Figure 14. Simultaneous time course and concentration response profiling for TCDD alteration of LPS-stimulated cell surface activation marker expression. Primary splenic B cells were isolated by negative selection and cultured at 3×10^6 cells/mL. Cells were treated with 0, 0.03, 0.3, 3, or 30 nM TCDD in DMSO vehicle (0.025%) and activated with LPS (30 µg/mL). 24, 48, and 72 h post-treatment cells were collected for FACS analysis of MHC Class II, CD69, CD80, and CD86 expression. Results depicted are geometric mean fluorescence ± SEM for at least 4 biological replicates. Results are representative of 2 experiments.

CD86

CD80

MHC Class II

CD69
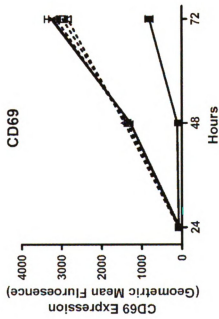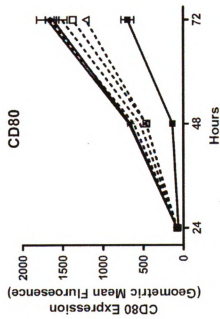
- Untreated
- LPS
- LPS + DMSO
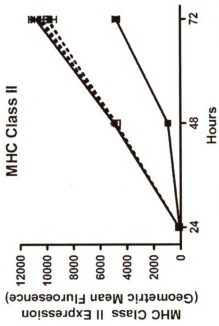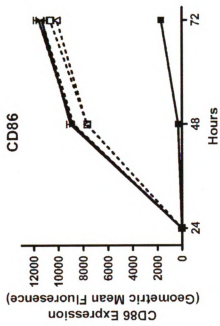
---- LPS + 0.03 nM TCDD
···· LPS + 0.3 nM TCDD
-□- LPS + 3 nM TCDD
-△- LPS + 30 nM TCDD
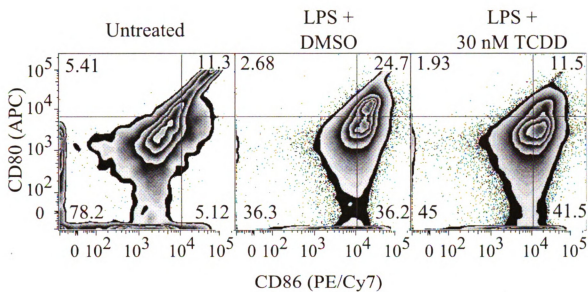
Figure 15. TCDD disrupts LPS-activated CD80 and CD86 expression. Purified B cells were treated with LPS (30 µg/mL) + DMSO vehicle or LPS + 30 nM TCDD. Cell surface expression of CD80 and CD86 was measured 72 h post-treatment. Results depicted immuno fluorescence from concatenated samples consisting of at least 4 biological replicates. Numbers in the corner of each quadrant depict the percentage of viable cells within the quadrant. Results are representative of 2 separate experiments.

Single parameter examination of LPS-activated expression for the costimulatory

molecules CD80 and CD86 was disrupted by TCDD in a concentration-related manner

(Figure 14). CD80 and CD86 stimulate T cells during the primary humoral response, and

knockout of either *CD80* or *CD86* results in significant impairment of humoral immunity.

However, even with knockout either allele can partially compensate for the loss of the

counterpart (Borriello *et al.* 1997). LPS treatment increased expression of both markers

simultaneously, causing 24.7% of B cells to express high levels both CD80 and CD86.

TCDD treatment impaired the generation CD80^{High} CD86^{High} B cells, reducing the

frequency of double positive cells to 11.5%, a level similar to that observed in untreated

B cells at 72 h.

While MHC Class II and CD69 were also inhibited by TCDD treatment at 72 h,

they decreased 9.0% and 12.7%, respectively, in LPS + 30 nM TCDD compared to LPS

+ DMSO treated B cells. In contrast, 30 nM TCDD caused at 23.5% decrease in CD80

expression relative to LPS + DMSO treated B cells at 72 h. TCDD treatment suppressed

LPS-activated CD86 expression 12.6%.

Simultaneous Time Course and Concentration Response Evaluation for TCDD-Induced Impairment of the TLR-stimulated In vitro Primary IgM Response

While results of *in vivo* and *in vitro* studies described above indicate TCDD-mediated disruption of LPS-activated Blimp-1 expression are consistent, a pivotal, direct mechanism for TCDD-mediated disruption of the primary IgM response could not be concluded. Based on the observation that TCDD disrupted Blimp-1 gene and protein expression, it was hypothesized that events preceding Blimp-1 upregulation may be altered by TCDD.

One pharmacologic approach for elucidating mechanisms involved in phenotype is to exploit different ligand-receptor interactions in order to understand underlying physiology. A classic example is use of α or β adrenoreceptor agonists and antagonists to illuminate the role of different adrenergic signal programs in control of sympathetic nervous system activity. LPS, used successfully both *in vivo* and *in vitro* to drive plasmacytic differentiation of B cells, is a TLR4 and CD180 ligand (Ogata *et al.* 2000). Other TLR ligands are also known to drive plasmacytic differentiation, in particular the small molecule R848 and CpG oligonucleotides, acting through TLR7/8 and TLR9, respectively (Genestier *et al.* 2007; Philbin *et al.* 2005). By utilizing different TLR ligands to activate plasmacytic differentiation it may be possible to identify discrete differences between responses that provide insight into TCDD-mediated disruption of the primary IgM response.

TCDD Suppression of TLR-induced Antibody Secretion in CH12.LX

Previous studies demonstrated that TCDD causes a concentration-dependent

inhibition of the LPS-activated IgM response in CH12.LX (Sulentic *et al.* 1998),

providing a useful *in vitro* model for elucidating intracellular mechanisms involved in

TCDD disruption of the IgM response. The TLR ligands LPS, CpG, and R848 all cause

increased secretion of IgM in CH12.LX cells (Bishop and Haughton 1986; Bishop *et al.*

2000; Krieg *et al.* 1995); however, the ability of TCDD to suppress IgM secretion

activated by CpG and R848 treatment was unknown. Both CpG and R848 induced

increases in IgM secretion comparable to that observed with LPS treatment. TCDD

caused a concentration-dependent suppression of the TLR ligand-induced IgM response

for all stimuli examined (Figure 16). Significant suppression occurred for all stimuli at

concentrations of 0.3 nM TCDD and higher. LPS- and CpG-activated IgM responses had

similar profiles of suppression caused by TCDD, with 3 nM TCDD causing a 72%

decrease in LPS-induced IgM secretion and 83% decrease in CpG-induced IgM secretion.

3 nM TCDD suppressed R848-induced IgM secretion more moderately compared to

other TLR ligands, declining 53%.
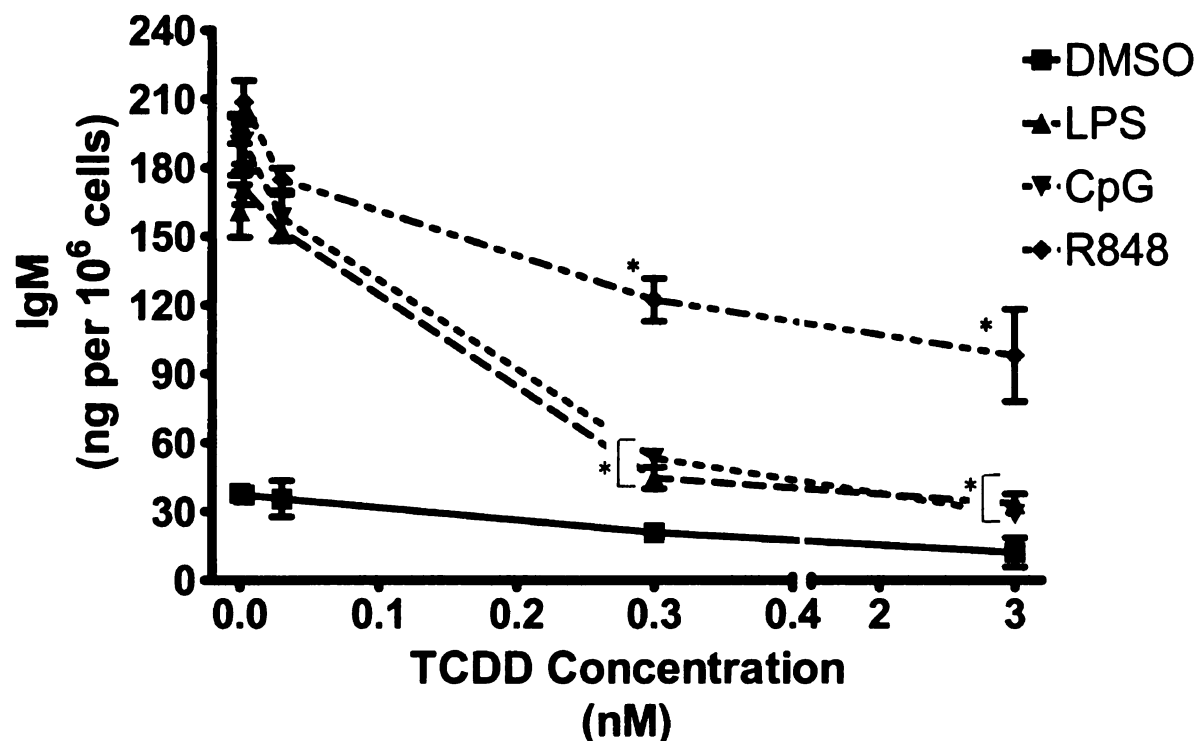
Figure 16. TCDD Suppression of TLR-activated IgM Responses in CH12.LX B cells.

CH12.LX cells (2x10^4 cells/mL) were activated with LPS (30 µg/mL), CpG (1.2 µg/mL),

or R848 (0.2 µg/mL) and treated with 0, 0.003, 0.03, 0.3, or 3 nM TCDD in DMSO

vehicle (0.035%). 48 h following activation culture supernatant IgM was determined by

ELISA and normalized to total cell count. Results from triplicate determinations are

*represented as mean IgM per 10^6 cells ± SEM. * indicates values that are significantly*

different from activated cells treated with vehicle at p<0.05. Results are representative of

more than four experiments.

TCDD alteration of TLR-activated kinase phosphorylation

Previous studies in CH12.LX cells established TCDD alteration in the LPS-activated DNA binding and transcriptional activity of AP-1 (Schneider *et al.* 2009; Suh *et al.* 2002a) as early as two hours following treatment. Jun was identified as one component of the AP-1 DNA binding complex, potentially resulting from TCDD disruption of LPS-induced translocation of c-Jun into the nucleus.

It was hypothesized that TCDD disrupts LPS-activated plasmacytic differentiation by altering the profile of kinase phosphorylation resulting from TLR activation because c-Jun is directly regulated by JNK and BCL-6 is directly regulated by ERK. AKT, or protein kinase B, is phosphorylated within minutes of BCR activation (Donahue and Fruman 2007) and is also known to be phosphorylated in B cells following LPS treatment (Bone and Williams 2001; Hebeis *et al.* 2005). Furthermore, AKT is a negative regulator of the transcription factor FoxO, which in turn is a positive regulator of BCL-6 expression; therefore, activated AKT can indirectly decrease BCL-6 expression by inactivating FoxO (Omori *et al.* 2006). Because TCDD impairs both LPS-activated and BCR-activated primary IgM responses, it was further hypothesized that TCDD impairs TLR-activated AKT phosphorylation.

Preliminary studies in primary B cells and CH12.LX cells established that LPS treatment stimulated modest phosphorylation of AKT, ERK, and JNK, consistent with the observations of others (Krutzik *et al.* 2005). In the absence of B cell activation it is difficult to discriminate between normal response variation versus inhibition, therefore alternative B cell activation stimuli were sought. Since it had already been established that CpG and R848 activated IgM responses are suppressed by TCDD in CH12.LX cells

(**Figure** 16), their relative effectiveness for JNK phosphorylation was examined. Both the

TLR9 ligand CpG and the TLR7/8 ligand R848 induced JNK phosphorylation on a level

equivalent to PMA/ionomycin within 15 min of treatment (Figure 17). While

PMA/ionomycin is not a TLR activator, it is a robust pharmacologic mimic of BCR

activation. Therefore, treatments that meet or exceed the stimulation induced by

PMA/ionomycin are considered robust inducers of kinase phosphorylation.

Treatment	Geometric Mean pJNK
Untreated	878.97
LPS	1116.87
PMA/Ionomycin	1566.27
CpG	1935.45
R848	1752.29
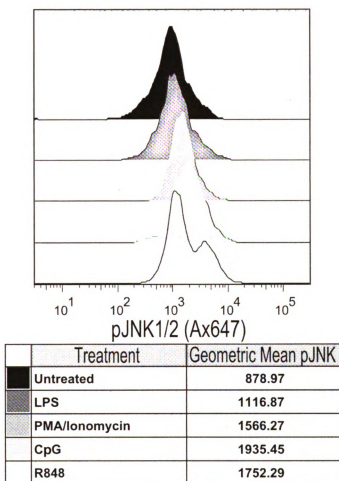
Figure 17. Relative TLR ligand efficacy for JNK phosphorylation. CH12.LX cells were activated by addition of LPS, PMA/Ionomycin, CpG, or R848. JNK phosphorylation status was frozen 15 min following activation by direct addition of concentrated paraformaldehyde to each group. Following methanol permeabilization CH12.LX cells were stained for phosphorylated JNK and analyzed by FACS. Histograms show the population distribution for JNK phosphorylation. Geometric mean fluorescence values are shown directly below the histograms for comparison of treatments.

FACS analysis of JNK phosphorylation demonstrated discrete activation patterns in response to TLR activation, particularly for R848. While LPS caused a 27% increase in JNK phosphorylation, PMA/ionomycin and CpG induced greater increases in JNK phosphorylation, 78% and 120% respectively. Viewed on a percent change basis, R848 appeared to be a more modest inducer of JNK phosphorylation when compared to CpG, increasing 99% over untreated CH12.LX. However, and only observable with FACS-based determination, R848 treatment generated two populations of CH12.LX cells, a majority population that did not phosphorylate JNK and a minority population, 33% of the total, that phosphorylates JNK to a high degree.

Because kinases, particularly MAPK, act as amplifiers in cell signaling cascades (Asthagiri and Lauffenburger 2001) small perturbations can profoundly alter phenotypic outcomes. Increases or decreases in the level of kinase phosphorylation, and therefore activation, can decrease both LPS-activated Blimp-1 mRNA expression and plasmacytic differentiation (Lin *et al.* 2006). To assess whether TCDD alters JNK, ERK, or AKT phosphorylation, CH12.LX cells were activated with single TLR ligands in combination with 0, 0.003, 0.03, or 0.3 nM TCDD in DMSO vehicle. Literature reports showing TLR ligand-induced kinase phosphorylation were used to select concentrations for stimulation of AKT, ERK, and JNK (Bishop *et al.* 2000; Yi and Krieg 1998; Yi *et al.* 1996). TCDD concentrations were selected on the basis of causing, respectively, no significant effect (0.003 nM TCDD), significant but submaximal (0.03 nM TCDD), or maximal (0.3 nM TCDD) inhibition of LPS-activated IgM secretion in CH12.LX cells.

Figure 18. Simultaneous time and concentration response profiling for TCDD alteration of TLR ligand-activated AKT phosphorylation. CH12.LX cells (6×10^5 cells/mL) were treated by simultaneous addition of vehicle, LPS, CpG, or R848 alone in combination with 0, 0.003, 0.03, or 0.3 nM TCDD in DMSO vehicle (0.1% final concentration). Phosphorylation status was fixed by direct addition of concentrated paraformaldehyde at 15, 30, or 60 min post-treatment, followed by permeabilization with methanol. CH12.LX cells were stained for phosphorylated forms of AKT, ERK, and JNK and analyzed by FACS. Results depicted are geometric mean fluorescence for AKT. Results are representative of 4 separate experiments.

Phosphorylated AKT (Serine 473)

CpG

R848

TCDD

LPS

- TLR Ligand + 0.003 nM TCDD
- TLR Ligand + 0.03 nM TCDD
- TLR Ligand + 0.3 nM TCDD

— Untreated
— DMSO
— TLR Ligand
— TLR Ligand + DMSO
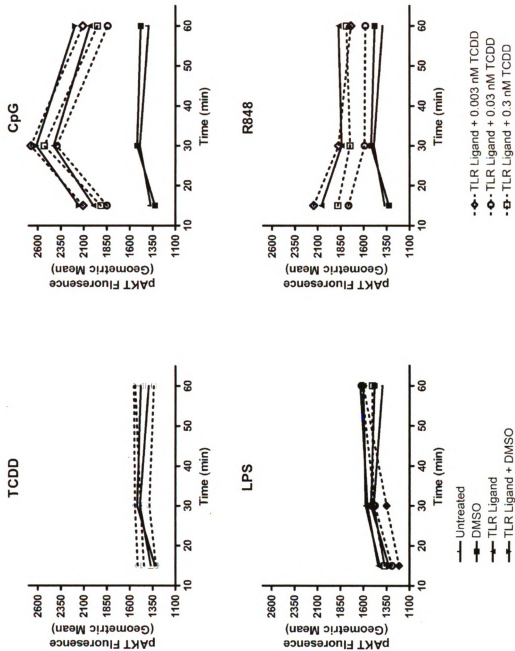
Figure 19. Simultaneous time and concentration response profiling for TCDD alteration of TLR ligand-activated ERK phosphorylation. CH12.LX cells (6×10^5 cells/mL) were treated by simultaneous addition of vehicle, LPS, CpG, or R848 alone in combination with 0, 0.003, 0.03, or 0.3 nM TCDD in DMSO vehicle (0.1% final concentration). Phosphorylation status was fixed by direct addition of concentrated paraformaldehyde at 15, 30, or 60 min post-treatment, followed by permeabilization with methanol. CH12.LX cells were stained for phosphorylated forms of AKT, ERK, and JNK and analyzed by FACS. Results depicted are geometric mean fluorescence for ERK. Results are representative of 4 separate experiments.

Phosphorylated ERK1/2 (Threonine 202/Tyrosine 204)

CpG

R848

TCDD

LPS

Legend:
- Untreated
- DMSO
- TLR Ligand
- TLR Ligand + DMSO
- TLR Ligand + 0.003 nM TCDD
- TLR Ligand + 0.03 nM TCDD
- TLR Ligand + 0.3 nM TCDD

Axes: pERK1/2 Fluorescence (Geometric Mean); Time (min)

Figure 20. Simultaneous time and concentration response profiling for TCDD alteration of TLR ligand-activated JNK phosphorylation. CH12.LX cells (6x10^5 cells/mL) were treated by simultaneous addition of vehicle, LPS, CpG or R848 alone in combination with 0, 0.003, 0.03, or 0.3 nM TCDD in DMSO vehicle (0.1% final concentration). Phosphorylation status was fixed by direct addition of concentrated paraformaldehyde at 15, 30, or 60 min post-treatment, followed by permeabilization with methanol. CH12.LX cells were stained for phosphorylated forms of AKT, ERK, and JNK and analyzed by FACS. Results depicted are geometric mean fluorescence for JNK. Results are representative of 4 separate experiments.

Phosphorylated JNK1/2 (Threonine 183/Tyrosine 185)
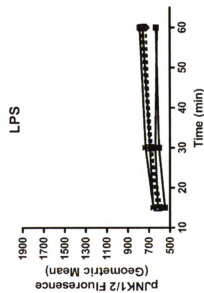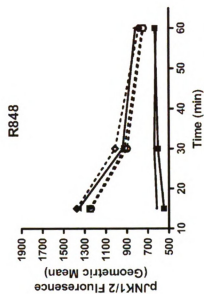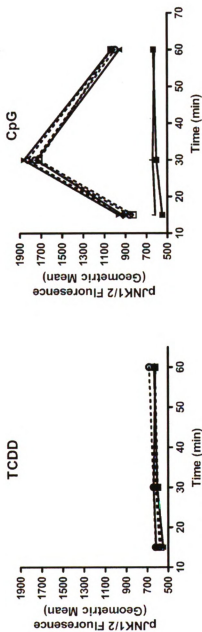
CpG

R848

TCDD

LPS

Legend (R848 panel):
- TLR Ligand + 0.003 nM TCDD
- TLR Ligand + 0.03 nM TCDD
- TLR Ligand + 0.3 nM TCDD

Legend (LPS panel):
- Untreated
- DMSO
- TLR Ligand
- TLR Ligand + DMSO

All panels:
- x-axis: Time (min)
- y-axis: pJNK1/2 Fluoresence (Geometric Mean)

Single treatment with TCDD or LPS typically altered kinase phosphorylation less than 20% relative to untreated CH12.LX cells. Serum addition to cell cultures is known to cause greater phosphorylation of ERK and JNK than TCDD (Tan *et al.* 2002), consistent with the modest induction observed above. As a result, many studies of TCDD-activated kinase phosphorylation have been performed under serum-starved conditions. Since the studies described above were all performed in cultures containing 10% serum, any alteration in ERK and JNK phosphorylation caused by TCDD must be robust relative to effects observed in published studies of other researchers using reduced serum conditions. While the relative effects of LPS on kinase phosphorylation are modest, LPS treatment induced a significant increase in IgM secretion at later time point, illustrative of the point that kinases act as signal amplifiers. Indeed, TCDD treatment alone, even with modest changes in kinase phosphorylation observed in this study, activated plasmacytic differentiation of B cells, albeit at very modest levels relative to classic humoral response activators (Kramer *et al.* 1987).

The kinetic and dynamic pattern of kinase phosphorylation resulting from TLR activation differs depending on the kinase examined and the TLR ligand applied. LPS treatment, as observed in preliminary studies, caused modest alterations in AKT, ERK, and JNK phosphorylation that peak at 60 min following treatment (Figure 18, Figure 19, and Figure 20). CpG treatment caused the largest increases in kinase phosphorylation, increasing as much as 132% for CpG + vehicle treatment at 30 min, and declining by 60 min post-activation. Kinase phosphorylation induced by R848 peaked earlier than other TLR ligands, increasing as much as 75% by 15 minutes post-activation, and declining at 30 and 60 min post-activation.

Viewed on a single parameter basis, effects of TCDD on TLR ligand-activated kinase phosphorylation are modest. TCDD at 0.003 nM did not significantly suppress kinase phosphorylation, consistent with a lack of immunosuppressive effects on the primary IgM response. TCDD alone caused no more than a 10% change in AKT, ERK, and JNK phosphorylation. ANOVA analysis of single parameters shows statistically significant impairments of kinase phosphorylation in 0.03 and 0.3 nM TCDD-treated CH12.LX cells relative to TLR ligand + vehicle treated cells. One of the strengths of flow cytometry is that it allows simultaneous collection of information on kinase phosphorylation from each individual cell, but ANOVA is not the best tool for analyzing such data. Probability binning analysis, which is designed for analysis of multiparametric flow cytometry (Roederer *et al.* 2001a; Roederer *et al.* 2001b), comparing TLR ligand + DMSO to TLR ligand + TCDD for AKT, ERK, and JNK phosphorylation suggested higher TCDD concentrations significantly decreased kinase phosphorylation. TLR-activated CH12.LX cells treated with 0.03 nM or 0.3 nM TCDD shifted at least 8 standard deviations ($T(\chi)$ greater than 8) away from the TLR ligand + DMSO treated groups.

To further extend and validate the biological relevance of TCDD disruption for kinase phosphorylation, *in vitro* experiments using splenocytes were performed. Based on results obtained in the CH12.LX cell line, R848 was chosen as the B cell activation stimulus because the kinase phosphorylation elicited by R848 was intermediate in magnitude when compared to LPS and CpG. At 15 min post-treatment primary B cells were assessed for AKT, ERK, and JNK phosphorylation.

As depicted in Figure 21, R848 caused phosphorylation of both AKT and ERK for the majority of B cells. Probability binning analysis comparing DMSO and 30 nM TCDD treated B cells showed no distinguishable difference for phosphorylation of AKT, ERK, or JNK. TCDD at 30 nM significantly suppressed R848-activated phosphorylation of AKT, ERK, and JNK (T(χ) of 11.5). pAKT^{High} pERK^{High} comprised 51.3% of R848-treated B cells, while 38.1% of R848 + TCDD cotreated B cells were pAKT^{High} pERK^{High} (Figure 21). The reciprocal pAKT^{Low} pERK^{Low} populations were 26.3% of R848 treated B cells and 32.0% of R848 + TCDD treated B cells.

Relative to pAKT and pERK, which increased 230.4% and 383.5% respectively, pJNK increased by 94.8% relative to DMSO treated B cells. While R848 induced a more modest relative increase in pJNK, TCDD caused a measurable decrease in pJNK. R848 + TCDD cotreated B cells increased pJNK by 79.5% over DMSO, a difference of 15.3% from single treatment with R848.

Figure 21. TCDD suppression of kinase phosphorylation in primary B cells. Isolated splenocytes were treated by simultaneous addition of DMSO vehicle, TCDD (30 nM), R848 (0.2 µg/mL), or a combined treatment of R848 + TCDD. 15 min after treatment splenocytes were fixed by direct addition of concentrated formaldehyde. Following permeabilization cells were blocked, then stained for B220, TCRβ, pAKT, pERK, and pJNK. B cells were identified as a B220$^+$ TCR$^-$ population, then analyzed for pAKT, pERK, and pJNK expression. Results depicted are immunofluoresence for pAKT and pERK. Percentages of viable cells within each quadrant are shown in the corner of each individual plot. Data is representative of more than 2 experiments.

Treatment	pJNK (GeoMean)
Untreated	62.63
DMSO	63.69
TCDD	58.89
R848	124.05
R848 + TCDD	114.31
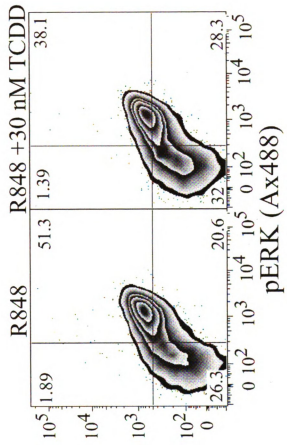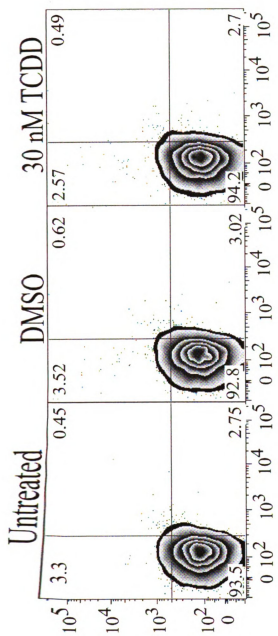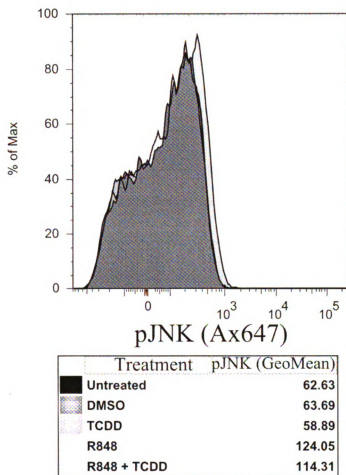
Figure 22. Effects of R848 and TCDD on JNK phosphorylation in primary B cells.

Isolated splenocytes were treated by simultaneous addition of DMSO vehicle, TCDD (30

nM), R848 (0.2 μg/mL), or a combined treatment of R848 + TCDD. 15 min after

treatment splenocytes were fixed by direct addition of concentrated formaldehyde.

Following permeabilization cells were blocked, then stained for B220, TCRβ, pAKT,

pERK, and pJNK. B cells were identified as a B220[+] TCR[-] population, then analyzed for

pAKT, pERK, and pJNK expression. Results depicted are immunofluorescence for pJNK.

Geometric mean fluorescence for individual treatments is shown below the histograms.

Data is representative of more than 2 experiments.

Discussion of Results from *In vivo* and *In vitro* Murine Models for TCDD Disruption of TLR-ligand Activated Plasmacytic Differentiation

In vitro models are valuable tools for examining intracellular events, but without the context of the whole animal limited information is gleaned. Science is well served when *in vitro* and *in vivo* models are used as complementary tools to develop basic understanding of life processes, thus verifying *in vitro* observations using *in vivo* models helps illuminate fundamental biology at work. Along those lines, utilization of the T-independent stimulus LPS for initiating a primary IgM response *in vivo* complemented *in vitro* LPS-activation models of humoral immunity. The kinetics of both the *in vivo* and *in vitro* response are similar, peaking 3 to 4 days following activation. Unlike sRBC-elicited responses that require interactions between multiple cell types, LPS can directly stimulate B cells. Direct stimulation increases the number of activated B cells during the initial phase of the immune response, potentially increasing the ability to detect effects occurring early in B cell activation that lead to suppression of the primary IgM response. Finally, to maintain similar intracellular signaling programs leading to plasmacytic differentiation it is important to utilize comparable activation stimuli. In assimilating the characteristics of the LPS-stimulated primary IgM response, the *in vivo* and *in vitro* models are highly compatible for exploring effects of TCDD on the B cell.

In examining *in vitro* events implicated in TCDD-mediated suppression of the primary IgM response using an *in vivo* T-independent humoral immune response many results were found to be consistent between models. TCDD modestly attenuated LPS-induced increases in splenocyte number, accompanied by profound suppression of the IgM response at all concentrations of TCDD evaluated. Assessment of multiple

phenotypic endpoints associated with AFCs confirms that TCDD prevents LPS-induced increases in XBP-1 and all components of pentameric IgM. The observations that CD138 expression, IgJ, and Igκ production are suppressed advance our understanding of TCDD's mechanism of action, as previous studies have not directly shown suppression of intracellular antibody production on a single cell basis, and as such could never conclusively establish whether TCDD suppression of the primary IgM response resulted from suppression of antibody secretion and production or the differentiation of B cells into AFC. TCDD impaired LPS-stimulated up-regulation of Blimp-1, a transcription factor established to be a central regulator of B cell differentiation. Collectively, these results strongly support the hypothesis that TCDD impairs B cell to plasma cell differentiation.

In agreement with moderate attenuation of LPS-stimulated increases in cell number observed in this *in vivo* study, TCDD treatment modestly decreased proliferation, as measured by $[^3H]$ thymidine incorporation, in isolated splenocytes activated *in vitro* with LPS (Morris *et al.* 1993). A minor decrease in proliferation is insufficient to explain the magnitude of suppression in the IgM response observed in the present study, especially since the IgM AFC response was normalized to cell number. However, the observed effect on decreased spleen cellularity was consistent with the possibility that an event upstream of antibody production is impaired by TCDD.

Disruption in the production of any single Ig component or protein important in antibody secretion impairs the primary IgM response. With that knowledge, *in vivo* studies examined expression of all immunoglobulin components. Expression of Igμ and Igκ are more modestly inhibited than the IgJ chain, and may provide insight on why the

111

IgM response is highly sensitive to suppression by TCDD. B cells must express antigen receptors on their surface to receive survival signals (Rajewsky 1996), hence the high constitutive levels of both Igμ and Igκ. TCDD inhibition of B cell antigen receptor components may result in deletion of some B cells, preventing detection of some affected B cells using current techniques. Additionally, suppression of Igμ and Igκ expression can be expected to impair expression of all forms of immunoglobulin, whereas the IgJ chain is essential only for IgM and IgA classes of immunoglobulin. TCDD strongly attenuates IgJ chain expression and can therefore be expected to impair markedly the assembly of pentameric IgM, an outcome verified by TCDD-mediated decrease in the AFC response. It is also plausible that less striking effects of TCDD on LPS-induced Igκ and Igμ expression are due to the high constitutive level of both Igκ and Igμ.

Impaired expression of Ig components disrupts antibody synthesis, but B cells must also resolve endoplasmic reticulum stress resulting from increased Ig protein synthesis necessary for robust secretion of antibody. Following activation B cells up-regulate expression of *XBP-1* mRNA, which can be spliced to an alternative mRNA translating to full length XBP-1, a transcription factor essential for resolution of the unfolded protein response (Reimold *et al.*, 2001). Consistent with an interpretation that TCDD blocks plasmacytic differentiation upstream of antibody production and secretion, TCDD treatment reduced both total and spliced *XBP-1* expression in LPS-treated mice (Figure 5). In addition, with the recent establishment of XBP-1 as a regulator of BCR signaling (Hu *et al.* 2009) and interacting with BOB-1 (Shen and Hendershot 2007), another key regulator of plasmacytic differentiation, it is even more apparent that TCDD-

mediated disruption of XBP-1 expression can feed back to alter early events in plasmacytic differentiation.

Importantly, recent studies of Blimp-1 conditional knockout mice and identification of XBP-1 as a regulator of hepatic lipid metabolism provide interesting, indirect links for two well-recognized human TCDD toxicities, chloracne and hepatosteatosis, to Blimp-1 expression. Magnúsdóttir and coworkers described a keratinocyte-specific knockout of Blimp-1 in mice resulting in a phenotype remarkably similar to the most consistently observed human health outcome produced by high dose TCDD exposure, chloracne (Zugerman 1990). Blimp-1 knockout in keratinocytes resulted in a sequela termed by the investigators as "a cyst-like structure that proved to be filled with lipid" in the skin of adult mice (Magnusdottir *et al.* 2007). If TCDD inhibits Blimp-1 expression in keratinocytes similarly to B cells, then a shared mechanism for TCDD toxicity involving deregulation of Blimp-1 in different tissues becomes more plausible. Along these lines, XBP-1, a transcription factor that is indirectly controlled by Blimp-1 in B cells, is a regulator of lipid homestasis in the mouse liver (Lee *et al.* 2008). Human serum dioxin-like chemical levels are associated with hepatosteatosis (Lee *et al.* 2006), and furthermore, TCDD induces hepatosteatosis in mice (Boverhof *et al.* 2005). Coupling the knowledge that TCDD reduced XBP-1 expression and is downstream of Blimp-1, it is tempting to speculate that TCDD-induced deregulation of Blimp-1 is a key event in some of the toxicities produced by TCDD.

Separate from their function in antibody synthesis and secretion, B cells change surface protein expression during transition into ASCs. Abundance of surface CD19, MHC Class II, and B cell antigen receptor all decrease during the later phase of

plasmacytic differentiation, while surface expression of CD138 is up-regulated (Fairfax

et al. 2007). CD138 has been commonly used as a marker to enumerate plasma cells, and

is a complementary phenotypic marker not directly involved in antibody secretion. LPS

and TCDD cotreated mice were impaired in their ability to generate $CD19^+ CD138^+$ cells

compared to mice treated with LPS in the absence of TCDD.

Cell surface activation markers such as MHC Class II, CD69, CD80, and CD86

initially increase following stimulation during the activation phase of plasmacytic

differentiation. TCDD suppression of MHC Class II upregulation in response to LPS

treatment was observed *in vivo*. *In vitro* examination of a more comprehensive panel of

activation markers following LPS activation demonstrated that TCDD suppresses more

than just MHC Class II. The significant impairment of CD80 and CD86 may be

particularly important to understanding the profound suppression of primary humoral

immunity caused by TCDD. The role of CD80 and CD86 is to provide costimulatory

signals to T cells, which in turn stimulate B cells via cytokine release. Because the

primary IgM response typically requires interaction between B and T cells, a failure of B

cells to provide sufficient stimulation to T cells would result in a spiraling failure of

costimulation, eventually resulting in considerable suppression of the humoral response.

Evidence indicates that TCDD interferes with LPS-induced Blimp-1 expression,

and taken collectively, points toward TCDD-mediated alteration of a fundamental control

switch during the primary IgM response. Blimp-1 expression is required for the

generation of plasma cells (Shapiro-Shelef *et al.* 2003), thus failure to up-regulate Blimp-

1 expression leads to decreased plasma cell appearance, consistent with TCDD-mediated

suppression of both IgM AFC response and in the frequency of $CD19^+ CD138^+$ B cells.

Direct evidence for deregulation of Blimp-1 expression *in vivo* comes from the observations that TCDD treatment dose-dependently decreased the frequency of CD19$^+$ Blimp-1^{elevated} B cells and *Blimp-1* mRNA abundance in LPS-treated mice. *In vitro* studies of purified B cells replicated *in vivo* suppression of Blimp-1 expression, and were also able to extend the effects of TCDD to an increase in BCL-6 expression. Based on Figure 3 a sustained expression of BCL-6 will, in the long term, prevent Blimp-1 expression. BCL-6 is also known to be a direct negative regulator of CD80 expression (Niu *et al.* 2003), thus the elevated levels of BCL-6 observed 48 and 72 h following TCDD treatment *in vitro* provide a partial explanation for the significant impairment of CD80 expression at 48 and 72 h in LPS + TCDD treated B cells.

AP-1 plays a fundamental role in initiating plasmacytic differentiation by activating Blimp-1 transcription (Ohkubo *et al.* 2005). *In vitro* treatment of B cells with TCDD significantly impaired LPS-activated phosphorylation of c-Jun, one component of the AP-1 transcription factor. AP-1 DNA binding in LPS-activated CH12.LX is almost completed abrogated by 10 nM TCDD 48 h post-treatment (Schneider *et al.* 2009), much more than what would be expected based on the impaired expression of phosphorylated c-Jun caused by 30 nM TCDD in primary B cells. While a portion of this difference is attributable to differences in model systems such as AHR expression, BCL-6 may be another important factor. Simple abundance of AP-1 components likely underestimates the effect on AP-1-mediated transcription because BCL-6 can directly bind and impair AP-1 activity (Vasanwala *et al.* 2002). It is likely that AP-1 transcriptional activity is significantly impaired given the observation that TCDD both inhibits c-Jun phosphorylation and increases BCL-6 expression.

Comparing the *in vitro* LPS + TCDD to LPS + DMSO treated cells by probability

binning showed that T(χ) values for both transcription factor and activation marker

expression correlate with the magnitude to which the IgM response was suppressed.

TCDD at 0.03 and 0.3 nM caused less LPS-activated IgM response suppression than at 3

and 30 nM, which was similarly reflected in the T(χ) values showing 0.03 and 0.3 nM

TCDD clustering nearer to LPS + DMSO treatment than 3 and 30 nM TCDD.

Application of more sophisticated statistical analysis tools to multiparametric FACS

allowed for better discrimination of TCDD effects by correlating changes for multiple

proteins within a single cell, which was previously unachievable using single parameter

analysis.

TCDD treatment consistently suppressed TLR-activated IgM responses in

CH12.LX cells, and a similar pattern for TCDD suppression of kinase phosphorylation

was observed regardless of the activating TLR ligand. While TCDD was less effective at

suppressing the R848-activated compared to LPS- and CpG-activated IgM responses,

TCDD at 0.3 nM consistently suppressed kinase phosphorylation 10-20% regardless of

the TLR ligand. There is likely to be additional factors beyond kinase phosphorylation

that contribute to the differences between R848 and non-R848 stimuli in TCDD-mediated

suppression of the IgM response.

Kinases are key regulators of AP-1 activation preceding plasmacytic

differentiation. Immunosuppressive concentrations of TCDD decreased TLR-activated

phosphorylation of the kinases AKT, ERK, and JNK in CH12.LX cells (Figure 18, Figure

19, and Figure 20). Primary B cells were also found to be sensitive to TCDD-mediated

disruption of TLR-activated kinase phosphorylation (Figure 21). TCDD impairment of

LPS-activated ERK and JNK phosphorylation provide novel mechanistic insight into alterations in BCL-6 and phosphorylated c-Jun expression observed *in vitro*. The observed increase in BCL-6 abundance caused by TCDD (Figure 10) is consistent with impairment of ERK activation, as active ERK phosphorylates BCL-6 leading to ubiquitination and degradation of BCL-6. JNK derives its name from one of its best characterized activities, the phosphorylation of c-Jun. Because TCDD impairs TLR-activated JNK phosphorylation, and therefore activity, TCDD suppression of phosphorylated c-Jun abundance is a natural consequence.

ERK plays an important role in differentiation processes beyond plasmacytic differentiation of B cells. Like plasmacytic differentiation, adipocytic differentiation is suppressed by TCDD. Treatments that induce ERK phosphorylation reversed TCDD suppression of adipocytic differentiation, leading the authors to speculate that TCDD suppression of differentiation requires a decreased activation of ERK in order to observe suppression (Hanlon *et al.* 2003). Results in Figure 19 demonstrated that TCDD treatment significantly impaired TLR-activated ERK phosphorylation, and coupled with the observations of Hanlon et al, suggest that TCDD impairment of ERK phosphorylation may play an important role in suppression of cellular differentiation in multiple cell types.

TCDD-mediated suppression of kinase phosphorylation may provide a partial explanation for the window of sensitivity that exists for *in vitro* disruption of the primary IgM response. Kinases in B cells respond rapidly to immunological stimuli, but the peak signal typically decays rapidly back to background level within hours of the initial activation (Irish *et al.* 2006). If the initial signaling cascade caused by TLR or BCR

activation has cycled from peak activation back to basal levels, and activated downstream transcription factors such as AP-1 and NFκB, the window of sensitivity may be closed for TCDD. The reported window of sensitivity for the LPS-activated IgM response is 3 h (Holsapple *et al.* 1986). ERK phosphorylation in B cells returns to background levels within 3 hours of LPS or CpG treatment (Banerjee *et al.* 2006). Integrating those observations, it is tempting to speculate that the window of sensitivity for TCDD disruption of the IgM response is attributable, at least in part, to alterations in kinase phosphorylation.

Observations described above, including TCDD suppression of kinase phosphorylation, disruption of transcription factor expression controlling plasmacytic differentiation, and impaired expression of activation markers could all individually impair humoral immunity, yet TCDD impairs normal TLR-activated expression for all. Furthermore, TCDD-activated AHR directly regulates the Igμ 3' α enhancer (Sulentic *et al.* 2004b), an event in the IgM response distal to Blimp-1 up-regulation during plasmacytic differentiation. Interference in both the initiation of plasmacytic differentiation, maintenance of costimulation necessary for humoral immunity, and Ig expression provides a partial explanation for the high sensitivity of B cells to TCDD. Taken together, the cumulative mechanism for TCDD-mediated suppression of the IgM response is multifaceted.

Experimental results presented in this chapter provide compelling evidence that TCDD impairs the primary IgM response via a block in plasmacytic differentiation upstream of Blimp-1 expression both *in vivo* and *in vitro*, not simply at the level of antibody production. Up-regulation of several phenotypic indicators for AFCs, including

118

CD138 and intracellular levels of Igκ and IgJ, were impaired by TCDD exposure. *In vitro* studies aimed to expand on results observed *in vivo* demonstrated both impaired activation marker expression and reduced phosphorylation of multiple kinases resulting from TCDD treatment. Collectively, these results validate and enhance the value of mechanistic *in vitro* studies establishing TCDD-induced deregulation of the Igμ 3' α enhancer (Sulentic *et al.* 2004a; Sulentic *et al.* 2004b), Pax5 (Schneider *et al.* 2008), and Blimp-1 (Schneider *et al.* 2009), and proceed to expand potential mechanisms for TCDD suppression of humoral immunity.

CHAPTER 4: EXPERIMENTAL RESULTS AND DISCUSSION FOR HUMAN MODELS

Development of a Human *in vitro* model for TCDD Disruption of the LPS-activated Primary IgM Response

Research efforts dedicated to elucidating the mechanism of TCDD immunotoxicity have used primarily rodent models, particularly the mouse. Unfortunately, the many significant advances in understanding the molecular biology underlying AHR function in the mouse have failed to produce information that can conclusively establish the health threat posed by TCDD and DLCs to human health. *In vivo* experimental evaluation of TCDD effects on humans is not ethical, however, availability of human tissues for *in vitro* experimentation presents the opportunity to validate that mechanisms of TCDD toxicity observed in mouse experimental models occur similarly for *in vitro* human experimental models.

While sources of primary human immune cells are commercially available there are several difficulties in their research application. Human immune cells tend to be expensive to obtain and process into useful experimental material. The purification required for modeling the direct effects of TCDD on human B cells results in significant cell loss during isolation. Due to these losses it is often difficult to obtain a sufficient number of cells for techniques such as immunoblotting, Northern Blot, or electromobility shift assays in individual donors. Additionally, the human population is likely to be polymorphic for both AHR and cell signaling components necessary for a functional primary IgM response, leading to increased variability of responses, and therefore uncertainty in analysis. Transgenic DNA alterations and introduction of foreign DNA

into primary human cells is difficult or impossible. Finally, unlike mouse splenic B cells, human peripheral blood B cells are not stimulated by LPS treatment to differentiate into ASC, making it impossible to make useful comparisons of LPS treated mouse cells to human cells.

Initial characterization of the SKW 6.4 cell line

An alternative approach to the use of primary human B cells circumventing many of the above limitations is use of immortalized human cell lines. Cell lines provide a theoretically unlimited supply of cells with homogeneous genetic makeup and responses, opening the possibility of performing analyses and manipulations that are impractical with primary cells. While many human B cell lines are available for research, few fulfill the prerequisites to make a useful model of the primary IgM response. Human B cells must, at the very least, increase secretion of IgM antibody in response to LPS treatment and express the AHR in order to compare TCDD effects on LPS activated mouse B cell responses to human B cell responses. The SKW 6.4 cell line, a subclone of the Daudi cell line identified for its low background IgM secretion under normal conditions with the capability for increased IgM secretion in response to B cell differentiation factor (Ralph *et al.* 1983), was found to respond to LPS treatment by increasing the secretion of IgM approximately 2-3 fold compared to vehicle treated cells (Figure 23). Immunoblot analysis of SKW 6.4 cell lysates showed that these cells to not express AHR (Figure 24) protein, further confirmed by a lack of AHR mRNA detected by QRT-PCR.
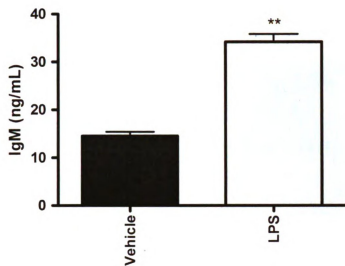
Figure 23. *LPS stimulates IgM secretion in SKW 6.4 cells.*

1x10⁵ SKW 6.4 cells were stimulated by addition of 100 µg/mL LPS. Following 96 h

incubation IgM secretion was quantified by human IgM ELISA. Results depicted are

*mean IgM ± standard error of the mean. ** P<0.01 as determined by 1 way ANOVA with*

Dunnet's post-hoc analysis comparing vehicle to LPS treatment.
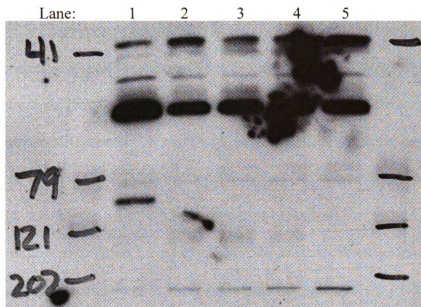
Figure 24. *Immunoblot analysis of AHR expression in SKW 6.4 cells. Total cell lysates from HepG2 (10 μg) and SKW 6.4 (100 μg) cells were assessed for human AHR expression. Lane 1 contains protein from HepG2 cells. A clear band at approximately 96 kilodaltons, the expected size of full length human AHR, is present in HepG2 cells. Lanes 2-5 contain cell lysates from SKW 6.4 cells. This figure includes handwritten/drawn annotation.*

While several approaches to enforced AHR expression were possible, the stable genomic integration of constitutively expressed human AHR was the most desirable outcome based on the expected consistency of results and cost of maintenance. The first attempt at generation of AHR expressing SKW 6.4 cells, called SKWA, was performed using the plasmid pcDNA3.1-TOPO with the open reading frame (ORF) for human AHR under the control of a Cytomegalovirus (CMV) promoter, a highly active promoter in most cell lines. 48 h post-transfection with pcDNA3.1-TOPO-HsAHR G418 antibiotic, which is inactivated by the neomycin resistance gene present within pcDNA3.1-TOPO-HsAHR, selection was initiated. Generation of G418-resistant cells required three weeks, after which the polyclonal pool of stable transfectants was screened for AHR gene expression by QRT-PCR. No AHR mRNA was detected. Further analysis of the polyclonal G418-resistant SKW 6.4 cells showed high levels of the neomycin resistance gene, demonstrating that the plasmid DNA had become stably integrated into the genome and was expressed, but AHR was not.

One potential cause for the failure of pcDNA3.1-TOPO-HsAHR to generate AHR expressing cells is the construction of the plasmid. To produce functional AHR an active promoter, complete cDNA sequence, and complete polyadenylation sequence must be present. The sequence beginning the CMV promoter of pcDNA3.1-TOPO-HsAHR through the end of the polyadenylation signal is approximately 4.5 kilobases. Given the entire vector is approximately 8.1 kilobases, the majority of the plasmid consists of components necessary for expression of AHR. When supercoiled plasmid DNA is transfected into any cell line it must first be linearized prior to genomic integration. The "break site" at which the plasmid linearizes occurs randomly. Accepting that the DNA

break site is random, and considering the size of the sequence necessary for AHR expression, it is most likely the break occurs in some portion of the sequence necessary for AHR expression. Based on the design of the plasmid, all the selection pressure is placed on the neomycin resistance cassette, with no advantage to expression of AHR. In such a situation, the likelihood for generating antibiotic resistant cell lines that do not express the gene of interest is greater than the likelihood of obtaining a cell line expressing the gene of interest, especially if there is a disadvantage to transgene expression.

Alternatively, another possible explanation for the lack of AHR expression in G418-resistant SKW 6.4 cells is a phenomenon known as "promoter neighboring", in which a highly active promoter recruits transcriptional machinery, outcompeting neighboring promoters for gene expression (Kimberland *et al.* 1999). To circumvent this issue an internal ribosome entry site (IRES) allows expression of two proteins from a single mRNA transcript. Use of an IRES addressed both the randomized break site issue and promoter neighboring effects that may have caused the failure of the pcDNA3.1-TOPO-HsAHR vector. Unlike the pcDNA3.1-TOPO-HsAHR, IRES-based vectors allow antibiotic selection pressure to be placed on both AHR and neomycin resistance gene expression simultaneously, thus the cell line cannot express the neomycin resistance cassette without also producing AHR mRNA. The ORF for human AHR was cloned into pIRESneo3 vector, generating a CMV driven AHR expression vector in which AHR and neomycin resistance should be coexpressed. SKW 6.4 cells were transfected by electroporation with pIRESneo3-HsAHR and selected with G418. This method did not produce any stable transfectants in four separate trials.

Following the failure of pIRESneo3-HsAHR to generate a stable transformant population it was suspected that the CMV promoter may be ineffective in the SKW 6.4 cell line. The G418 resistant SKW 6.4 cells generated using the pcDNA3.1-TOPO-HsAHR plasmid used the SV40 promoter to drive expression of neomycin resistance. A SV40 driven protein expression plasmid, pZeoSV2, was obtained based on the prior knowledge that SV40 was a sufficiently active promoter to drive expression of the neomycin resistance gene. No drug resistant colonies were ever obtained using pZeoSV2-HsAHR despite multiple attempts to generate antibiotic resistant populations.

To determine relative promoter activity in SKW 6.4 cells several different luciferase reporter plasmids were obtained, each containing alternative forms of CMV or a CMV/β-actin chimeric promoter coupled with different polyadenylation signals (SV40 or Bovine Growth Hormone). SKW 6.4 cells were electroporated and luciferase activity was measured at 24, 48, and 72 h post-electroporation. Figure 25 demonstrates that CMV promoters have relatively strong activity in the SKW 6.4 cell line, which can be modestly altered depending on the polyadenylation sequence used. Additionally, even with single transient transfection sustained activity of the CMV promoter is observed.
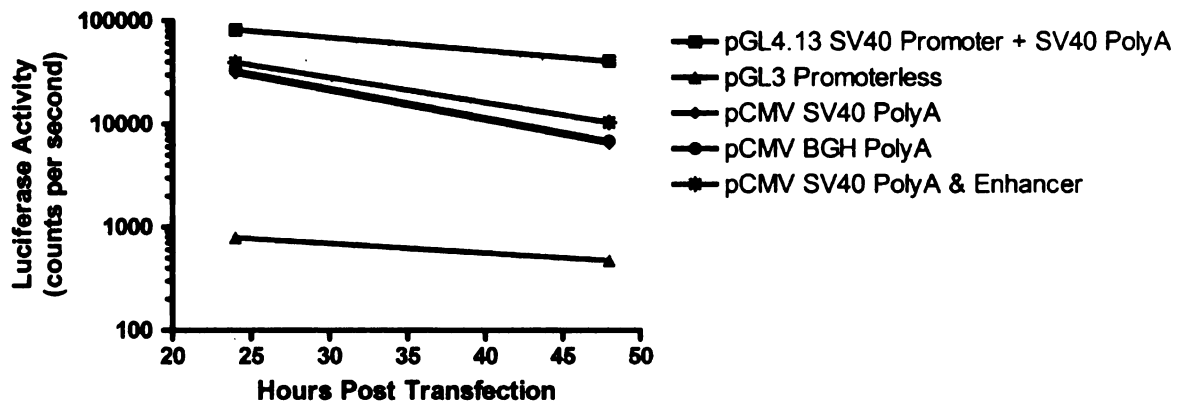
Figure 25. Relative Promoter Activities in SKW 6.4 cells. SKW 6.4 cells were

electroporated with equal quantities of plasmid DNA and assayed for luciferase activity

24 and 48 h post-transfection.

Based on the observation that CMV promoters generated relatively high luciferase

reporter activity and robust GFP expression from transient transfections in SKW 6.4

cells, a new expression vector was constructed utilizing a highly active form of CMV.

The promoter of the pmaxGFP vector used in transient transfection of SKW 6.4 cells to

assess transfection efficiency is a CMV promoter coupled with intron A, a modification

of the CMV promoter that drives higher transcriptional activity than other CMV

promoters lacking intron A (Chapman *et al.* 1991). By selecting a highly active promoter

and fusing AHR to GFP it was believed that the probability of successfully generating

AHR expressing SKW 6.4 cells was improved. GFP was cloned in-frame with the C-

terminus of AHR in the vector phCMV-CGFP by mutating the native stop codon of AHR

to a leucine residue, with the resulting ORF generating a GFP-fused form of AHR. A

nonfused form of AHR was also generated, leaving the normal AHR stop codon intact.

phCMV-HsAHR and phCMV-HsAHR-GFP were individually electroporated into

separate pools of SKW 6.4 cells, then following 72 h recovery, treated with G418 to

select stable cell lines. No cell lines containing AHR-GFP were ever identified in three

separate electroportations. Two pools of G418 resistant phCMV-AHR electroporated

cells were identified following 6 weeks of culture and screened for AHR mRNA by

QRT-PCR (Figure 26). Both pools contained cells expressing detectable levels of AHR

mRNA, but following the recovery of frozen stocks AHR mRNA could not be detected.
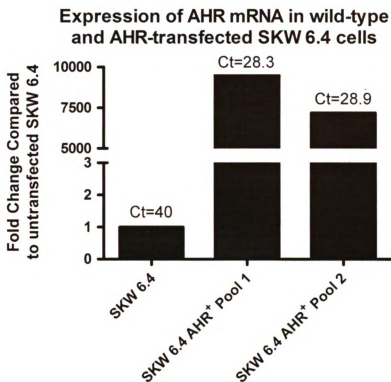
Figure 26. AHR expression in G418-resistant pools of SKW 6.4 cells. SKW 6.4 cells were electroporated with phCMV-AHR plasmids. Following 72 h recovery cells were grown in the presence of 1.2 mg/mL G418 for 6 weeks. G418 resistant cells were assessed for AHR mRNA expression by QRT-PCR. For graphing purposes the Ct value for AHR expression in native SKW 6.4 cells was set at 40.

Following the failure of plasmid-based vectors to generate sustainable populations of AHR expressing cells an alternative approach to integration of DNA into host genomes was utilized, in which lentiviral transduction of SKW 6.4 cells with replication incompetent virus consisting of an expression cassette for a single mRNA containing both HsAHR and puromycin resistance (PuroR) was performed. Lentiviral genomes are randomly inserted by the enzyme Integrase into open regions of chromatin, and unlike supercoiled plasmid DNA, without a requirement for linearization by random breakage prior to integration. Recognizing that CMV sequences differ between vendor plasmids, the CMV with intron A promoter was selected based on the knowledge that the promoter had provided transient AHR expression in the phCMV-HsAHR vector. DNA for the CMV sequence containing intron A combined with either HsAHR or HsAHR-GFP was PCR amplified from phCMV-based vectors and cloned into the pLEX-MCS vector after removing the vendor supplied CMV promoter without intron A. Initial evaluations of lentivirus produced from the pLEX-CMVi-HsAHR and pLEX-CMVi-HsAHR-GFP showed very low titers of infectious virus, from 500-1000 transfection units per mL. This contrasted sharply with titers of GFP virus obtained from pLEX-Jred/TurboGFP, ranging from $3x10^6$ to $8x10^6$ transfection units per mL. In consultation with OpenBiosystems technical support it was learned that the inclusion of intron A provided a splice acceptor site in the mRNA produced during viral production. The ψ packaging sequence of HIV, the parental virus for the pLEX-MCS vector, contains a strong splice donor. During viral production the splice donor finds the splice acceptor in the intron and excises itself, resulting in removal of both the ψ packaging sequence and CMV promoter for AHR

expression. The final outcome is low production of functional lentiviral vector (John Wakefield, personal communication).

Following the explanation for the low viral production the pLEX-based vectors were rederived by excising the HsAHR and HsAHR-GFP sequences from phCMV and inserting them into pLEX-MCS to generate new transfer vector plasmids lacking intron A. Newly generated lentiviruses, pLEX-HsAHR and pLEX-HsAHR-GFP, were used separately to transduce SKW 6.4 cells. Following puromycin selection, stable pools of transformants were identified and screened for GFP expression by FACS (Figure 27), and termed SKWAG to indicate "SKW 6.4 expressing AHR-GFP". Following puromycin selection, GFP expression occurred in more than 95% of all cells.
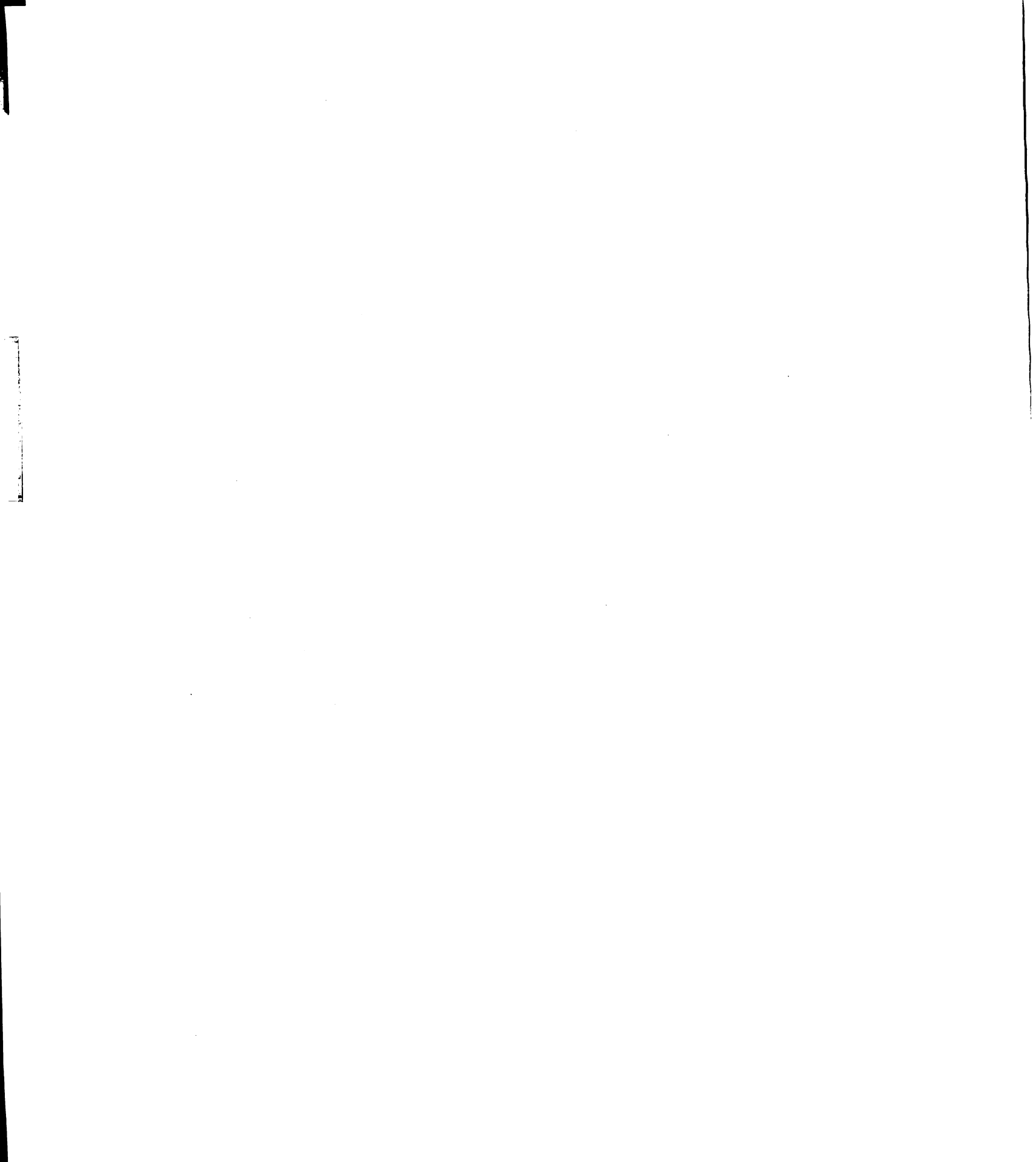
Figure 27. GFP expression in transduced SKW 6.4 cells. SKW 6.4 cells were transduced with a lentiviral expression vector pLEX-HsAHR-GFP. Transduced cells were selected by resistance to varying concentrations of puromycin (1, 3, 5, or 10 µg/mL). Nonviable cells were detected using the viability dye TO-PRO-3.

Native SKW 6.4 — SKWAG 1

| 0.05 | 0.07 | 0.60 |
| 97.62 | 2.26 | 2.47 | 1.35 |

95.58

SKWAG 3 — SKWAG 5 — SKWAG 10

| 0.95 | 27.01 | 6.90 | 94.33 | 1.29 |
| 95.72 | 1.87 | 64.22 | 0.57 | 3.8 |

| 2.99 | 0.34 |
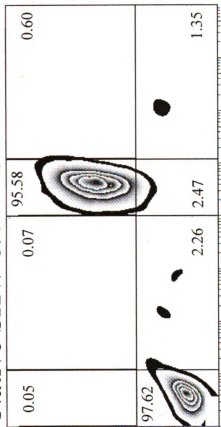
AHR-GFP (GFP Fluorescence)
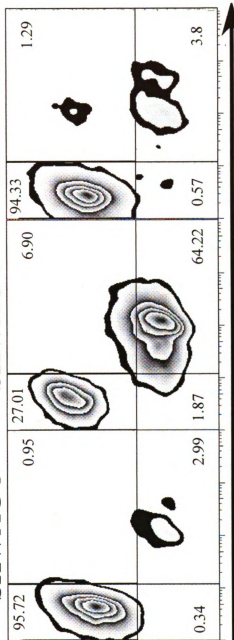
Viability (TO-PRO-3)

133

Pools of puromycin resistant cells were grown in the presence of different

concentrations of puromycin. Increasing antibiotic concentration allows crude control

over expression of the antibiotic resistance gene, and by proxy the expression of AHR.

Different pools of SKWAG were given the suffix 0.5, 1, 3, 5, or 10 to indicate the

concentration of puromycin in which they were selected. Following positive

identification of a GFP$^+$ population SKWAG10 cells, antibiotic selection pressure was

removed and cells rescreened by FACS one week later. Removal from puromycin

selection resulted in a temporary increase in GFP expression, believed to be indicative of

AHR, in SKWAG10 cells (Figure 28). Extended maintenance in the absence of

puromycin resulted in progressive loss in GFP fluorescence (Figure 29), potentially

resulting from silencing of lentiviral DNA following removal of selection pressure. This

finding led to the decision to maintain cell lines in continuous puromycin. Following

several weeks in culture a polyclonal pool of SKWAG cells arose, which was in turn

screened for AHR expression by QRT-PCR. Despite relatively high levels of GFP

fluorescence, no expression of AHR was detectable in any SKWAG cell lines.
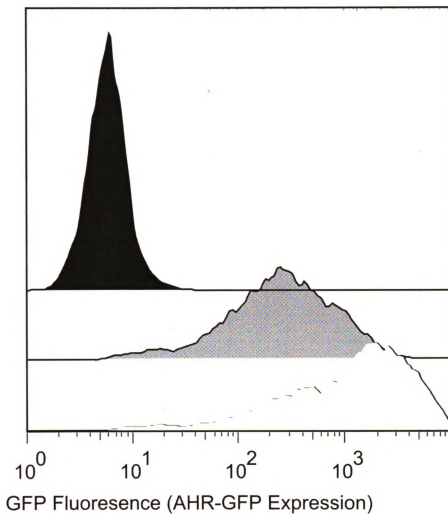
	TUBE NAME	Geom. Mean , FL1-H
⬛	Native SKW 6.4	5.65
▨	SKWAG 10 with Puromy...	239.93
☐	SKWAG 10 without Puro...	981.20

Figure 28. GFP expression in the presence and absence of puromycin. SKW 6.4 and SKWAG10 cells lines were evaluated for GFP fluorescence by flow cytometry. SKWAG 10 cells were grown in the absence of puromycin for 48 h and compared to SKWAG 10 cells grown in the continuous presence of puromycin. Native SKW 6.4 cells are presented as an indicator of background fluorescence.
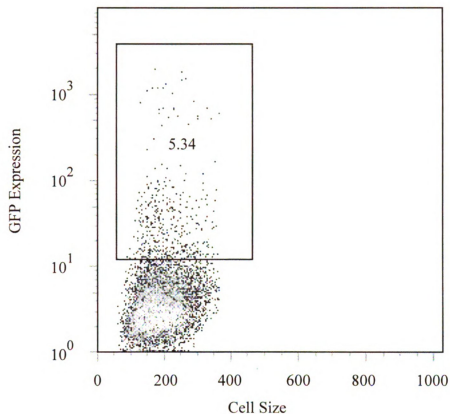
Figure 29. GFP expression loss following 1 week of culture in the absence of puromycin. SKWAG1 cells were removed from puromycin selection 1 week prior to sorting by FACS. GFP^+ cells were identified based on GFP fluorescence greater than 99% of native SKW 6.4 cells.

A second polyclonal cell line was derived from the HsAHR-GFP lentivirus using 293T cells, called 293T-HAG. Immunoblot of cell lysates from 293T-HAG, in contrast to the experience with SKWAG, demonstrate high expression of a protein of approximately 120 kDa that reacts with AHR specific antibodies (Figure 30), confirming the production of a GFP fused form of AHR. Immunoblot analysis also demonstrated multiple smaller bands in 293T-HAG that are detected by the anti-human AHR antibody used, suggestive of either AHR degradation or alternative splice products in the polyclonal 293T-HAG pool. Several SKW 6.4 cell lines transduced or transfected with AHR expression vectors were also assessed, but none were found to express significant amounts of AHR or AHR-GFP.

Development of 293T-HAG cell line provided the material to develop a FACS-based AHR detection method, allowing for more rapid determination of AHR expression in a pooled population. Additionally, if a minority population of SKWAG cells exists expressing AHR-GFP and is at a growth disadvantage relative to SKWAG cells expressing GFP alone it may not be possible to discriminate between populations in an immunoblot, whereas this can be immediately detected using FACS.
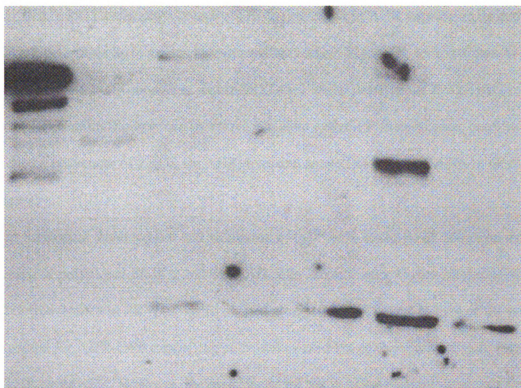
Figure 30. AHR immunoblot in 293T-HAG, HepG2, and SKW 6.4 cell lines. Total cellular protein was separated by SDS-PAGE and probed for AHR protein by immunoblot. From left to right lane assignments are as follows: 293T-HAG, HepG2, native SKW 6.4, SKW 6.4 transduced with pTZV-HsAHR-GFP, SKW 6.4 transfected with phCMV-HsAHR, SKWAG1 cells, and SKW 6.4 transduced with pTZV-HsAHR. The single band in lane 2, HepG2, corresponds with human AHR of approximately 96 kDa.

While 293T cells natively express AHR, increases in AHR expression detected by FACS are detectable as increases in immunofluoresence. Figure 31 demonstrates AHR expression is relatively consistent within 293T-GFP cells. Analysis of 293T-HAG cells shows AHR immunofluoresence increases correlate with GFP fluorescence, confirming both the effectiveness of FACS for AHR detection as well as fusion of AHR to GFP (Figure 31).

Following development and validation of the FACS-based AHR detection the screening of polyclonal SKWA and SKWAG cells was initiated. Figure 32 shows AHR immunofluoresence in SKWAG cells, shifted along both the X- and Y-axes of the graph as expected for AHR-GFP expressing cells, with over 11% of the screened cells viable and AHR expressing. However, the majority of the SKWAG cells were dead, and for the SKWA cell line less than 9% of cells were viable. Dead cell populations for both the SKWA and SKWAG cell lines are AHR positive, and were slightly, though nonsignificantly, higher in AHR immunofluoresence than their viable counterparts. The loss of viability in cultures expressing AHR could be explained by potential toxicity associated with expression of HsAHR (Craig Rowlands, personal communication).
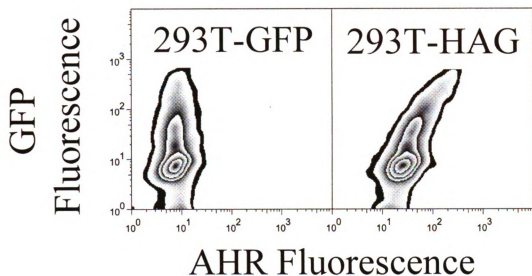
Figure 31. Correlation of AHR immunofluoresence with GFP fluorescence in 293T cell lines. 293T human kidney cells were transduced with pLEX-GFP or pLEX-HsAHR-GFP lentivirus. Following establishment of a puromycin resistant cell lines intracellular AHR expression was assessed by FACS.

Figure 32. AHR expression correlates with nonviability. SKW 6.4 cells were transduced with pLEX-HsAHR-GFP or pLEX-HsAHR. Puromycin resistant populations stained for viability then assessed for AHR immunofluoresence by FACS.
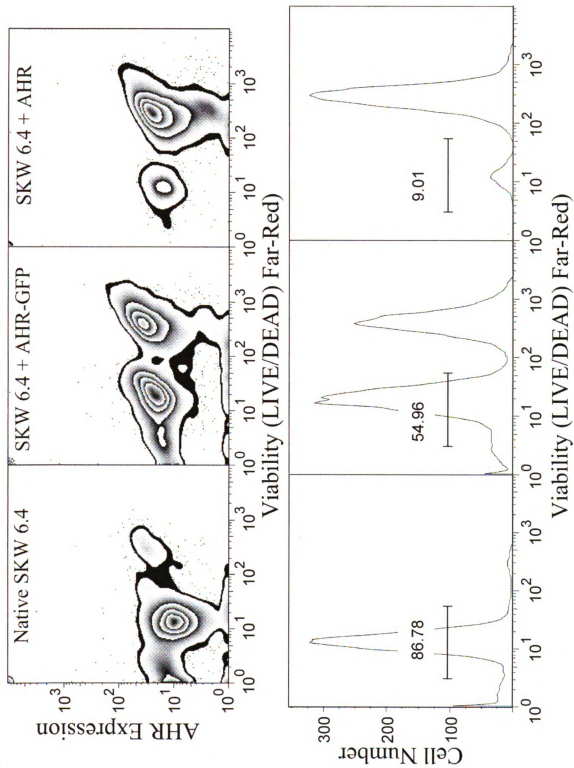
With the knowledge that the lentiviral HsAHR-GFP vector produced the desired protein, but not in SKWAG cells, it was clear that previously unanticipated difficulties in the generation of stable B cell lines were present. Transfer plasmid identity had been verified by restriction digestion prior to viral production, and the successful generation of GFP$^+$ and puromycin resistant cell lines demonstrated packaged lentivirus was competent for gene transfer. However, the actual composition of the lentiviral pool had not been examined.

Several methods for measurement of lentiviral vector exist, including QRT-PCR based techniques (Sastry *et al.* 2002). pLEX-HsAHR and pLEX-HsAHR-GFP lentiviral vector RNA was isolated and assessed by QRT-PCR for AHR, GFP, or puromycin resistance genes. Since the lentiviral genome is a single strand of mRNA, if a single form of virus is produced then equal quantities of each gene should be detected. QRT-PCR analysis of separate lots of virus revealed that quantities of viral genes, putatively on the same single mRNA strand, were not equal. After subtracting Ct values obtained from non-reverse transcribed samples, the pTZV-HsAHR-GFP lentivirus was found to contain no AHR mRNA but did contain significant quantities of GFP mRNA. Plasmid DNA for the pTZV-HsAHR-GFP vector was verified by QRT-PCR to contain equal copy numbers of AHR, GFP, and puromycin resistance genes. After subtracting Ct values obtained from non-reverse transcribed samples, pLEX-HsAHR-GFP-20080707 contained no lentiviral RNA. Some lots of virus, pTZV-HsAHR, pLEX-HsAHR-20080613, and pLEX-HsAHR-GFP-20080404, did contain detectable amounts of lentiviral RNA for AHR, but Ct values were not equal for PuroR. This observation is indicative of multiple isoforms of lentivirus being produced (Table 1).

Because polyclonal isoforms of virus were also generated from an AHR expression vector produced by an offsite collaborator (pTZV-based vectors), evidence suggests that splicing issues are not restricted simply to pLEX-HsAHR and pLEX-HsAHR-GFP, but extend to other lentiviral gene transfer vectors as well. This observation provides a potential explanation for generation of SKWAG cells that do not express AHR mRNA, as a spliced form of the virus may remove AHR entirely or remove significant portions of the gene, while leaving GFP and PuroR intact. Isoforms that spliced out PuroR would be killed during the selection process, eliminating cell lines that contained AHR or AHR-GFP alone. Confirmation of the polyclonal viral pool was obtained from puromycin resistant cell lines SKWAG and SKWA. In the pLEX-derived vectors AHR, GFP, and PuroR are all transcribed as a single strand of mRNA, thus Ct values should be equal if every copy of the genome-integrated lentiviral vector contains the same sequence. QRT-PCR analysis of gene expression for AHR, GFP, and PuroR demonstrated variations in amounts of mRNA for each gene (Table 2), suggestive of transduction with a pool of lentiviruses containing multiple spliced isoforms.

| | AHR Ct | | |
Virus Lot Name	Value	GFP Ct Value	PuroR Ct Value
pTZV-HsAHR-GFP	33.58	22.75	Not Evaluated
pTZV-HsAHR	16.46	16.13	Not Evaluated
pLEX-HsAHR- 20080613	15.48	Not Evaluated	17.26
pLEX-HsAHR-GFP- 20080707	21.17	Not Evaluated	21.55
pLEX-HsAHR-GFP- 20080404	18.71	Not Evaluated	19.85
pLEX-GFP	Undetected	Not Evaluated	14.7

Table 1. Direct assessment of lentiviral RNA. RNA was isolated from cell culture
supernatants following lentiviral vector packaging. Following reverse transcription QRT-
PCR was used to directly quantify the amount of RNA present for genes included in the
gene transfer vector. PuroR gene expression was not evaluated in pTZV-based vectors
because the gene is not included in the plasmid source used for packaging lentivirus.

Cell Line	AHR Ct Value	GFP Ct Value	PuroR Ct Value
SKWAG	30.6	16.28	22.41
SKWA	29.35	22.1	36.09

Table 2. Direct assessment of vector gene expression in antibiotic-resistant cell lines.

QRT-PCR was performed on RNA from antibiotic-resistant cell lines.

While evidence shows that the lentiviral pool contained multiple isoforms of HsAHR and HsAHR-GFP, one method to circumvent the problem of polyclonal populations is to derive a monoclonal line of SKWAG cells expressing only full length HsAHR or HsAHR-GFP. A polyclonal pool of approximately 100×10^6 puromycin resistant GFP^+ cells previously transduced with lentiviral HsAHR-GFP vector were sorted by FACS and cloned by limiting dilution. Out of approximately 600 viable cells recovered following sorting and plating, 50 monoclonal colonies of SKWAG cells were picked from 96 well plates during the weeks following cloning. 30 of 50 monoclonal colonies expanded, albeit at dramatically different rates, to populations of at least 5×10^5 cells, sufficient to screen for AHR protein expression by FACS. The earliest screenings were performed within 2 weeks of colony expansion, while the last colonies screen were not sufficiently expanded until 2 months following cloning. Of the 30 monoclonal cell lines screened none showed AHR immunofluoresence above the background observed with normal SKW 6.4 cells.

Extensive efforts to establish AHR^+ SKW 6.4 cells were ineffective. Based on the relatively low viability of SKWAG and SKWA lines, difficulty in maintaining cultures with viability in excess of 90%, variable doubling times, and occasional collapse of the viable population, evidence suggests SKW 6.4 cells expressing AHR are, at the very least, at a growth disadvantage compared to cells not expressing AHR. One consequence of a growth disadvantage is that AHR mRNA may be detectable in the days or weeks following initial gene transfer, but over time will be diluted out of the heterogeneous population of cells as the non-AHR expressing cells increase number. Several approaches

may be fruitful in future efforts to develop AHR$^+$ SKW 6.4 cells, including coexpression

of chaperone proteins HSP90 and XAP2 in the case that HsAHR misfolding is

responsible for toxicity associated with high AHR expression, or use of an inducible

expression systems activated by tetracycline, ecdysone, or isopropyl β-D-1-

thiogalactopyranoside. Techniques allowing for reporter indication of functional AHR

expression may also provide a useful method of detection, such as incorporation of a

DRE driven red fluorescent protein in the lentiviral vector. Activation with an AHR

ligand such as 6-formylindolo[3,2-b] carbazole, which is subsequently degraded by

metabolism, would drive expression of a long-lived, highly fluorescent marker which is

readily detectable by FACS, facilitating sorting for the cell population containing

functional AHR.

CHAPTER 5: CONCLUDING DISCUSSION

Results presented within this dissertation can be broadly classified as technical or scientific advances for the field of toxicology. Applied together, both advances revealed insights regarding the mechanism for TCDD disruption of primary humoral immunity, resulting in reduced uncertainty pertaining to the health hazard posed by dioxins and DLCs.

The most significant technical advance came from application of FACS to perform single cell, multiparametric analyses of the transcription factor network regulating plasmacytic differentiation. While the field of toxicology has utilized FACS to analyze changes in the composition of the immune system, only in recent years have investigators begun to examine intracellular events involved in chemical disruption of homeostasis. Analyzing expression and activation of transcription factors, and evaluating how TCDD disrupts their expression, is a novel technical advance in immunotoxicology. Single cell analysis is particularly useful for generating computational models of biological processes, as it allows for identification and characterization of subpopulations that are not apparent in bulk lysis techniques. For example, in R848-activated CH12.LX cells there are two populations, a group that phosphorylates JNK and a group that does not (Figure 17). Bulk lysis would show that JNK was phosphorylated in the population, but would erase the ability to observe that only a minority population is actually responding strongly to immune response activation. Most illustrative of the power of multiparametric flow cytometry is the difference in the amount of information gleaned from a single experiment. A single immunoblot give two basic pieces of information, molecular weight and relative protein expression. A simple 4-color FACS experiment

asking the most basic question of whether a protein is expressed provides at least 24 combinations of measurements within a single cell. That does not consider the wealth of information that comes from the relative expression of a given protein.

A single series of experiments measuring transcription factor expression, activation marker expression, and kinase phosphorylation can be accomplished simultaneously using splenocytes from less than three mice. As efforts to reduce, refine, and replace models employing intact animals, techniques such as multiparametric FACS can assist investigators to garner more information with less starting material. Along these lines, the experiments described in Chapter 3 provide a proof of principle that multiparametric analyses are a powerful method facilitating reduced animal use.

Studies examining TCDD effects on transcription factor expression are typically performed only at times of peak abundance with a limited range of TCDD concentrations, often covering only a single order of magnitude. The experiments described in Chapter 3 not only examine TCDD-mediated effects across a wider range of concentrations, but also across time. Moreover, the multiparametric analysis of protein expression allows single cell correlations between transcription factor expression and cell surface protein abundance. The dynamic combination of evaluating multiple times, TCDD concentrations, and proteins in a systematic manner resolves the effects of TCDD on a resolution never achieved before.

Many scientific advances were made in the progress of this dissertation research, most noteworthy the improved understanding of TCDD effects on the plasmacytic differentiation control circuit both *in vivo* and *in vitro*. The solid evidence for suppression of LPS-induced Blimp-1 expression by TCDD *in vivo* led to examination of additional

regulatory events preceding increases in Blimp-1. The findings that LPS-elicited changes in BCL-6 expression are disrupted by TCDD is a novel discovery, and provides another avenue of research to understand how TCDD alters the plasmacytic differentiation control circuit. Suppression by TCDD of LPS-activated c-Jun phosphorylation (Figure 10) provided supportive evidence for results showing impairment of AP-1 DNA binding and activity (Schneider *et al.* 2009; Suh *et al.* 2002a), further validating the CH12.LX cell line as a useful model for investigating TCDD immunotoxicity. Viewed cumulatively, TCDD alters expression of several transcription factors, leading to failure of B cells to achieve the ASC phenotype.

One persistent difficulty in application of scientific research to policy making is the uncertainty resulting from cross-species extrapolation. The validation that *in vitro* disruption of Blimp-1 expression occurs *in vivo* suggests a persistent, nonartifactual mechanism for TCDD-mediated suppression of the primary IgM response in the mouse. Because the plasmacytic differentiation control circuit is conserved between human and mouse, validating results from murine models in human models will be indispensable in understanding dioxin and DLC effects on B cells.

Concomitant with disrupted plasmacytic differentiation, the observation that TCDD impaired LPS-elicited cell surface activation marker expression is another potentially important event. Impairments of MHC Class II, CD80, and CD86 will decrease B cell – T cell interaction, resulting in compromised humoral immunity against most pathogens. In part, effects of TCDD on MHC Class II, CD80, and CD86 explain why the sRBC-elicited primary IgM response is more sensitive to TCDD than the LPS-elicited primary IgM response. LPS-activated B cells do not require presence of

accessory cell types to differentiate into antibody-secreting cells, whereas the sRBC-elicited primary IgM response is dependent on cell-cell interactions between T cells and B cells, interactions dependent on MHC Class II, CD80, and CD86. Going forward, evaluation of surface markers essential for cell-cell communication in the immune system has the potential for helping to identify mechanisms responsible for suppression of immune responses by chemicals beyond dioxins and DLCs.

FACS-based methods for evaluation of phosphorylation of specific kinases were unknown prior to 2002 (Perez and Nolan 2002) and have only recently been applied to understanding pharmacology (Krutzik *et al.* 2008). Studies described in Chapter 3 are the first to apply single cell, multiparametric analysis for phosphorylation status of specific kinases in the context of toxicology research. Examining multiple kinases within the same cell illuminates the signaling network engaged by immune response stimuli, and potentially identifying nodes within the signaling network that are altered by environmental chemicals. For example, results from Figure 21 show that in primary B cells the majority of cells increase AKT and ERK phosphorylation, but there are minority populations that upregulate neither kinase, or only single kinases. Because chemicals have the potential of affecting subsets within a given population, and examining single parameters using bulk lysis techniques such as immunoblot can obscure important biological events occurring within minority subpopulations, the potential for missing important indicators of toxicity cannot be understated. Multiparametric interrogations of single cells address some of the limitations of bulk lysis methods and represent a valuable avenue of assessment with tremendous potential for aiding toxicology studies. Additional information gleaned from dissecting the kinase signaling network can be used to add a

new layer of refinement on computational models designed to predict disruption of plasmacytic differentiation.

While literature reports exist showing that TLR ligands cause AKT phosphorylation (Francois *et al.* 2005; Hebeis *et al.* 2005; Vivarelli *et al.* 2004), no reported evidence exists for R848- or CpG-activated AKT phosphorylation in B cells. Most studies of TCDD effects on specific kinases have not been performed in the context of an activated immune response. Studies in Chapter 3 are the first to illustrate TCDD impairs AKT, ERK, and JNK phosphorylation in B cells even when considering only single parameter analysis, and was further extended to show TCDD impairs activation of all three kinases simultaneously within single cells.

Uniting findings presented in Chapter 3, evidence suggests that TCDD suppression of the primary IgM response results from a cascade of effects, potentially beginning during the activation of kinases by immunologic stimuli. Because the window of sensitivity for TCDD-mediated suppression of the IgM response occurs early in B cell activation, and evidence presented in Chapter 3 shows TCDD disrupted TLR-activated events during the first hour following treatment, future efforts to examine TCDD effects on cell signaling may be fundamental in understanding the mechanism of TCDD immunotoxicity. There are many basic questions to be addressed in the future, such as whether AHR is required for suppression of AKT, ERK, or JNK phosphorylation. Disruption of early events in the immune response is amplified and propagated into later stages of differentiation, and coupled with direct effects of AHR on the *IgH* 3'α enhancer, resulting in a significant impairment of the primary IgM response.

Based on results obtained and described within this thesis, Figure 33 depicts the putative regulation of the plasmacytic differentiation control circuit in the presence and absence of TCDD. TLR activation causes increased phosphorylation and activation of the kinases AKT, ERK, and JNK. In turn, BCL-6 and AP-1 activity is changed by reducing the abundance of BCL-6 and increasing the transcriptional activity of AP-1, allowing increased expression of Blimp-1. As Blimp-1 levels increase there is a concomitant increase in phenotypic indicators of plasmacytic differentiation.

Figure 33. Summary figure for LPS-activated changes in kinase and transcription factor activity in the presence and absence of TCDD. Positive regulation in depicted as ➔ *and negative regulation as* ⊣*. Kinases are depicted as* ⬭ *and transcription factors are depicted as* ◇ *. Line thickness and object size represent, respectively, relative activity and abundance.*

Transcription Factor Network Following LPS Treatment
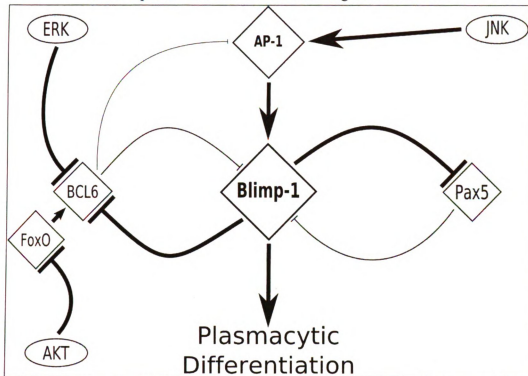
Transcription Factor Network Following LPS + TCDD Treatment
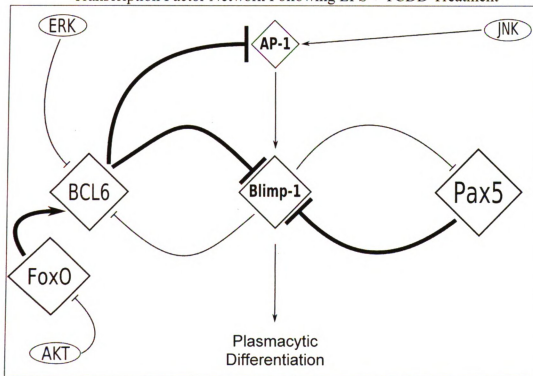
Extending the observations gained using *in vitro* and *in vivo* mouse models to human *in vitro* models would be a significant advance in understanding health risks posed by DLCs. Extensive efforts to develop an *in vitro* human model suitable for modeling LPS-activated plasmacytic differentiation were successful in a limited scope. The SKW 6.4 cell line was established as LPS-responsive and proved amenable to both transient and persistent genetic manipulations. However, to make a suitable model for investigating DLC effects, the expression of HsAHR was essential. Transient expression of HsAHR was observed in SKW 6.4 cells using both plasmid-based and lentiviral expression vectors, but unremitting expression of HsAHR proved untenable. Sustained expression of HsAHR, likely at higher than normal physiologic levels, caused cell death in SKW 6.4 cells. Other cell lines, in particular 293T, can accommodate high level long term expression of HsAHR. At this point there are unidentified factors in the SKW 6.4 and 293T cell lines that account for the difference in sensitivity to HsAHR. The clearest benefit to the experiences gained with HsAHR and HsAHR-GFP expression vectors was an improved understanding of how to develop future expression vectors. Secondarily, confirmation of lentiviral vector splicing as a major factor affecting both viral production and protein isoforms is valuable in preventing future failures when working with lentiviral, and likely retroviral, gene transfer vectors.

In summary, significant scientific progress came in the extension of *in vitro* observations regarding disruption of the plasmacytic differentiation control circuit to *in vivo* models, establishment of several novel mechanisms of action for TCDD in affecting the both transcription factor expression and the cellular activation process, development of a more rapid method for moderate to high throughput detection of human AHR, and

from efforts to develop a human model suitable for assessing TCDD effects *in vitro*. While data gaps still exist in fundamental understanding for TCDD suppression of humoral immunity, efforts to address the unknowns have advanced the field of dioxin immunotoxicology and opened new avenues of exploration.

APPENDIX A. Antibodies

Target	Fluoro-phore	Host	Isotype	Type	Catalog #	Supplier
AHR	None or APC	Rabbit	IgG	polyclonal	sc-5579	Santa Cruz Biotech
B220 (CD45R)	PerCP-Cy5.5	Rat	$IgG_{2a, \kappa}$	monoclonal, RA3-6B2	103235	Biolegend
BCL-6	None	Rabbit	IgG	polyclonal	sc-368	Santa Cruz Biotech
BCL-6	None	Rabbit	IgG	polyclonal	ab19011-100	Abcam
Blimp-1	None or PE	Goat	IgG	polyclonal	sc-13206	Santa Cruz Biotech
c-jun	FITC	Rabbit	IgG	polyclonal	sc-1694	Santa Cruz Biotech
CD16/32	None	Mouse	$IgG_{2b, \kappa}$	monoclonal, 2.4G2	553142	BD Biosciences
CD19	PE	Rat	$IgG_{2a, \kappa}$	monoclonal. 2D4	553786	BD Biosciences
CD69	PE	Armenian Hamster	IgG	monoclonal, H1.2F3	104508	Biolegend
CD80	APC	Armenian Hamster	IgG	monoclonal, 16-10A1	104714	Biolegend
CD86	PE/Cy7	Rat	$IgG_{2a, \kappa}$	monoclonal, GL-1	105014	Biolegend
goat IgG	APC	Donkey	IgG $F(ab')_2$	polyclonal	sc-3860	Santa Cruz Biotech
Ig J-chain	None	Goat	IgG	polyclonal	sc-34654	Santa Cruz Biotech
Igκ light chain	FITC	Rat	IgG_1	monoclonal	sc-53080	Santa Cruz Biotech

Igμ chain	FITC	Goat	IgG	polyclonal	FI-2020	Vector Laboratories
goat IgG	FITC	Donkey	IgG F(ab')$_2$	polyclonal	sc-3853	Santa Cruz Biotech
MHC Class II I-A^B	FITC	Mouse	IgG$_{2a, κ}$	monoclonal, AF6-120.1	116406	Biolegend
MHC Class II I-A^P	FITC	Mouse	IgG$_{2a, κ}$	monoclonal, 7-16.17	558921	BD Biosciences
Pax5	AF647	Goat	IgG	polyclonal	sc-1974	Santa Cruz Biotech
Phosphorylated c-jun (Ser 63)	AF647	Mouse	IgG$_1$	monoclonal, KM-1	sc-822	Santa Cruz Biotech
Phosphorylated AKT (Ser473)	PE	Mouse	IgG	monoclonal, M89-61	560378	BD Biosciences
Phosphorylated JNK (Thr183/Tyr185)	AF647	Mouse	IgG	monoclonal, G9	9257	Cell Signaling
Phosphorylated ERK1/2 (Thr202/Tyr204)	AF488	Rabbit	IgG	monoclonal, D13.14.4E	4344	Cell Signaling
Rabbit IgG	AF647	Donkey	IgG	polyclonal	A31573	Invitrogen
Rabbit IgG	PerCP	Bovine	IgG	polyclonal	sc-45099	Santa Cruz Biotech
Rabbit IgG	PE-Cy5.5	Goat	IgG F(ab')$_2$	polyclonal	L43018	Invitrogen
Rabbit IgG	APC	Goat	IgG F(ab')$_2$	polyclonal	sc-3846	Santa Cruz Biotech
TCRβ	PE/Cy7	Armenian Hamster	IgG	monoclonal, H57-597	109221	Biolegend
Isotype	APC	Goat	IgG	polyclonal	sc-3867	Santa Cruz Biotech
Isotype	None	Goat	IgG	polyclonal	sc-3887	Santa Cruz Biotech

Isotype	AF647	Mouse	IgG_1	polyclonal	sc-24636	Santa Cruz Biotech
Isotype	FITC	Mouse	IgG_1	polyclonal	sc-2855	Santa Cruz Biotech
Isotype	FITC	Mouse	$IgG_{2a, \kappa}$	polyclonal	554647	BD Biosciences
Isotype	FITC	Mouse	IgM	polyclonal	sc-2859	Santa Cruz Biotech
Isotype	FITC	Rabbit	IgG	polyclonal	sc-3870	Santa Cruz Biotech
Isotype	None	Rabbit	IgG	polyclonal	sc-3888	Santa Cruz Biotech
Isotype	PE	Rat	$IgG_{2a, \kappa}$	polyclonal	554689	BD Biosciences

APPENDIX B. TaqMan Primers and Probes

Gene	Probe	Catalog #	Ref Seq
18S	VIC-MGB	4319413E	X03205.1
CD138	FAM-MGB	Mm00448918_m1	NM_011519.2
Ig μ Chain	FAM-MGB	Mm01718955_g1	No RefSeq #
Ig κ Chain	FAM-MGB	Custom synthesized using Forward primer: GGAAGATTGATGGCAGTGAACGA Reverse Primer: GCTGTCCTGATCAGTCCAACT Probe: TCAGGACGCCATTTTG	NG_005612
Ig J-Chain	FAM-MGB	Mm00461780_m1	NM_152839.2
XBP-1 (total)	FAM-MGB	Mm00457359_m1	NM_013842.2
XBP-1 (spliced)	FAM-MGB	Custom synthesized, see (Skalet *et al.* 2005) for details	No RefSeq #
Pax5 (BSAP)	FAM-MGB	Mm00435501_m1	NM_008782.2
Blimp-1 (prdm1)	FAM-MGB	Mm00476128_m1	NM_007548.3
BCL6	FAM-MGB	Mm00477633_m1	NM_009744.3
c-fos	FAM-MGB	Mm00487425_m1	NM_010234.2
c-jun	FAM-MGB	Mm00495062_s1	NM_010591.2

BIBLIOGRAPHY

Abbott, B. D. and Birnbaum, L. S. (1989). TCDD alters medial epithelial cell differentiation during palatogenesis. *Toxicology and applied pharmacology* **99**, 276-286.

Alsharif, N. Z. and Hassoun, E. A. (2004). Protective effects of vitamin A and vitamin E succinate against 2,3,7,8-tetrachlorodibenzo-p-dioxin (TCDD)-induced body wasting, hepatomegaly, thymic atrophy, production of reactive oxygen species and DNA damage in C57BL/6J mice. *Basic Clin Pharmacol Toxicol* **95**, 131-8.

Arulampalam, V., Grant, P. A., Samuelsson, A., Lendahl, U. and Pettersson, S. (1994). Lipopolysaccharide-dependent transactivation of the temporally regulated immunoglobulin heavy chain 3' enhancer. *Eur J Immunol* **24**, 1671-7.

Asthagiri, A. R. and Lauffenburger, D. A. (2001). A computational study of feedback effects on signal dynamics in a mitogen-activated protein kinase (MAPK) pathway model. *Biotechnol Prog* **17**, 227-39.

Balazs, M., Martin, F., Zhou, T. and Kearney, J. (2002). Blood dendritic cells interact with splenic marginal zone B cells to initiate T-independent immune responses. *Immunity* **17**, 341-52.

Banerjee, A., Gugasyan, R., McMahon, M. and Gerondakis, S. (2006). Diverse Toll-like receptors utilize Tpl2 to activate extracellular signal-regulated kinase (ERK) in hemopoietic cells. *Proc Natl Acad Sci U S A* **103**, 3274-9.

Bendelac, A., Bonneville, M. and Kearney, J. F. (2001). Autoreactivity by design: innate B and T lymphocytes. *Nat Rev Immunol* **1**, 177-86.

Bishop, G. A. and Haughton, G. (1986). Induced differentiation of a transformed clone of Ly-1+ B cells by clonal T cells and antigen. *Proc Natl Acad Sci U S A* **83**, 7410-4.

Bishop, G. A., Hsing, Y., Hostager, B. S., Jalukar, S. V., Ramirez, L. M. and Tomai, M. A. (2000). Molecular mechanisms of B lymphocyte activation by the immune response modifier R-848. *J Immunol* **165**, 5552-7.

Bone, H. and Williams, N. A. (2001). Antigen-receptor cross-linking and lipopolysaccharide trigger distinct phosphoinositide 3-kinase-dependent pathways to NF-kappa B activation in primary B cells. *Int Immunol* **13**, 807-16.

Borriello, F., Sethna, M. P., Boyd, S. D., Schweitzer, A. N., Tivol, E. A., Jacoby, D., Strom, T. B., Simpson, E. M., Freeman, G. J. and Sharpe, A. H. (1997). B7-1 and B7-2 have overlapping, critical roles in immunoglobulin class switching and germinal center formation. *Immunity* **6**, 303-13.

Boverhof, D. R., Burgoon, L. D., Tashiro, C., Chittim, B., Harkema, J. R., Jump, D. B. and Zacharewski, T. R. (2005). Temporal and dose-dependent hepatic gene expression patterns in mice provide new insights into TCDD-Mediated hepatotoxicity. *Toxicol Sci* **85**, 1048-63.

Bowen, S. S. and Moursund, M. P. (1957). Chloracne in the manufacture of DDT. *AMA Arch Derm* **75**, 743-6.

Bradfield, C. A., Glover, E. and Poland, A. (1991). Purification and N-terminal amino acid sequence of the Ah receptor from the C57BL/6J mouse. *Mol Pharmacol* **39**, 13-9.

Burbach, K. M., Poland, A. and Bradfield, C. A. (1992). Cloning of the Ah-receptor cDNA reveals a distinctive ligand-activated transcription factor. *Proc Natl Acad Sci U S A* **89**, 8185-9.

Calame, K. L., Lin, K.-I. and Tunyaplin, C. (2003). Regulatory Mechanisms that Determine the Development and Function of Plasma Cells. *Annual Review of Immunology* **21**, 205-230, doi:10.1146/annurev.immunol.21.120601.141138.

Campbell, K. S. (1999). Signal transduction from the B cell antigen-receptor. *Curr Opin Immunol* **11**, 256-64.

Chapman, B. S., Thayer, R. M., Vincent, K. A. and Haigwood, N. L. (1991). Effect of intron A from human cytomegalovirus (Towne) immediate-early gene on heterologous expression in mammalian cells. *Nucleic Acids Res* **19**, 3979-86.

Clark, A. J. (1933). The mode of action of drugs on cells. The Williams & Wilkins company.

Clark, D. A., Sweeney, G., Safe, S., Hancock, E., Kilburn, D. G. and Gauldie, J. (1983). Cellular and genetic basis for suppression of cytotoxic T cell generation by haloaromatic hydrocarbons. *Immunopharmacology* **6**, 143-53.

Clark, G. C., Blank, J. A., Germolec, D. R. and Luster, M. I. (1991). 2,3,7,8-Tetrachlorodibenzo-p-dioxin stimulation of tyrosine phosphorylation in B lymphocytes: potential role in immunosuppression. *Mol Pharmacol* **39**, 495-501.

Cobaleda, C., Jochum, W. and Busslinger, M. (2007a). Conversion of mature B cells into T cells by dedifferentiation to uncommitted progenitors. *Nature* **449**, 473-7.

Cobaleda, C., Schebesta, A., Delogu, A. and Busslinger, M. (2007b). Pax5: the guardian of B cell identity and function. *Nat Immunol* **8**, 463-70.

Corcoran, L. M., Hasbold, J., Dietrich, W., Hawkins, E., Kallies, A., Nutt, S. L., Tarlinton, D. M., Matthias, P. and Hodgkin, P. D. (2005). Differential requirement for OBF-1 during antibody-secreting cell differentiation. *J Exp Med* **201**, 1385-96.

Crawford, R. B., Holsapple, M. P. and Kaminski, N. E. (1997). Leukocyte activation induces aryl hydrocarbon receptor up-regulation, DNA binding, and increased Cyp1a1 expression in the absence of exogenous ligand. *Mol Pharmacol* **52**, 921-7.

Dariavach, P., Williams, G. T., Campbell, K., Pettersson, S. and Neuberger, M. S. (1991). The mouse IgH 3'-enhancer. *Eur J Immunol* **21**, 1499-504.

DeFranco, A. L., Raveche, E. S. and Paul, W. E. (1985). Separate control of B lymphocyte early activation and proliferation in response to anti-IgM antibodies. *J Immunol* **135**, 87-94.

Delogu, A., Schebesta, A., Sun, Q., Aschenbrenner, K., Perlot, T. and Busslinger, M. (2006). Gene repression by Pax5 in B cells is essential for blood cell homeostasis and is reversed in plasma cells. *Immunity* **24**, 269-81.

Denison, M. S. and Nagy, S. R. (2003). Activation of the aryl hydrocarbon receptor by structurally diverse exogenous and endogenous chemicals. *Annu Rev Pharmacol Toxicol* **43**, 309-34.

Donahue, A. C. and Fruman, D. A. (2007). Distinct signaling mechanisms activate the target of rapamycin in response to different B-cell stimuli. *European Journal of Immunology* **37**, 2923-2936.

Dooley, R. K. and Holsapple, M. P. (1988). Elucidation of cellular targets responsible for tetrachlorodibenzo-p-dioxin (TCDD)-induced suppression of antibody responses: I. The role of the B lymphocyte. *Immunopharmacology* **16**, 167-80.

Dooley, R. K., Morris, D. L. and Holsapple, M. P. (1990). Elucidation of cellular targets responsible for tetrachlorodibenzo-p-dioxin (TCDD)-induced suppression of antibody responses: II. The role of the T-lymphocyte. *Immunopharmacology* **19**, 47-58.

Fagarasan, S., Watanabe, N. and Honjo, T. (2000). Generation, expansion, migration and activation of mouse B1 cells. *Immunol Rev* **176**, 205-15.

Fairfax, K. A., Corcoran, L. M., Pridans, C., Huntington, N. D., Kallies, A., Nutt, S. L. and Tarlinton, D. M. (2007). Different kinetics of blimp-1 induction in B cell subsets revealed by reporter gene. *J Immunol* **178**, 4104-11.

Fan, F., Wierda, D. and Rozman, K. K. (1996). Effects of 2,3,7,8-tetrachlorodibenzo-p-dioxin on humoral and cell-mediated immunity in Sprague-Dawley rats. *Toxicology* **106**, 221-8.

Francois, S., El Benna, J., Dang, P. M., Pedruzzi, E., Gougerot-Pocidalo, M. A. and Elbim, C. (2005). Inhibition of neutrophil apoptosis by TLR agonists in whole blood: involvement of the phosphoinositide 3-kinase/Akt and NF-kappaB signaling pathways, leading to increased levels of Mcl-1, A1, and phosphorylated Bad. *J Immunol* **174**, 3633-42.

Genestier, L., Taillardet, M., Mondiere, P., Gheit, H., Bella, C. and Defrance, T. (2007). TLR agonists selectively promote terminal plasma cell differentiation of B cell subsets specialized in thymus-independent responses. *J Immunol* **178**, 7779-86.

Gilman, H. and Dietrich, J. J. (1957). Halogen Derivatives of Dibenzo-Para-Dioxin. *J. Am. Chem. Soc.* **79**, 1439-1441.

Grant, P. A., Thompson, C. B. and Pettersson, S. (1995). IgM receptor-mediated transactivation of the IgH 3' enhancer couples a novel Elf-1-AP-1 protein complex to the developmental control of enhancer function. *Embo J* **14**, 4501-13.

Hanlon, P. R., Ganem, L. G., Cho, Y. C., Yamamoto, M. and Jefcoate, C. R. (2003). AhR- and ERK-dependent pathways function synergistically to mediate 2,3,7,8-tetrachlorodibenzo-p-dioxin suppression of peroxisome proliferator-activated receptor-gamma1 expression and subsequent adipocyte differentiation. *Toxicol Appl Pharmacol* **189**, 11-27.

Harnett, M. M., Katz, E. and Ford, C. A. (2005). Differential signalling during B-cell maturation. *Immunol Lett* **98**, 33-44.

Harper, N., Connor, K., Steinberg, M. and Safe, S. (1995a). Immunosuppressive activity of polychlorinated biphenyl mixtures and congeners: nonadditive (antagonistic) interactions. *Fundam Appl Toxicol* **27**, 131-9.

Harper, N., Steinberg, M., Thomsen, J. and Safe, S. (1995b). Halogenated aromatic hydrocarbon-induced suppression of the plaque-forming cell response in B6C3F1 splenocytes cultured with allogenic mouse serum: Ah receptor structure activity relationships. *Toxicology* **99**, 199-206.

Hayakawa, K., Hardy, R. R., Herzenberg, L. A. and Herzenberg, L. A. (1985). Progenitors for Ly-1 B cells are distinct from progenitors for other B cells. *J Exp Med* **161**, 1554-68.

Hebeis, B., Vigorito, E., Kovesdi, D. and Turner, M. (2005). Vav proteins are required for B-lymphocyte responses to LPS. *Blood* **106**, 635-40.

Holladay, S. D., Lindstrom, P., Blaylock, B. L., Comment, C. E., Germolec, D. R., Heindell, J. J. and Luster, M. I. (1991). Perinatal thymocyte antigen expression and postnatal immune development altered by gestational exposure to tetrachlorodibenzo-p-dioxin (TCDD). *Teratology* **44**, 385-93.

Holsapple, M. P., Tucker, A. N., McNerney, P. J. and White, K. L., Jr. (1984). Effects of N-nitrosodimethylamine on humoral immunity. *J Pharmacol Exp Ther* **229**, 493-500.

Holsapple, M. P., Dooley, R. K., McNerney, P. J. and McCay, J. A. (1986). Direct suppression of antibody responses by chlorinated dibenzodioxins in cultured spleen cells from (C57BL/6 x C3H)F1 and DBA/2 mice. *Immunopharmacology* **12**, 175-86.

Hsu, S. M., Cossman, J. and Jaffe, E. S. (1983). Lymphocyte subsets in normal human lymphoid tissues. *Am J Clin Pathol* **80**, 21-30.

Hu, C. C., Dougan, S. K., McGehee, A. M., Love, J. C. and Ploegh, H. L. (2009). XBP-1 regulates signal transduction, transcription factors and bone marrow colonization in B cells. *Embo J* **28**, 1624-36.

Huff, J. E., Salmon, A. G., Hooper, N. K. and Zeise, L. (1991). Long-term carcinogenesis studies on 2, 3, 7, 8-tetrachlorodibenzo-p-dioxin and hexachlorodibenzo-p-dioxins. *Cell biology and toxicology* **7**, 67-94.

Igarashi, K., Ochiai, K. and Muto, A. (2007). Architecture and Dynamics of the Transcription Factor Network that Regulates B-to-Plasma Cell Differentiation. *J Biochem* **141**, 783-789, 10.1093/jb/mvm106.

Irish, J. M., Czerwinski, D. K., Nolan, G. P. and Levy, R. (2006). Kinetics of B cell receptor signaling in human B cell subsets mapped by phosphospecific flow cytometry. *J Immunol* **177**, 1581-9.

Jensen, N. E., Sneddon, I. B. and Walker, A. E. (1972). Tetrachlorobenzodioxin and chloracne. *Trans St Johns Hosp Dermatol Soc* **58**, 172-7.

Jeong, H. G., Jeong, T. C. and Yang, K. H. (1993). Mouse interferon gamma pretreated hepatocytes conditioned media suppress cytochrome P-450 induction by TCDD in mouse hepatoma cells. *Biochem Mol Biol Int* **29**, 197-202.

Kallies, A., Hasbold, J., Tarlinton, D. M., Dietrich, W., Corcoran, L. M., Hodgkin, P. D. and Nutt, S. L. (2004). Plasma Cell Ontogeny Defined by Quantitative Changes in Blimp-1 Expression. *J. Exp. Med.* **200**, 967-977, 10.1084/jem.20040973.

Kanda, K., Hu, H. M., Zhang, L., Grandchamps, J. and Boxer, L. M. (2000). NF-kappa B activity is required for the deregulation of c-myc expression by the immunoglobulin heavy chain enhancer. *J Biol Chem* **275**, 32338-46.

Kantor, A. B. and Herzenberg, L. A. (1993). Origin of murine B cell lineages. *Annu Rev Immunol* **11**, 501-38.

Karin, M., Liu, Z. and Zandi, E. (1997). AP-1 function and regulation. *Curr Opin Cell Biol* **9**, 240-6.

Karras, J. G. and Holsapple, M. P. (1994). Inhibition of calcium-dependent B cell activation by 2,3,7,8-tetrachlorodibenzo-p-dioxin. *Toxicol Appl Pharmacol* **125**, 264-70.

Karras, J. G., Morris, D. L., Matulka, R. A., Kramer, C. M. and Holsapple, M. P. (1996). 2,3,7,8-tetrachlorodibenzo-p-dioxin (TCDD) elevates basal B-cell intracellular calcium concentration and suppresses surface Ig- but not CD40-induced antibody secretion. *Toxicol Appl Pharmacol* **137**, 275-84.

Kelly, B. C., Ikonomou, M. G., Blair, J. D., Morin, A. E. and Gobas, F. A. P. C. (2007). Food Web-Specific Biomagnification of Persistent Organic Pollutants. *Science* **317**, 236-239, 10.1126/science.1138275.

Kimberland, M. L., Divoky, V., Prchal, J., Schwahn, U., Berger, W. and Kazazian, H. H., Jr. (1999). Full-length human L1 insertions retain the capacity for high frequency retrotransposition in cultured cells. *Hum Mol Genet* **8**, 1557-60.

Kramer, C. M., Johnson, K. W., Dooley, R. K. and Holsapple, M. P. (1987). 2,3,7,8-Tetrachlorodibenzo-p-dioxin (TCDD) enhances antibody production and protein kinase activity in murine B cells. *Biochem Biophys Res Commun* **145**, 25-33.

Krieg, A. M., Yi, A. K., Matson, S., Waldschmidt, T. J., Bishop, G. A., Teasdale, R., Koretzky, G. A. and Klinman, D. M. (1995). CpG motifs in bacterial DNA trigger direct B-cell activation. *Nature* **374**, 546-9.

Krutzik, P. O., Hale, M. B. and Nolan, G. P. (2005). Characterization of the murine immunological signaling network with phosphospecific flow cytometry. *J Immunol* **175**, 2366-73.

Krutzik, P. O., Crane, J. M., Clutter, M. R. and Nolan, G. P. (2008). High-content single-cell drug screening with phosphospecific flow cytometry. *Nat Chem Biol* **4**, 132-42.

Kumagai, S., Koda, S., Miyakita, T., Yamaguchi, H., Katagi, K. and Yasuda, N. (2000). Polychlorinated dibenzo-p-dioxin and dibenzofuran concentrations in the serum samples of workers at continuously burning municipal waste incinerators in Japan. *Occup Environ Med* **57**, 204-10.

Lee, A.-H., Scapa, E. F., Cohen, D. E. and Glimcher, L. H. (2008). Regulation of Hepatic Lipogenesis by the Transcription Factor XBP1. *Science* **320**, 1492-1496, 10.1126/science.1158042.

Lee, C. C., Yao, Y. J., Chen, H. L., Guo, Y. L. and Su, H. J. (2006). Fatty liver and hepatic function for residents with markedly high serum PCDD/Fs levels in Taiwan. *J Toxicol Environ Health A* **69**, 367-80.

Lin, K.-I., Angelin-Duclos, C., Kuo, T. C. and Calame, K. (2002). Blimp-1-dependent repression of Pax-5 is required for differentiation of B cells to immunoglobulin M-secreting plasma cells. *Mol Cell Biol* **22**, 4771-80.

Lin, K. I., Kao, Y. Y., Kuo, H. K., Yang, W. B., Chou, A., Lin, H. H., Yu, A. L. and Wong, C. H. (2006). Reishi polysaccharides induce immunoglobulin production through the TLR4/TLR2-mediated induction of transcription factor Blimp-1. *J Biol Chem* **281**, 24111-23.

Lindenmann, J. (1984). Origin of the terms 'antibody' and 'antigen'. *Scand J Immunol* **19**, 281-5.

Livak, K. J. and Schmittgen, T. D. (2001). Analysis of relative gene expression data using real-time quantitative PCR and the 2(-Delta Delta C(T)) Method. *Methods* **25**, 402-8.

Lloyd, R. V., Erickson, L. A., Jin, L., Kulig, E., Qian, X., Cheville, J. C. and Scheithauer, B. W. (1999). p27kip1: a multifunctional cyclin-dependent kinase inhibitor with prognostic significance in human cancers. *Am J Pathol* **154**, 313-23.

Lopes-Carvalho, T., Foote, J. and Kearney, J. F. (2005). Marginal zone B cells in lymphocyte activation and regulation. *Curr Opin Immunol* **17**, 244-50.

Luebke, R. W., Chen, D. H., Dietert, R., Yang, Y., King, M. and Luster, M. I. (2006). The comparative immunotoxicity of five selected compounds following developmental or adult exposure. *J Toxicol Environ Health B Crit Rev* **9**, 1-26.

Luster, M. I., Germolec, D. R., Clark, G., Wiegand, G. and Rosenthal, G. J. (1988). Selective effects of 2,3,7,8-tetrachlorodibenzo-p-dioxin and corticosteroid on in vitro lymphocyte maturation. *J Immunol* **140**, 928-35.

Magnusdottir, E., Kalachikov, S., Mizukoshi, K., Savitsky, D., Ishida-Yamamoto, A., Panteleyev, A. A. and Calame, K. (2007). Epidermal terminal differentiation depends on B lymphocyte-induced maturation protein-1. *Proc Natl Acad Sci U S A* **104**, 14988-93.

Maitra, S. and Atchison, M. (2000). BSAP Can Repress Enhancer Activity by Targeting PU.1 Function. *Mol. Cell. Biol.* **20**, 1911-1922, 10.1128/mcb.20.6.1911-1922.2000.

Markevich, N. I., Hoek, J. B. and Kholodenko, B. N. (2004). Signaling switches and bistability arising from multisite phosphorylation in protein kinase cascades. *J Cell Biol* **164**, 353-9.

Martin, F., Oliver, A. M. and Kearney, J. F. (2001). Marginal zone and B1 B cells unite in the early response against T-independent blood-borne particulate antigens. *Immunity* **14**, 617-29.

Matthias, P. and Baltimore, D. (1993). The immunoglobulin heavy chain locus contains another B-cell-specific 3' enhancer close to the alpha constant region. *Mol Cell Biol* **13**, 1547-53.

May, G. (1973). Chloracne from the accidental production of tetrachlorodibenzodioxin. *Br J Ind Med* **30**, 276-83.

Meigs, J. W., Albom, J. J. and Kartin, B. L. (1954). Chloracne from an unusual exposure to arochlor. *J Am Med Assoc* **154**, 1417-8.

Mikkola, I., Heavey, B., Horcher, M. and Busslinger, M. (2002). Reversion of B cell commitment upon loss of Pax5 expression. *Science* **297**, 110-3.

Morris, D. L. and Holsapple, M. P. (1991). Effects of 2,3,7,8-tetrachlorodibenzo-p-dioxin (TCDD) on humoral immunity: II. B cell activation. *Immunopharmacology* **21**, 171-81.

Morris, D. L., Karras, J. G. and Holsapple, M. P. (1993). Direct effects of 2,3,7,8-tetrachlorodibenzo-p-dioxin (TCDD) on responses to lipopolysaccharide (LPS) by isolated murine B-cells. *Immunopharmacology* **26**, 105-12.

Morris, D. L., Jeong, H. G., Stevens, W. D., Chun, Y. J., Karras, J. G. and Holsapple, M. P. (1994). Serum modulation of the effects of TCDD on the in vitro antibody response and on enzyme induction in primary hepatocytes. *Immunopharmacology* **27**, 93-105.

Nebert, D. W., Goujon, F. M. and Gielen, J. E. (1972). Aryl hydrocarbon hydroxylase induction by polycyclic hydrocarbons: simple autosomal dominant trait in the mouse. *Nat New Biol* **236**, 107-10.

Nera, K.-P., Kohonen, P., Narvi, E., Peippo, A., Mustonen, L., Terho, P., Koskela, K., Buerstedde, J.-M. and Lassila, O. (2006). Loss of Pax5 Promotes Plasma Cell Differentiation. *Immunity* **24**, 283-293.

Niu, H., Ye, B. H. and Dalla-Favera, R. (1998). Antigen receptor signaling induces MAP kinase-mediated phosphorylation and degradation of the BCL-6 transcription factor. *Genes Dev* **12**, 1953-61.

Niu, H., Cattoretti, G. and Dalla-Favera, R. (2003). BCL6 controls the expression of the B7-1/CD80 costimulatory receptor in germinal center B cells. *J Exp Med* **198**, 211-21.

Nutt, S. L., Fairfax, K. A. and Kallies, A. (2007). BLIMP1 guides the fate of effector B and T cells. *Nat Rev Immunol* **7**, 923-7.

Ogata, H., Su, I., Miyake, K., Nagai, Y., Akashi, S., Mecklenbrauker, I., Rajewsky, K., Kimoto, M. and Tarakhovsky, A. (2000). The toll-like receptor protein RP105 regulates lipopolysaccharide signaling in B cells. *J Exp Med* **192**, 23-9.

Ohkubo, Y., Arima, M., Arguni, E., Okada, S., Yamashita, K., Asari, S., Obata, S., Sakamoto, A., Hatano, M., J, O. W., Ebara, M., Saisho, H. and Tokuhisa, T. (2005). A role for c-fos/activator protein 1 in B lymphocyte terminal differentiation. *J Immunol* **174**, 7703-10.

Omori, S. A., Cato, M. H., Anzelon-Mills, A., Puri, K. D., Shapiro-Shelef, M., Calame, K. and Rickert, R. C. (2006). Regulation of class-switch recombination and plasma cell differentiation by phosphatidylinositol 3-kinase signaling. *Immunity* **25**, 545-57.

Patterson, D. G., Jr., Fingerhut, M. A., Roberts, D. W., Needham, L. L., Sweeney, M. H., Marlow, D. A., Andrews, J. S., Jr. and Halperin, W. E. (1989). Levels of polychlorinated dibenzo-p-dioxins and dibenzofurans in workers exposed to 2,3,7,8-tetrachlorodibenzo-p-dioxin. *Am J Ind Med* **16**, 135-46.

Perdew, G. H. and Poland, A. (1988). Purification of the Ah receptor from C57BL/6J mouse liver. *J Biol Chem* **263**, 9848-52.

Perez, O. D. and Nolan, G. P. (2002). Simultaneous measurement of multiple active kinase states using polychromatic flow cytometry. *Nat Biotechnol* **20**, 155-62.

Pettersson, S., Cook, G. P., Bruggemann, M., Williams, G. T. and Neuberger, M. S. (1990). A second B cell-specific enhancer 3' of the immunoglobulin heavy-chain locus. *Nature* **344**, 165-8.

Pettersson, S., Arulampalam, V. and Neurath, M. (1997). Temporal control of IgH gene expression in developing B cells by the 3' locus control region. *Immunobiology* **198**, 236-48.

Philbin, V. J., Iqbal, M., Boyd, Y., Goodchild, M. J., Beal, R. K., Bumstead, N., Young, J. and Smith, A. L. (2005). Identification and characterization of a functional, alternatively spliced Toll-like receptor 7 (TLR7) and genomic disruption of TLR8 in chickens. *Immunology* **114**, 507-21.

Poland, A. and Glover, E. (1974). Comparison of 2,3,7,8-tetrachlorodibenzo-p-dioxin, a potent inducer of aryl hydrocarbon hydroxylase, with 3-methylcholanthrene. *Mol Pharmacol* **10**, 349-59.

Poland, A., Glover, E. and Kende, A. S. (1976). Stereospecific, high affinity binding of 2,3,7,8-tetrachlorodibenzo-p-dioxin by hepatic cytosol. Evidence that the binding species is receptor for induction of aryl hydrocarbon hydroxylase. *J Biol Chem* **251**, 4936-46.

Poland, A., Greenlee, W. F. and Kende, A. S. (1979). Studies on the mechanism of action of the chlorinated dibenzo-p-dioxins and related compounds. *Ann N Y Acad Sci* **320**, 214-30.

Prell, R. A. and Kerkvliet, N. I. (1997). Involvement of altered B7 expression in dioxin immunotoxicity: B7 transfection restores the CTL but not the autoantibody response to the P815 mastocytoma. *J Immunol* **158**, 2695-703.

Rajewsky, K. (1996). Clonal selection and learning in the antibody system. *Nature* **381**, 751-8.

Ralph, P., Saiki, O., Maurer, D. H. and Welte, K. (1983). IgM and IgG secretion in human B-cell lines regulated by B-cell-inducing factors (BIF) and phorbol ester. *Immunol Lett* **7**, 17-23.

Rehli, M. (2002). Of mice and men: species variations of Toll-like receptor expression. *Trends Immunol* **23**, 375-8.

Reimold, A. M., Ponath, P. D., Li, Y. S., Hardy, R. R., David, C. S., Strominger, J. L. and Glimcher, L. H. (1996). Transcription factor B cell lineage-specific activator protein regulates the gene for human X-box binding protein 1. *J. Exp. Med.* **183**, 393-401, 10.1084/jem.183.2.393.

Rittenberg, M. B. and Pratt, K. L. (1969). Antitrinitrophenyl (TNP) plaque assay. Primary response of Balb/c mice to soluble and particulate immunogen. *Proc Soc Exp Biol Med* **132**, 575-81.

Roederer, M., Moore, W., Treister, A., Hardy, R. R. and Herzenberg, L. A. (2001a). Probability binning comparison: a metric for quantitating multivariate distribution differences. *Cytometry* **45**, 47-55.

Roederer, M., Treister, A., Moore, W. and Herzenberg, L. A. (2001b). Probability binning comparison: a metric for quantitating univariate distribution differences. *Cytometry* **45**, 37-46.

Rui, L., Healy, J. I., Blasioli, J. and Goodnow, C. C. (2006). ERK signaling is a molecular switch integrating opposing inputs from B cell receptor and T cell cytokines to control TLR4-driven plasma cell differentiation. *J Immunol* **177**, 5337-46.

Safe, S. H. (1995). Modulation of gene expression and endocrine response pathways by 2,3,7,8-tetrachlorodibenzo-p-dioxin and related compounds. *Pharmacol Ther* **67**, 247-81.

Sastry, L., Johnson, T., Hobson, M. J., Smucker, B. and Cornetta, K. (2002). Titering lentiviral vectors: comparison of DNA, RNA and marker expression methods. *Gene Ther* **9**, 1155-62.

Schneider, D., Manzan, M. A., Crawford, R. B., Chen, W. and Kaminski, N. E. (2008). 2,3,7,8-Tetrachlorodibenzo-p-dioxin-mediated impairment of B cell differentiation involves dysregulation of paired box 5 (Pax5) isoform, Pax5a. *J Pharmacol Exp Ther* **326**, 463-74.

Schneider, D., Manzan, M. A., Yoo, B. S., Crawford, R. B. and Kaminski, N. (2009). Involvement of Blimp-1 and AP-1 dysregulation in the 2,3,7,8-tetrachlorodibenzo-p-dioxin-mediated suppression of the IgM response by B cells. *Toxicol Sci.*

Schrantz, N., Beney, G. E., Auffredou, M. T., Bourgeade, M. F., Leca, G. and Vazquez, A. (2000). The expression of p18INK4 and p27kip1 cyclin-dependent kinase inhibitors is regulated differently during human B cell differentiation. *J Immunol* **165**, 4346-52.

Seefeld, M. D., Corbett, S. W., Keesey, R. E. and Peterson, R. E. (1984). Characterization of the wasting syndrome in rats treated with 2, 3, 7, 8-tetrachlorodibenzo-p-dioxin. *Toxicology and applied pharmacology* **73**, 311-322.

Shaffer, A. L., Yu, X., He, Y., Boldrick, J., Chan, E. P. and Staudt, L. M. (2000). BCL-6 represses genes that function in lymphocyte differentiation, inflammation, and cell cycle control. *Immunity* **13**, 199-212.

Shaffer, A. L., Lin, K.-I., Kuo, T. C., Yu, X., Hurt, E. M., Rosenwald, A., Giltnane, J. M., Yang, L., Zhao, H., Calame, K. and Staudt, L. M. (2002). Blimp-1 Orchestrates Plasma Cell Differentiation by Extinguishing the Mature B Cell Gene Expression Program. *Immunity* **17**, 51-62.

Shapiro-Shelef, M., Lin, K. I., McHeyzer-Williams, L. J., Liao, J., McHeyzer-Williams, M. G. and Calame, K. (2003). Blimp-1 is required for the formation of immunoglobulin secreting plasma cells and pre-plasma memory B cells. *Immunity* **19**, 607-20.

Shen, Y. and Hendershot, L. M. (2007). Identification of ERdj3 and OBF-1/BOB-1/OCA-B as direct targets of XBP-1 during plasma cell differentiation. *J Immunol* **179**, 2969-78.

Singh, M. and Birshtein, B. K. (1993). NF-HB (BSAP) is a repressor of the murine immunoglobulin heavy-chain 3' alpha enhancer at early stages of B-cell differentiation. *Mol Cell Biol* **13**, 3611-22.

Skalet, A. H., Isler, J. A., King, L. B., Harding, H. P., Ron, D. and Monroe, J. G. (2005). Rapid B cell receptor-induced unfolded protein response in nonsecretory B cells correlates with pro- versus antiapoptotic cell fate. *J Biol Chem* **280**, 39762-71.

Smeal, T., Binetruy, B., Mercola, D. A., Birrer, M. and Karin, M. (1991). Oncogenic and transcriptional cooperation with Ha-Ras requires phosphorylation of c-Jun on serines 63 and 73. *Nature* **354**, 494-6.

Smialowicz, R. J., Riddle, M. M., Williams, W. C. and Diliberto, J. J. (1994). Effects of 2,3,7,8-tetrachlorodibenzo-p-dioxin (TCDD) on humoral immunity and lymphocyte subpopulations: differences between mice and rats. *Toxicol Appl Pharmacol* **124**, 248-56.

Snyder, N. K., Kramer, C. M., Dooley, R. K. and Holsapple, M. P. (1993). Characterization of protein phosphorylation by 2,3,7,8-tetrachlorodibenzo-p-dioxin in murine lymphocytes: indirect evidence for a role in the suppression of humoral immunity. *Drug Chem Toxicol* **16**, 135-63.

Suh, J., Jeon, Y. J., Kim, H. M., Kang, J. S., Kaminski, N. E. and Yang, K.-H. (2002a). Aryl hydrocarbon receptor-dependent inhibition of AP-1 activity by 2,3,7,8-tetrachlorodibenzo-p-dioxin in activated B cells. *Toxicol Appl Pharmacol* **181**, 116-23.

Suh, J., Jeon, Y. J., Kim, H. M., Kang, J. S., Kaminski, N. E. and Yang, K. H. (2002b). Aryl hydrocarbon receptor-dependent inhibition of AP-1 activity by 2,3,7,8-tetrachlorodibenzo-p-dioxin in activated B cells. *Toxicol Appl Pharmacol* **181**, 116-23.

Sulentic, C. E., Holsapple, M. P. and Kaminski, N. E. (1998). Aryl hydrocarbon receptor-dependent suppression by 2,3,7, 8-tetrachlorodibenzo-p-dioxin of IgM secretion in activated B cells. *Mol Pharmacol* **53**, 623-9.

Sulentic, C. E., Holsapple, M. P. and Kaminski, N. E. (2000). Putative link between transcriptional regulation of IgM expression by 2,3,7,8-tetrachlorodibenzo-p-dioxin and the aryl hydrocarbon receptor/dioxin-responsive enhancer signaling pathway. *J Pharmacol Exp Ther* **295**, 705-16.

Sulentic, C. E. W., Kang, J. S., Na, Y. J. and Kaminski, N. E. (2004a). Interactions at a dioxin responsive element (DRE) and an overlapping kappaB site within the hs4 domain of the 3'alpha immunoglobulin heavy chain enhancer. *Toxicology* **200**, 235-46.

Sulentic, C. E. W., Zhang, W., Na, Y. J. and Kaminski, N. E. (2004b). 2,3,7,8-tetrachlorodibenzo-p-dioxin, an exogenous modulator of the 3'alpha immunoglobulin heavy chain enhancer in the CH12.LX mouse cell line. *J Pharmacol Exp Ther* **309**, 71-8.

Tan, Z., Chang, X., Puga, A. and Xia, Y. (2002). Activation of mitogen-activated protein kinases (MAPKs) by aromatic hydrocarbons: role in the regulation of aryl hydrocarbon receptor (AHR) function. *Biochem Pharmacol* **64**, 771-80.

Tucker, A. N., Vore, S. J. and Luster, M. I. (1986). Suppression of B cell differentiation by 2,3,7,8-tetrachlorodibenzo-p-dioxin. *Mol Pharmacol* **29**, 372-7.

Tunyaplin, C., Shaffer, A. L., Angelin-Duclos, C. D., Yu, X., Staudt, L. M. and Calame, K. L. (2004). Direct Repression of prdm1 by Bcl-6 Inhibits Plasmacytic Differentiation. *J Immunol* **173**, 1158-1165.

Vasanwala, F. H., Kusam, S., Toney, L. M. and Dent, A. L. (2002). Repression of AP-1 Function: A Mechanism for the Regulation of Blimp-1 Expression and B Lymphocyte Differentiation by the B Cell Lymphoma-6 Protooncogene. *J Immunol* **169**, 1922-1929.

Vecchi, A., Mantovani, A., Sironi, M., Luini, W., Cairo, M. and Garattini, S. (1980a). Effect of acute exposure to 2,3,7,8-tetrachlorodibenzo-p-dioxin on humoral antibody production in mice. *Chem Biol Interact* **30**, 337-42.

Vecchi, A., Mantovani, A., Sironi, M., Luini, W., Spreafico, F. and Garattini, S. (1980b). The effect of acute administration of 2,3,7,8-tetrachlorodibenzo-p-dioxin (TCDD) on humoral antibody production and cell-mediated activities in mice. *Arch Toxicol Suppl* **4**, 163-5.

Vecchi, A., Sironi, M., Canegrati, M. A., Recchia, M. and Garattini, S. (1983). Immunosuppressive effects of 2,3,7,8-tetrachlorodibenzo-p-dioxin in strains of mice with different susceptibility to induction of aryl hydrocarbon hydroxylase. *Toxicol Appl Pharmacol* **68**, 434-41.

Vivarelli, M. S., McDonald, D., Miller, M., Cusson, N., Kelliher, M. and Geha, R. S. (2004). RIP links TLR4 to Akt and is essential for cell survival in response to LPS stimulation. *J Exp Med* **200**, 399-404.

Vorderstrasse, B. A., Steppan, L. B., Silverstone, A. E. and Kerkvliet, N. I. (2001). Aryl Hydrocarbon Receptor-Deficient Mice Generate Normal Immune Responses to Model Antigens and Are Resistant to TCDD-Induced Immune Suppression. *Toxicology and Applied Pharmacology* **171**, 157-164.

Vos, J. G., Moore, J. A. and Zinkl, J. G. (1973). Effect of 2,3,7,8-tetrachlorodibenzo-p-dioxin on the immune system of laboratory animals. *Environ Health Perspect* **5**, 149-62.

Vos, J. G., Moore, J. A. and Zinkl, J. G. (1974). Toxicity of 2,3,7,8-tetrachlorodibenzo-p-dioxin (TCDD) in C57B1/6 mice. *Toxicology and Applied Pharmacology* **29**, 229-241.

Weber, R., Tysklind, M. and Gaus, C. (2008). Dioxin-contemporary and future challenges of historical legacies. *Environmental Science and Pollution Research* **15**, 96-100.

Williams, C. E., Crawford, R. B., Holsapple, M. P. and Kaminski, N. E. (1996). Identification of functional aryl hydrocarbon receptor and aryl hydrocarbon receptor nuclear translocator in murine splenocytes. *Biochem Pharmacol* **52**, 771-80.

Wortis, H. H. (1971). Immunological responses of 'nude' mice. *Clin Exp Immunol* **8**, 305-17.

Yi, A.-K. and Krieg, A. M. (1998). Cutting Edge: Rapid Induction of Mitogen-Activated Protein Kinases by Immune Stimulatory CpG DNA. *J Immunol* **161**, 4493-4497.

Yi, A. K., Chace, J. H., Cowdery, J. S. and Krieg, A. M. (1996). IFN-gamma promotes IL-6 and IgM secretion in response to CpG motifs in bacterial DNA and oligodeoxynucleotides. *J Immunol* **156**, 558-564.

Yoo, B. S., Boverhof, D. R., Shnaider, D., Crawford, R. B., Zacharewski, T. R. and Kaminski, N. E. (2004). 2,3,7,8-Tetrachlorodibenzo-p-dioxin (TCDD) Alters the Regulation of Pax5 in Lipopolysaccharide-Activated B Cells. *Toxicol. Sci.* **77**, 272-279, 10.1093/toxsci/kfh013.

Yoshida, H., Matsui, T., Yamamoto, A., Okada, T. and Mori, K. (2001). XBP1 mRNA is induced by ATF6 and spliced by IRE1 in response to ER stress to produce a highly active transcription factor. *Cell* **107**, 881-91.

Zugerman, C. (1990). Chloracne. Clinical manifestations and etiology. *Journal Name: Dermatologic Clinics; (USA); Journal Volume: 8:1*, Medium: X; Size: Pages: 209-213.